

MINIMIZING ENERGY CONSUMPTION AND DOWNTIME IN OIL AND GAS
DRILLING EXPLORATION THROUGH TRIBOLOGY

A Thesis

by

JEVON HENDRA KUSUMA PHANDI

Submitted to the Office of Graduate and Professional Studies of
Texas A&M University
in partial fulfillment of the requirements for the degree of

MASTER OF SCIENCE

Chair of Committee,	Andreas Polycarpou
Committee Members,	Hong Liang
	Homero Castaneda-Lopez
Head of Department,	Andreas Polycarpou

December 2018

Major Subject: Mechanical Engineering

Copyright 2018 Jevon Hendra Kusuma Phandi

ABSTRACT

The scarcity of conventional oil reservoirs has led the oil and gas (O&G) industry to develop non-conventional extraction techniques such as extended-reach drilling (ERD) that brings new engineering challenges. Challenges such as high frictional torque and drag increases O&G exploration and production (E&P) costs in terms of time, energy consumption, tool replacement, and environmental restoration. One technical way to tackle the challenge is to improve the tribological performance of the drilling mud used as lubricating fluid to decrease friction and wear in the drilling process. In this study, a tribological approach is used to investigate the effect of organic friction modifiers (OFM) on drilling fluid friction reduction and wear protection. The results show that the use of a high molecular amide OFM in drilling mud reduces friction by 36% and wear by 90%. Additionally, the tribological effects of these friction modifiers on water-based mud (WBM) is studied to increase its technical performance. WBM is desirable due to two important aspects such as its lower cost and milder environmental impact in comparison to OBM. This study shows that the main source of COF and wear reductions are the mechanical and chemical properties of lubricating compounds called tribochemical layers which is produced during tribological processes. A characterization technique called Secondary Ion Mass Spectroscopy (SIMS) is used to characterize the surface chemistry of the best tribological interfaces for developing more superior friction modifier additives.

ACKNOWLEDGEMENTS

Above all else, I would like to thank God for all the blessings and people that He has put in my life. I would never have reached this far if not for the countless grace and miraculous healings that He has done in my life. Through all the experiences and chances that I have been given, I learn to live a life full of purposes to share the blessings to other people.

I would like to thank my advisor, Dr. Andreas Polycarpou, for giving me the guidance and opportunities to be a part of the Microtribodynamics Laboratory. Thank you for trusting me with the responsibilities and being an example of a good leader. I have learn so much from you.

I would like to thank my family, especially my mom, dad, and grandmothers, who have done their best to provide my siblings and I with shelter, food, educations, and good moral compass in every season. Thank you for not giving up on me when I was terminally ill in my early age. Thank you for always praying and supporting me, for trusting my own judgements, and for letting me pursue my dreams. I can never repay the sacrifices that you have done for me. I will forever love you and make you proud.

Last but not least I would like to thank all of my friends and colleagues that has become my family and support system. Each of you are special and have influenced my life in a way. I believe there is nothing that you cannot achieve if you commit to reach it. Don't focus on your weaknesses or failures, but use them to grow instead, and know that each of you have a special purpose.

CONTRIBUTORS AND FUNDING SOURCES

Contributors

This work was supervised by a thesis (or) dissertation committee consisting of Dr. Andreas Polycarpou and Dr. Hong Liang of the Department of Mechanical Engineering and Dr. Homero Castaneda-Lopez of the Department of Material Science.

The TOF SIMS in Chapter 4 was conducted by the Department of Chemistry and Materials Characterization Facility with a special thanks to the scientist working there, Dr. Stanislav Verkothurov.

All other work conducted for the thesis was completed by the student independently.

Funding Sources

This work was also made possible in part by collaboration with ExxonMobil Chemical. Its contents are solely the responsibility of the authors and do not necessarily represent the official views of ExxonMobil Chemical.

NOMENCLATURE

O & G	Oil and gas
E & P	Exploration and production
BF	Base fluid
DF	Drilling fluid
OBM	Oil-based mud
WBM	Water-based mud
SBM	Synthetic-based mud
FM	Friction modifier
OFM	Organic friction modifier
COF (μ)	Coefficient of friction
ToF SIMS	Time-of-Flight Secondary Ion Mass Spectroscopy
w	Wear rate (m^3/Nm)
L	Sliding distance (m)
P	Applied load (kg)
p_o	Contact pressure (Pa)
F	Tangential force (N)
W	Normal force
L	Length of contact
U	Relative sliding speed
η	Dynamic viscosity
N	Entrainment speed of fluid

H	Surface hardness
f	Friction force (g)
l	Torsional arm length (cm)
E^*	Effective modulus of elasticity
$\nu_{1,2}$	Poisson's ratio of sphere 1, 2
R^*	Effective radius of sphere
$R_{1,2}$	Radius of sphere 1, 2
A	Surface area under contact (m^2)
V	Wear volume (m^3)
a	Wear radius (m)
r	Steel ball radius (m)
d	Height of dome shaped wear (m)
MW	Molecular weight

TABLE OF CONTENTS

	Page
ABSTRACT.....	ii
ACKNOWLEDGEMENTS.....	iii
CONTRIBUTORS AND FUNDING SOURCES	iv
NOMENCLATURE	v
TABLE OF CONTENTS.....	vii
LIST OF FIGURES	x
LIST OF TABLES.....	xiv
CHAPTER 1 INTRODUCTION AND LITERATURE REVIEW	1
1.1. Engineering Challenges in Non-Conventional Oil and Gas Exploration and Production	1
1.2. Application of Tribology in Upstream Sector.....	2
1.2.1 Friction and Lubrication	2
1.2.2. Wear.....	7
1.3. Drilling Mud.....	10
1.4. Lubricant Additives.....	12
1.5. Thesis Flowchart	14
CHAPTER 2 EXPERIMENTAL SETUP AND MATERIALS.....	16
2.1. Equipment and Experimental Procedure.....	16
2.1.1. Falex Four-Ball Machine	16
2.1.2. Surface Analysis	19
2.2. Materials.....	20
2.2.1. SAE 52100 Alloy Steel Balls.....	20
2.2.2. Escaid/ Base Fluid (BF).....	21
2.2.3. Oil-based Mud (OBM)/ Oil-based Drilling Fluid.....	22
2.2.4. Water-based Mud (WBM)/ Water-based Drilling Fluid.....	24
2.2.5. Friction Modifier Additives	26
2.3. Tribological and Tribochemical Analysis.....	28
2.3.1. Coefficient of Friction.....	28
2.3.2. Hertzian Contact Stress for Sphere-on-Sphere Contact [³⁹]	29
2.3.3. Nominal Contact Pressure.....	30
2.3.4. Wear.....	31
2.3.5. Secondary Ion Mass Spectroscopy [⁴⁰].....	32

CHAPTER 3 TRIBOLOGICAL TESTING AND ANALYSIS.....	34
3.1. Escaid/ Base Fluid Experiments.....	35
3.1.1. No Additives	35
3.1.2. EMamide-2 and EMamide-7 Additives	36
3.1.3. UltraLube II Additive	38
3.1.4. Amphiphile S Additives.....	39
3.1.5. Summary	40
3.2. Oil-Based Drilling Mud Experiments	44
3.2.1. No Additives	44
3.2.2. EMamide-2 and EMamide-7 Additives	45
3.2.3. UltraLube 2 Additive	47
3.2.4. Amphiphile S Additives.....	48
3.2.5. Summary	49
3.3. Water-Based Drilling Mud Experiments.....	52
3.3.1. No Additives	53
3.3.2. EMamide-2 and EMamide-7.....	54
3.3.3. Amphiphile S and Amphiphile S-13.....	55
3.3.4. UltraLube II	57
3.3.5. EvoLube G	58
3.3.6. Summary	60
3.4. COF vs Wear Masterchart.....	64
3.5. Nominal Contact Pressure.....	69
3.6. Electrochemistry and Tribo-corrosion	70
3.7. Surface Profile.....	73
CHAPTER 4 TRIBOCHEMISTRY OF FRICTION AND WEAR REDUCTION	76
4.1. Chemical Analysis of Lubricating Fluid/ Additive Mixture	77
4.2. Tribochemical Analysis of Tribological Surface	79
4.2.1. Escaid.....	80
4.2.2. Water-Based Mud	84
4.3. Coverage Level Analysis and Summary	88
CHAPTER 5 CONCLUSION AND FUTURE WORK.....	90
REFERENCES	93
APPENDIX A FOUR-BALL TEST PROCEDURE	98
APPENDIX B FALEX FOUR-BALL TESTER DAQ WIRING.....	102
APPENDIX C SECONDARY ION MASS SPECTROSCOPY	103
APPENDIX D ADDITIONAL TRIBOLOGICAL DATA	106

APPENDIX E EFFECTS OF SURFACE HARDENING AND LUBRICANT VISCOSITY

ON SURFACE SEIZURE 107

LIST OF FIGURES

	Page
Figure 1: Curved drill string and hole-casing illustrating horizontal drilling.....	4
Figure 2: Schematic of Stribeck curve.....	6
Figure 3: Schematics of solid surfaces under different lubrication regimes. Not to scale.....	7
Figure 4: Lubricant additives breakdown [¹¹][²⁵].....	13
Figure 5: Solvent class vs polarity [²⁷].....	14
Figure 6: Thesis flowchart	15
Figure 7: Four-ball schematic	16
Figure 8: Four-ball data acquisition NI LabVIEW user interface	18
Figure 9: Four-ball tester data acquisition block diagram	18
Figure 10: VHX-600 Digital microscope	19
Figure 11: KLA-Tencor P-6 Stylus Profiler	20
Figure 12: Escaid as base fluid (BF) of oil-based mud (OBM).....	22
Figure 13: Oil-based mud (OBM) also known as drilling fluid (DF).....	24
Figure 14: Physical appearance of additives. A) EvoLube-G, B) Amphiphile S-13, C) EMamide-2, D) UltraLube II, E) Amphiphile S	26
Figure 15: Chemical structure of amide group, simple amide, substituted amide, and carboxylic acid [³⁶].....	27
Figure 16: Chemical structure of propanoic acid.....	28
Figure 17: Dome shaped wear on bottom stationary ball	31
Figure 18: Partial view of top (rotating) ball analyzed with ToF SIMS	33
Figure 19: Temperature, speed, and applied load profile with respect to time.....	35

Figure 20: COF versus time of Escaid lubricated interface	36
Figure 21: COF versus time of Escaid + EMamide-2 lubricated interface	37
Figure 22: COF versus time of Escaid + EMamide-2 lubricated interface	38
Figure 23: COF versus time of Escaid + UltraLube II Lubricated Interface	39
Figure 24: COF versus time of Escaid + Amphiphile S Lubricated Interface.....	40
Figure 25: COF versus time of all the additives tested in Escaid	40
Figure 26: Micro-images of one of the three bottom stationary ball a) Escaid (BF), b) Escaid + EMamide-2, c) Escaid + Amphiphile S, d) Escaid + UltraLube II, e) Escaid + EMamide-7, and f), g), h), i), j) respectively for the top ball.....	42
Figure 27: Wear rate of interface versus test duration.....	44
Figure 28: COF versus time of OBM lubricated interface	45
Figure 29: COF versus time of OBM + EMamide-2 lubricated interface	46
Figure 30: COF versus time of OBM + EMamide-7 lubricated interface	47
Figure 31: COF versus time of OBM + UltraLube II lubricated interface	48
Figure 32: COF versus time of OBM + Amphiphile S lubricated interface.....	49
Figure 33: COF versus time of all the additives tested in OBM.....	49
Figure 34: Micro-images of a) oil-based mud (OBM), b) OBM + EMamide-2, c) OBM + Amphiphile S, d) OBM + UltraLube II, e) OBM + EMamide-7 bottom stationary balls, and f), g), h), i), j) respectively for the top balls.....	51
Figure 35: Wear rate of OBM, OBM + EM-2, and OBM + Amphiphile S lubricated interfaces after 15, 30, and 60 minutes test duration.....	52
Figure 36: COF versus time of WBM lubricated interface.....	53
Figure 37: COF versus time of WBM + EMamide-2 lubricated interface	54

Figure 38: COF versus time of WBM + EMamide-7 lubricated interface	55
Figure 39: COF versus time of WBM + Amphiphile S lubricated interface	56
Figure 40: COF versus time of WBM + Amphiphile S-13 lubricated interface.....	56
Figure 41: COF versus time of WBM + 1/4 dosage Amphiphile S lubricated interface.....	57
Figure 42: COF versus time of WBM + UltraLube II lubricated interface	58
Figure 43: COF versus time of WBM + EvoLube G lubricated interface.....	59
Figure 44: COF versus time of WBM + 1/4 dosage EvoLube G lubricated interface	59
Figure 45: Effect of OFMs on WBM COF versus time.....	61
Figure 46: Micro-images of bottom stationary ball of a) water-based mud (WBM), b) WBM + EMamide-2, c) WBM + UltraLube II, d) WBM + EMamide-7, e) WBM + Amphiphile S, f) WBM + Amphiphile S-13, g) WBM + EvoLube G, and h) WBM + ¼ dosage EvoLube G.....	62
Figure 47: Micro-images of top rotating ball of a) water-based mud (WBM), b) WBM + EMamide-2, c) WBM + UltraLube II, d) WBM + EMamide-7, e) WBM + Amphiphile S, f) WBM + Amphiphile S-13, g) WBM + EvoLube G, and h) WBM + ¼ dosage EvoLube G.....	63
Figure 48: COF vs. wear radius	66
Figure 49: COF versus wear rate	67
Figure 50: Nominal contact pressure of interfaces at the end of testing.....	70
Figure 51: Surface profile of BF and BF + EMamide-2.....	74
Figure 52: Surface profile of OBM and OBM + EMamide-2	74
Figure 53: Surface profile of WBM and WBM + EvoLube-G 25% dosage	75

Figure 54: Mass spectrum of a) Escaid (BF), b) Escaid + EMamide-2, c) Escaid + Amphiphile S in carbon nanotube (CNT) structure	77
Figure 55: Mass spectrum of wear track surface on sample lubricated with Escaid	80
Figure 56: Mass spectrum of surfaces on sample lubricated by Escaid + EMamide-2	81
Figure 57: Mass spectrum of surfaces on sample lubricated by Escaid + Amphiphile S	82
Figure 58: Mass spectrum of surfaces on sample lubricated by WBM	86
Figure 59: Mass spectrum of surfaces on sample lubricated by WBM + EvoLube G	87
Figure 60: Falex Foue-Ball user interface	100
Figure 61: Falex Four-Ball setup before experiment.....	101
Figure 62: Falex Four-Ball setup during experiment.....	101
Figure 63: NI USB-6001 takes analog input from Falex Four-Ball tester.....	102
Figure 64: Analog inputs are in the form of negative and positive voltage.....	102
Figure 65. SIMS working principle	104
Figure 66. Cation and Anion usage for different target elements.....	104
Figure 67. Dynamic SIMS ion beam interaction	105
Figure 68. Static SIMS ion beam interaction.....	105
Figure 69: Master Chart of additional Four-Ball results.....	106
Figure 70: High-pressure tribometer (HPT) used for testing.....	108
Figure 71: Summary of load at seizure for different interfaces	109
Figure 72: Average failure load of interfaces	110
Figure 73: Average failure temperature of interfaces	110

LIST OF TABLES

	Page
Table 1: Relative comparison of WBM and OBM performance	11
Table 2: Modified ASTM D5183-05 [29] to resemble drilling condition	17
Table 3: Alloying Material of 52100 Alloy Steel [30].....	21
Table 4: Composition of OBM from field [33].....	23
Table 5: Solid composition of WBM [35]	25
Table 6: Tabulated COF, wear radius, and wear rate of interfaces.....	68
Table 7: Standard reduction potentials of species found in drilling system at 25°C[41]	71
Table 8: Testing matrix.....	109
Table 9: Summary of results	111

CHAPTER 1

INTRODUCTION AND LITERATURE REVIEW

1.1. Engineering Challenges in Non-Conventional Oil and Gas Exploration and Production

The depletion of conventional oil reserve has pushed oil and gas industry to develop non-conventional oil recovery techniques such as extended-reach drilling (ERD). ERD enables optimization of field development through the reduction of drilling sites and structures and provides access to otherwise unavailable reserves [1]. This is done by deep and directional drilling, including wells with tangent angles of up to 82° that pose engineering challenges such as extreme frictional torque and drag, and difficulty in hole-cleaning [2]. Frictional torque proportionally translates to the amount of energy needed in the drilling process, thus its reduction is desirable for cost saving. This can be achieved through friction reduction which depends heavily on mud lubricity and is one of the important technologies critical to the success of ERD [1]. Another way of reducing friction is to use low friction hardfacing material on tool joint surfaces where contact is most critical [3].

Different types of drilling fluid is used for different well conditions. The common types of drilling fluids used in field are oil-based mud (OBM) and water-based mud (WBM) each of which has its advantages and disadvantages against the other. OBM is usually used to drill wells that requires higher performance such as horizontal drilling. WBM is used in most drilling application due to its low cost and environmental friendliness. Another type of drilling fluid, synthetic-based mud (SBM), is used for wells requiring even higher performance with lower environmental impact than OBM.

The friction force from drag and torque of drilling mud can be reduced further using friction modifier (FM) additives. There are different types of FM such as organic friction modifiers (OFM), organo-molybdenum friction modifiers, nanoparticles, and functionalized polymers. This study will focus only on OFM due to their superior lubricating performance among the other types. Historically, OFMs were fatty acids which are corrosive to some bearing metal, and later replaced by amphiphiles such as amides, amines, and ester, or more complex organo-acid-based compounds that gave insoluble metal salts passivating layers [4, 5, 6, 7, 8, 9].

The chemical reaction occurring between lubricant/ environment and the surfaces under boundary condition is known as tribochemistry. However the precise nature of the reaction is not well understood [10]. Although the precise chemical structure of the additives used in this study are unknown, they are suspected to have predominantly linear alkyl chain with one or more functional head groups at one end [11]. The additives used in this study are selected based on a study of the effect of functional head group that reveals carboxylic acid and amine groups are generally more effective lubricants than alcohol, ester, nitrile or halide groups on ferrous substrates [12, 13, 14]. This study will focus on the effect of these amphiphilic OFMs on mud lubricity.

1.2. Application of Tribology in Upstream Sector

1.2.1 Friction and Lubrication

Friction is the resistance encountered when one body moves tangentially over another with which it is in contact [15]. Friction has no useful contribution to the overall operation and ultimately must be dissipated as waste heat. Thus every engineering application aims to keep these frictional force as small as possible to reduce energy consumption.

Based on Holmberg and Erdemir, ~23% (119 EJ) of the world's total energy consumption originates from tribological contacts. Of that 20% (103 EJ) is used to overcome friction and 3% (16 EJ) is used to remanufacture worn parts and spare equipment due to wear and wear-related failures. Improving friction performance will not only save cost, but also reduce consumption of resources and global CO₂ emissions [16].

In oil and gas drilling, friction comes in the form of torque and drag. The energy consumed by torque and drag may become much higher during drilling of deviated wells such as ERD leading to considerable operational problems and increased drilling costs. The torque of a drillstring is generally determined by three phenomena: the friction between the drill string/ pipe and the casing (cased hole), the friction between the drillstring and the borehole wall (open hole), and the drill bit [17].

This study will explore the effects of organic friction modifiers (OFM) on mud lubricity for a drill string and casing interface. The contact geometry of drill string and casing is modeled using a simplified journal bearing contact as shown in Figure 1 due to its geometrical similarity.

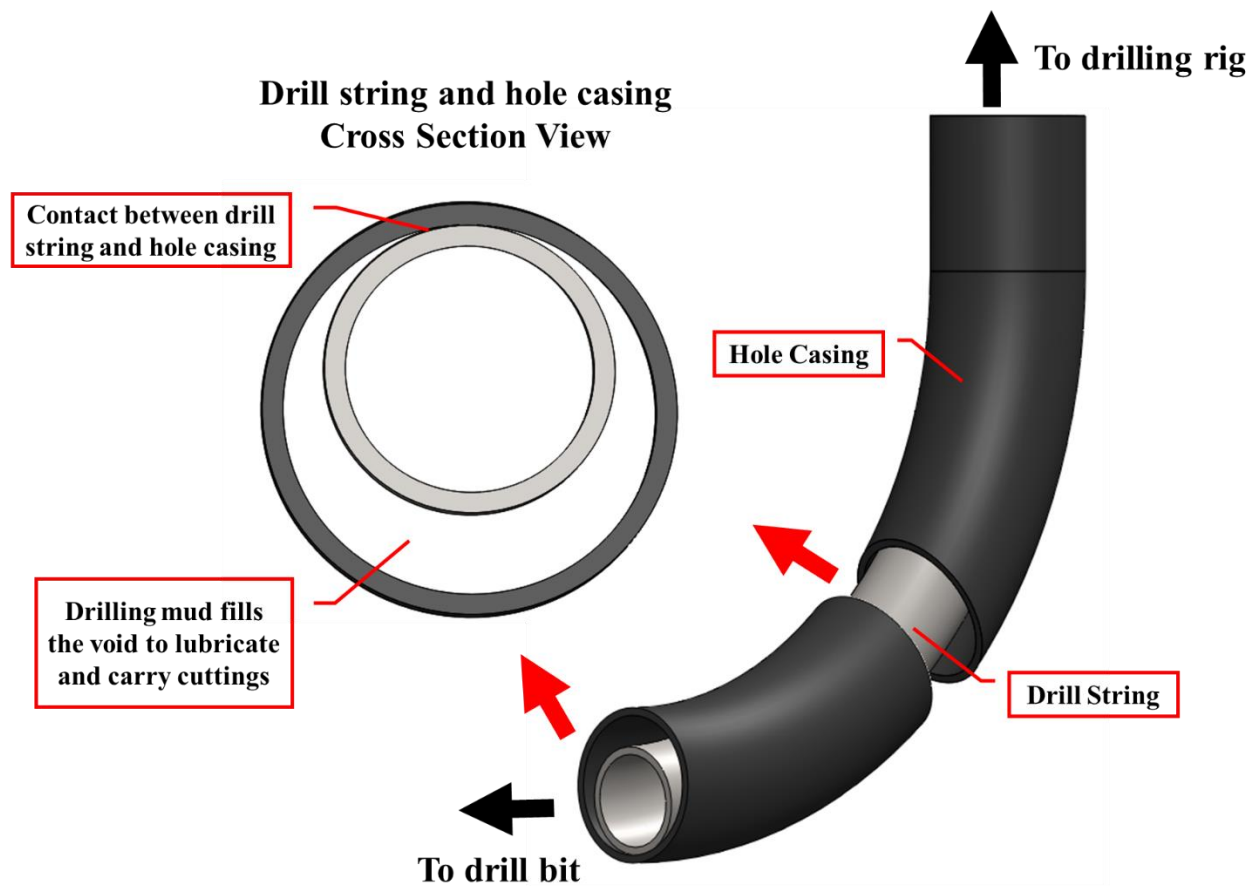


Figure 1: Curved drill string and hole-casing illustrating horizontal drilling

In an ideal lubrication scenario, lubricant will separate two contacting surfaces in the form of a lubricant film and load is supported fully by a lubricant film. This condition is known as hydrodynamic lubrication regime. At this lubrication condition, frictional force comes solely from shearing of hydrodynamic lubrication film also known as hydrodynamic drag. Parameters such as lubricant viscosity, sliding speed, and normal load will determine the drag/ friction force. Coefficient of friction (COF) of hydrodynamic lubrication is given by Equation 1 shown below.

$$\mu = \frac{F}{W} = \frac{7}{2\sqrt{2}} \sqrt{\frac{L U \eta}{W}} \quad \text{Equation 1}$$

Where,

μ = Coefficient of friction

F = Tangential friction force

W = Normal force

L = Length of contact

U = Relative sliding speed

η = Dynamic viscosity

Based on this equation, an increase of loading, or decrease in speed, the COF will drop. However there is a limitation to the COF decrease. At some point when speed is insufficient or load is too high, the lubrication film cannot be formed and COF increases rapidly due to solid-to-solid contact of surface asperities. At this condition, lubrication is known as boundary lubrication regime and load is mainly supported by asperities contact. Between these two lubrication regimes, there is mixed lubrication, where solid-to-solid contact and hydrodynamic film thickness is optimal resulting in a very low COF. The different regimes are illustrated in Figure 2 which is also known as Stribeck Curve attributed to Richard Stribeck and Mayo D. Hersey [18].

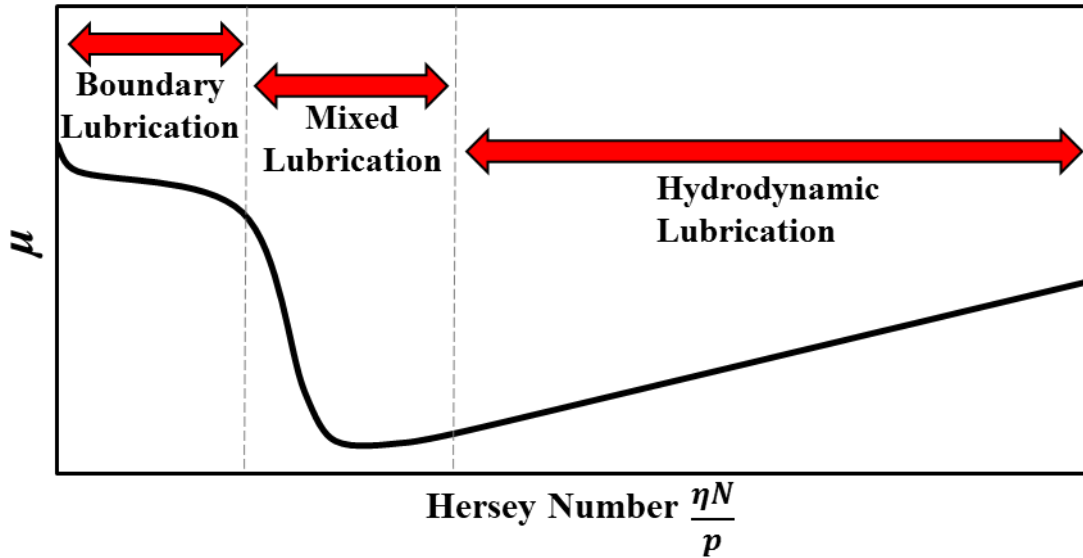


Figure 2: Schematic of Stribeck curve

The Stribeck curve separates lubrication into three regimes such as hydrodynamic lubrication, mixed lubrication, and boundary lubrication. The Stribeck curve shows the relationship between Hersey number with COF. Thus with this number, the resulting lubrication regime and COF can be predicted. The Hersey number is defined as shown in Equation 2 below.

$$\text{Hersey number} = \frac{\eta N}{P} \quad \text{Equation 2}$$

Where,

η = Dynamic viscosity

N = Entrainment speed of fluid

W = Normal force

The types of contacts under different lubrication regimes is illustrated in Figure 3 below.

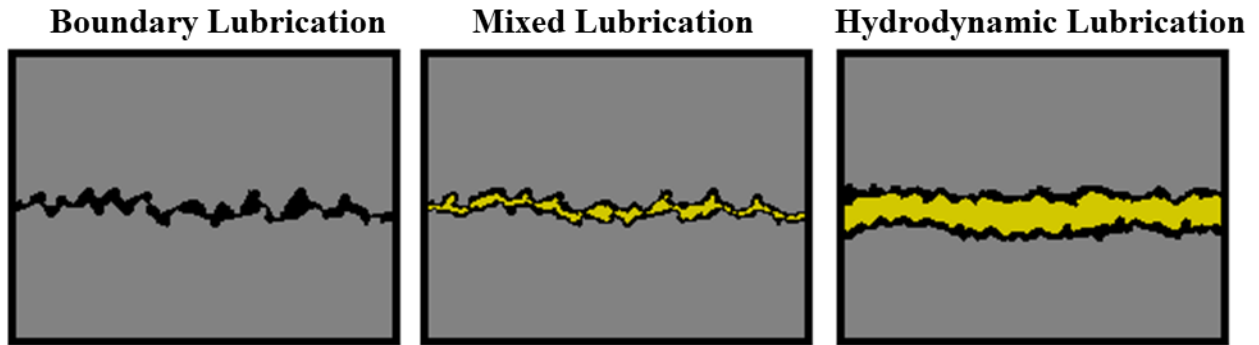


Figure 3: Schematics of solid surfaces under different lubrication regimes. Not to scale

This study will focus on the reduction of COF of a boundary lubrication regime. One possible solution is by using friction modifier (FM) additives that will reduce the COF by creating a separation between solid-to-solid contact depending on the type of FM used. Specifically, this study compares the performances of different organic friction modifiers that are known to chemically react with certain drill string materials creating protective surface films that reduces the COF in boundary lubrication.

1.2.2. Wear

Wear is progressive damage, involving material loss, which occurs on the surface of a component as a result of its motion relative to the adjacent working parts. The economic consequences of wear are widespread and pervasive, including not only the cost of replacement parts, but also the expenses involved in turnaround, lost production, the consequent loss of business opportunities, and chain processes associated to wear that lead to reduced machine performance and increased energy consumption [19]. Compared to friction, wear appears to be more critical as it may result in catastrophic failures and operational breakdowns that can adversely impact productivity and hence cost. [16]

JA Williams classified the mechanism of wear into seven types such as seizure, melt wear, oxidation dominated wear, mechanical wear, fatigue wear, fretting and corrosion wear, and erosive wear [19].

1. Seizure: When metal surfaces are brought into contact the real area over which they touch is a comparatively small fraction of the nominal contact area. The high normal pressures generated at these asperity contacts forge metallic junctions which, when they are sheared by the application of a load tangential to the interface can grow until the actual area of metallic contact approaches the nominal area and seizure happens.
2. Melt wear: Localized melting of the uppermost layer of the wearing solid due to high speed or high pressure that produces heat.
3. Oxidation-dominated wear: When dry surfaces slide at higher speed, heat generates flash temperature sufficient to cause oxidation when oxidizing agent such as oxygen is present. Oxide film may spall from the surface exposing more metal which rapidly oxidize again.
4. Mechanical wear: When surface heating is negligible, the effect of the frictional force is principally to deform the metal surface, shearing it in the sliding direction and ultimately causing the removal of material, usually in the form of small particles of wear debris. Mechanical wear behavior often follows the Archard equation which asserts that wear rate (w) is directly proportional to the load (W) on the contact, but inversely proportional to the surface hardness (H) of the wearing material given by Equation 3 shown below.

$$w = K \frac{W}{H} \quad \text{Equation 3}$$

Mechanical wear is then classified into different processes such as:

- Running in: process that improves conformity, topography, and frictional compatibility, also known as breaking-in wear
 - Adhesive wear: When touching asperities adhere together and plastic shearing of the junctions detach the tips of the softer asperities leaving them adhering to the harder surface. Then these tips can become detached and wear builds up. Severe damage of this type may cause tearing of macroscopic chunks of material from the surface known as galling which is a particular problem when the tribological contacts are made of the same materials. In another case called scuffing, lubricant film breaks down and fails, leading to adhesive wear.
 - Abrasive wear: When damage of a surface is caused by relative motion to that surface of either harder asperities or hard particles trapped at the interface. Hard particles may be introduced by contaminants from outside particles or formed by oxidation of the worn particles itself. If wear depends on free particles, the situation is known as three-body abrasion; if the wear-producing agent is the hard counterface itself, it is called two-body abrasion. Abrasive wear gives a characteristic surface topography consisting of long parallel grooves running in the rubbing direction caused by ploughing of material. Industrial surveys show that abrasive wear accounts for up to about 50% of wear problems. Abrasive wear is also what is mostly seen on samples tested in this study.
 - Delamination wear: When material is lost in the form of thin flakes or platelets it is called delamination wear. This wear is often seen in coated tribological pairs.
5. Fatigue wear in rolling contact: When there is little to no slip at the interface, there is no adhesive, abrasive, or oxidative wear. However, material may still spall from the surface

after long operation. This wear generates a characteristic pitted surface caused by fatigue induced subsurface crack propagation.

6. Fretting and corrosion wear: When two surfaces have a relative oscillatory motion of small amplitude, fretting can occur. The characteristic of fretting contact is formation of metal oxide wear particle with hardness depending the metal itself. Abrasive and adhesive wear can also be induced by fretting wear.
7. Erosive wear: When material is removed by the impingement of particles on the surface, it is called erosive wear. The particles do not have to be solid. The effect of impact angle on rates of erosion have been studied on ductile metal and brittle solids. The study shows that for ductile materials, material is removed by ploughing during impact, while in brittle solids wear is induced by formation and intersections of cracks.

1.3. Drilling Mud

Drilling mud is a type of lubricating fluid used in oil and gas drilling exploration. It is also known as drilling fluid (DF) and is a colloidal suspension made by mixing base fluid (BF), additives, weighting agent such as bentonite clay, and lost-circulation prevention materials (LCM).

Some of the main functions of drilling fluids are:

1. Carry cuttings from the hole and permit their separation at the surface.
2. Cool and clean the bit.
3. Reduce friction between the drill pipe and wellbore or casing.
4. Maintain the stability of the wellbore.
5. Prevent the inflow of fluids from the wellbore.
6. Form a thin, low-permeable filter cake.

7. Be non-damaging to the producing formation.
8. Be non-hazardous to the environment and personnel [20, 21].

At any time in the process of drilling a well, one or more of these functions may take precedence over the others. In the case of extended-reach and horizontal drilling, hole cleaning and maintaining wellbore integrity are generally considered the most important [22]. Additionally, there are various types of drilling fluids (DF) such as water-based mud (WBM), oil-based mud (OBM), drill-in fluids, and synthetic-based mud (SBM) which are all designed and used for specific well conditions. Table 1 shows some of the technical performance comparison between WBM and OBM.

Table 1: Relative comparison of WBM and OBM performance

Technical Criteria	WBM	OBM
Heat reduction during operation	Good	Bad
Friction	Bad	Good
Wear	Bad	Good
Protection to corrosion and biological growth	Bad	Good
Flammability & environmental friendliness	Good	Bad
Cost	Low	High

The three key factors that drive the decision about which type of DF is selected for a specific well are cost, technical performance, and environmental impact [23]. Among the different types, SBM is known to have excellent lubricity, non-polluting, and minimally toxic making it

preferable than OBM for ERD [24]. The performance of the DF can then be improved further to meet different criteria using lubricant additives. One ideal scenario is to improve technical performance of WBM where it is lacking, such as friction, wear, and corrosion protection, without impairing its low cost, environmental friendliness, and excellent heat reducing properties.

1.4. Lubricant Additives

Lubricant additives come with a broad variety of different functions. The three common types are surface protective additive, performance improver additive, and lubricant protective additives. The roles of these lubricant additives are (1) to enhance existing base oil properties with antioxidants, corrosion inhibitors, anti-foam agents, and demulsifying agents, (2) to suppress undesirable base oil properties with pour-point depressants, and viscosity index (VI) improvers, (3) to impart new properties to base oils with extreme pressure (EP) additives, detergents, friction modifier (FM), and anti-wear (AW) [25]. Figure 4 shows a breakdown of lubricant additive types and their functions. In improving technical performance of drilling mud, FM additives are especially important in reducing friction and wear, and are classified to four variants such as:

1. Organic Friction Modifier (OFM)
2. Organo-Molybdenum Friction Modifier
3. Functionalized Polymer
4. Nanoparticle Friction Modifier

Each of these FM types provide lubrication in different ways. OFM generates a passive lubrication film also known as tribochemical film while nanoparticle friction modifier, functionalized polymer, and organo-molybdenum friction modifier acts as molecular bearing and

may also be adsorbed on the interacting surface as protective film [11]. OFM may also bind with lubricating fluid suspending it as part of the tribochemical film. The focus of this thesis is to understand the lubricating mechanism of some of these FMs especially OFM and their limitation in friction and wear reduction as well as to recommend incorporation of higher performances additives such as extreme pressure additives.

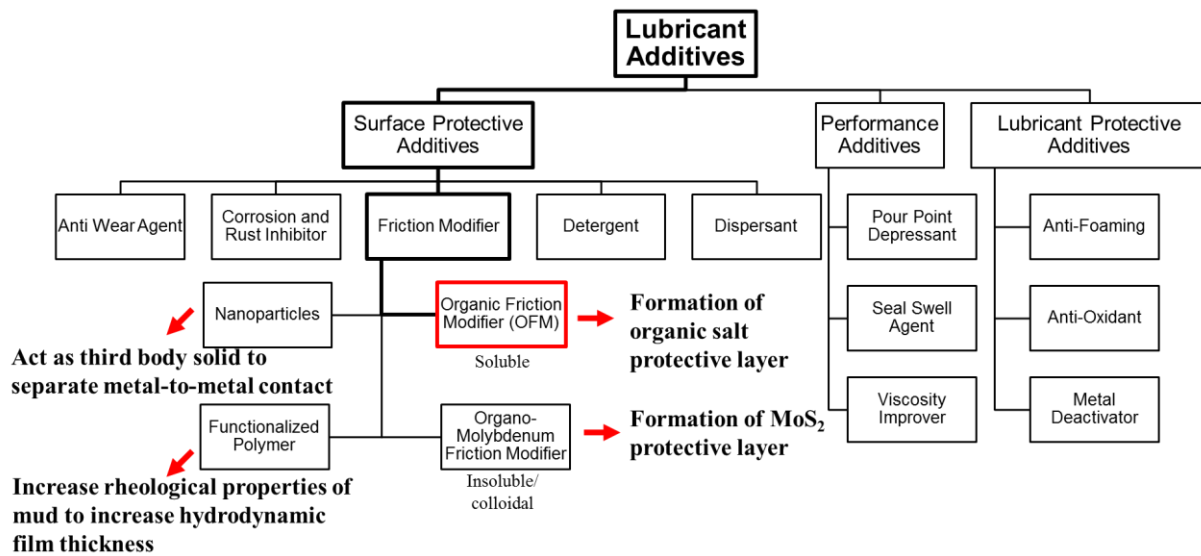


Figure 4: Lubricant additives breakdown [11][25]

Additionally, additives such as OFM may have different levels of polarity depending on where it is derived, as shown in Figure 5. In oil and gas drilling applications, this information is very important to determine whether or not an additive is compatible with the types of drilling fluid used. As an example drawn from Figure 5, OFM sourced from an amide is more compatible in water-based lubricants due to its similarity in polarity compared to haloalkanes/ alkyl halides. However, it is also important to note that most amides, carboxylic acids, and amines are amphiphilic in nature which means that they have both lipophilic (“fat loving”) and hydrophilic (“water-loving”) characteristics that will allow them to bind with both polar and non-polar

molecules [26]. This important information should be considered especially when choosing the additives for certain lubricant types.

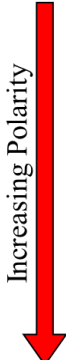
Relative Polarity	Compound Formula	Group	Representative Solvent Compounds
Nonpolar	R – H	Alkanes	Petroleum ethers, ligroin, hexanes
	Ar – H	Aromatics	Toluene, benzene
	R – O – R	Ethers	Diethyl ether
	R – X	Alkyl Halides	Tetrachloromethane
	R – COOR	Esters	Ethyl acetate
	R – CO – R	Aldehydes and ketones	Acetone, ketone
	R – NH ₂	Amines	Triethylamine
	R – OH	Alcohols	Methanol, isopropanol
	R – COHN ₂	Amides	Dimethylformamide
	R – COOH	Carboxylic acids	Propanoic acid
	Polar	H – OH	Water

Figure 5: Solvent class vs polarity [27]

1.5. Thesis Flowchart

This study will discuss a tribological approach to improve the technical performance of drilling fluids used in non-conventional oil and gas recovery techniques such as ERD. It is desirable for the oil and gas industry to minimize energy consumption and downtime while lowering environmental damage during exploration and production (E&P). One way to achieve increased drilling fluid performance is using organic friction modifier (OFM) additives to alter friction and wear of the interfaces in drilling such as drill string and hole-casing as shown on Figure 1.

Tribological improvements of a selection of OFMs mixture in oil-based and water-based drilling fluids are tested using a Four-ball Friction and Wear Machine as discussed in Chapter 3.

Coefficient of friction and wear are qualitatively and quantitatively analyzed to determine the best performing OFM. In Chapter 4, the tribological interfaces tested are chemically

characterized to determine the tribochemical reaction in the boundary lubrication that plays a key role in friction and wear reduction of both oil-based and water-based drilling fluid. The flowchart of the thesis is depicted in Figure 6.

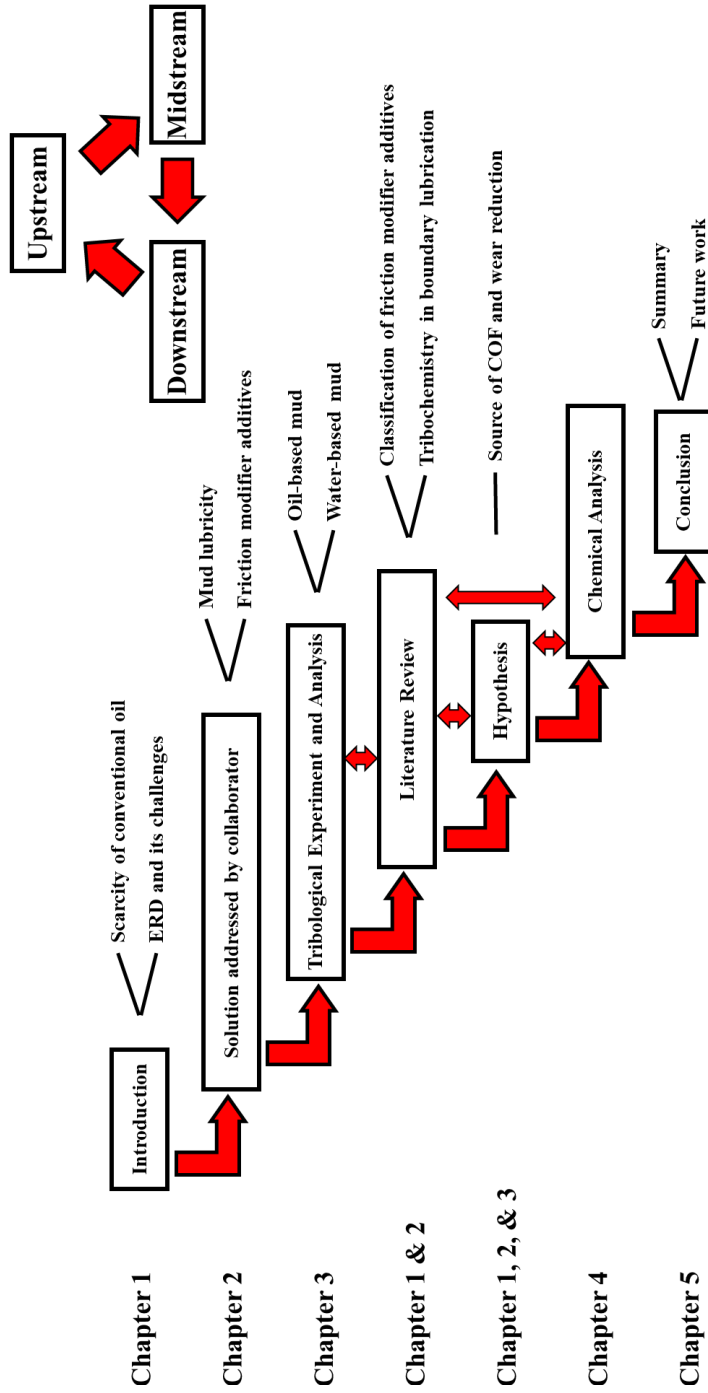


Figure 6: Thesis flowchart

CHAPTER 2

EXPERIMENTAL SETUP AND MATERIALS

2.1. Equipment and Experimental Procedure

2.1.1. Falex Four-Ball Machine

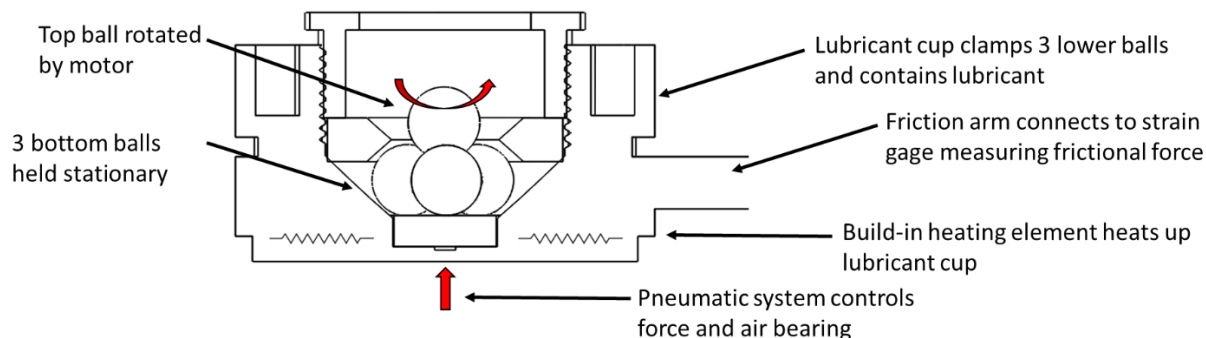


Figure 7: Four-ball schematic

A Falex 4 Ball friction and wear test machine is used to study the tribological performance of drilling fluids and selection of friction modifiers. The schematic of the setup is shown in Figure 7. The bottom stationary balls are clamped inside a heating cup filled with lubricant, while the top ball is held by a collet that is rotated by a motor. A pneumatic loading system pushes the lubricant cup up exerting the load against the top ball. The frictional force between the top and bottom balls exerts a torque to the lubricant cup forcing it to spin. An air bearing under the lubricant reservoir allows it to spin while its friction arm that connects to a strain gage restrains it from spinning, thus the resulting frictional force is measured. Details of the hardware user interface is shown in Appendix A.

ASTM D2783-03 [28] standard is used for testing the lubricant performance and is slightly modified to resemble boundary lubrication conditions between the drill string with casing in oil and gas drilling process, shown in Table 2.

Table 2: Modified ASTM D5183-05 [29] to resemble drilling condition

Test Parameters	Setting
Load	15 ± 0.2 kg
Speed	400 ± 10 rpm
Temperature	75 ± 2 °C
Duration	15, 30, 60 minutes

The friction data is automatically collected with a National Instrument USB-6003 multifunction DAQ. A LabVIEW script is written to acquire the voltage output of the DAQ hardware. The voltage can be converted to friction load in units of grams by multiplying the output with a conversion factor of 500. The user interface program and the LabVIEW block diagram script are shown in Figure 8 and Figure 9 below. Details of DAQ wiring is discussed in Appendix B.

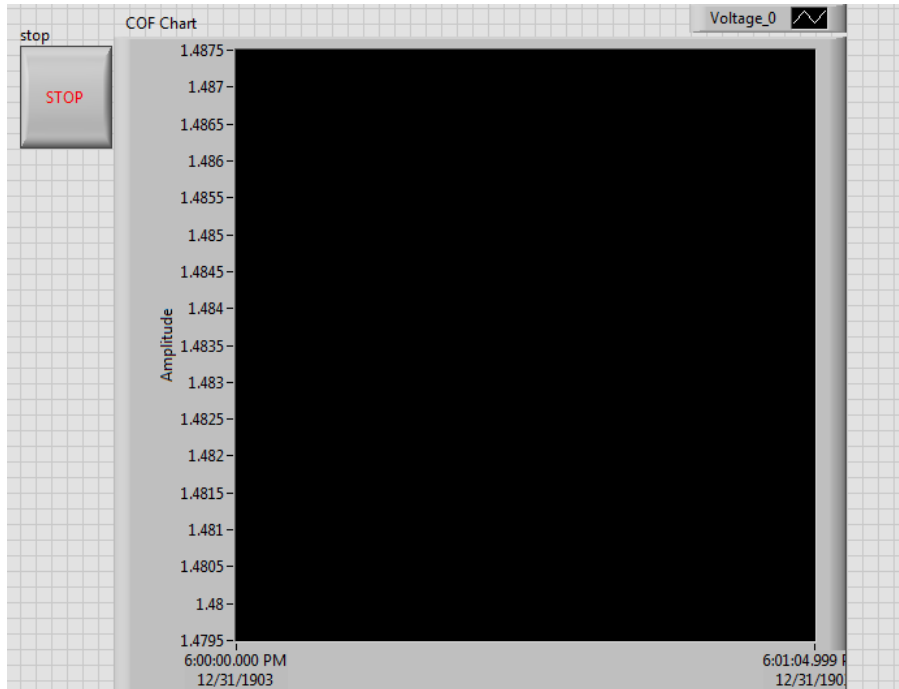


Figure 8: Four-ball data acquisition NI LabVIEW user interface

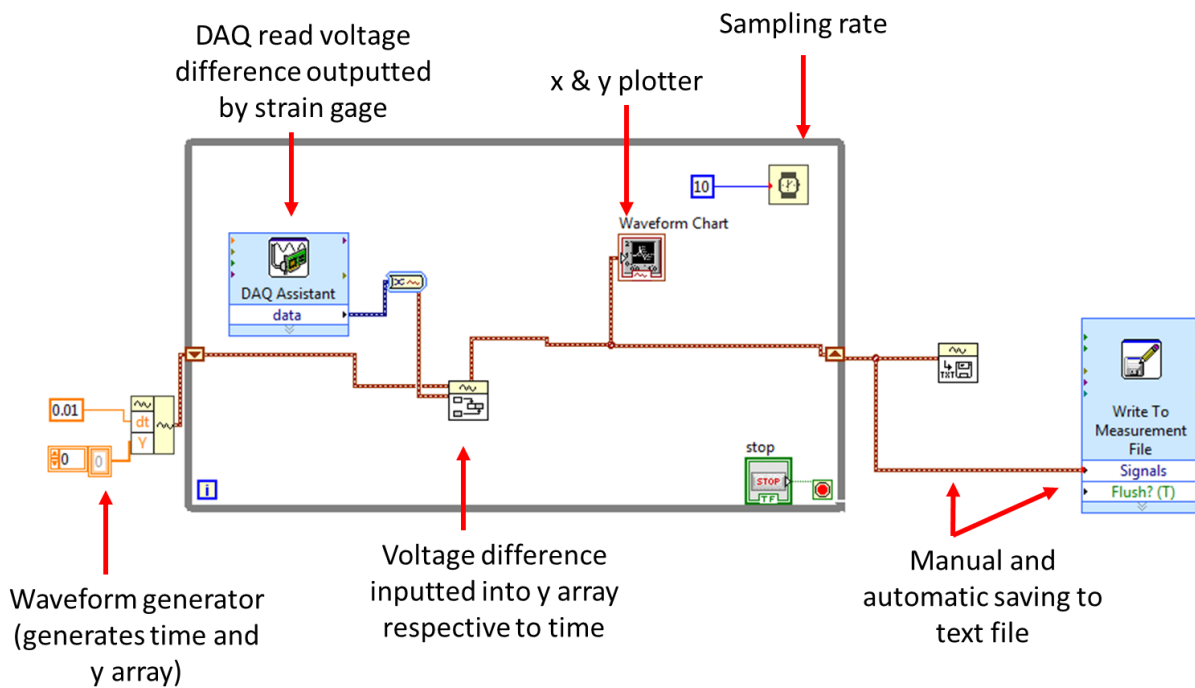


Figure 9: Four-ball tester data acquisition block diagram

2.1.2. Surface Analysis

Imaging

A VHX-600 Digital Microscope from Texas A&M Mechanical Engineering Shared Facility as shown in Figure 10 below is used to measure microimages of the tested samples. Microimages are useful to qualitatively and quantitatively analyze the wear characteristics such as measuring wear volume and detecting corrosion and wear types that determine the tribological performance of the interfaces.



Figure 10: VHX-600 Digital microscope

Surface Profile

KLA-Tencor P-6 Stylus Profiler located at the Texas A&M Mechanical Engineering Shared Facility as shown in Figure 11 is used to analyze the surface profile of the tested samples. These data will provide information such as depth and shape of wear that will be useful in calculating wear rate and determining the tribological performance of the interfaces.



Figure 11: KLA-Tencor P-6 Stylus Profiler

2.2. Materials

2.2.1. SAE 52100 Alloy Steel Balls

52100 alloy steel ball samples are chosen for their high iron content and low cost to resemble drilling tools material that is typically made of various stainless steel or aluminum alloys based on specific applications. Detailed composition of the material is depicted in Table 3. It is available for purchase from third party suppliers.

Table 3: Alloying Material of 52100 Alloy Steel [³⁰]

Composition	Weight %	Composition	Weight %	Composition	Weight %
Aluminum	0-0.050	Copper	0-0.30	Oxygen	0-0.0015
Iron	95.75- 97.37	Manganese	0.25-0.45	Phosphorus	0.025 Max.
Carbon	0.93-1.10	Molybdenum	0-0.10	Silicon	0.15-0.35
Chromium	1.30-1.60	Nickel	0-0.25	Sulfur	0.25 Max.

2.2.2. Escaid/ Base Fluid (BF)

Escaid 110TM, low viscosity Group III is a hydrocarbon derived base fluid with low aromatics/ environmental toxicity, used as base stock for drilling fluids in deep water or extended reach applications. It can also be referred as petroleum distillates (hydrotreated light) or base fluid (BF) and will be mixed with other ingredients to make drilling fluid with specific properties depending on the well/ application. Physical appearance of Escaid is shown in Figure 12.

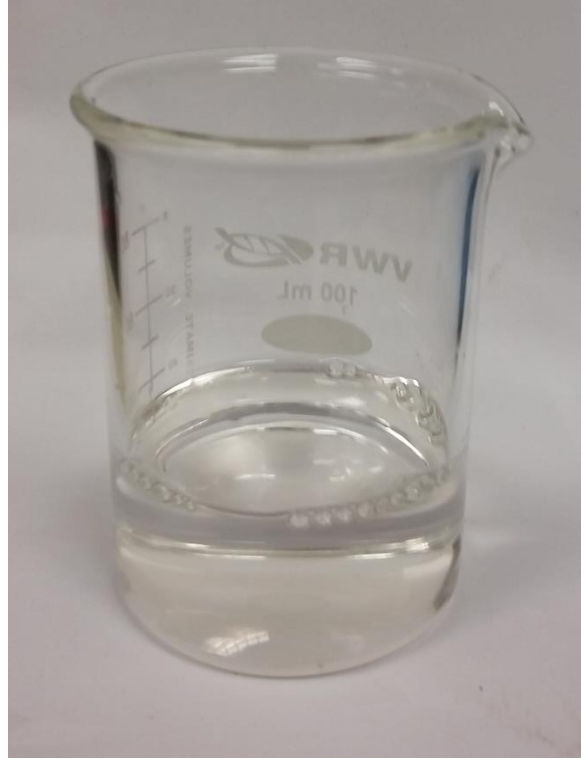


Figure 12: Escald as base fluid (BF) of oil-based mud (OBM)

2.2.3. Oil-based Mud (OBM)/ Oil-based Drilling Fluid

Oil-based Mud (OBM) as actual drilling fluid obtained from the field. Composition is shown in Table 4. OBM is usually formulated in many ways to meet specific drilling requirements for unique well conditions. The complete functions of OBM are to remove cutting from well, suspend and release cuttings, control formation pressures, seal permeable formations, maintain wellbore stability, minimize formation damage, cool, lubricate, and support the bit and drilling assembly, transmit hydraulic energy to tools and bit, ensure adequate formation evaluation, control corrosion, facilitate cementing and completion, and minimize impact on environment [31]. Barite, a mineral containing barium sulfate, is used as weighting agent that will help transport cutting debris out of the borehole to the surface when mixed with base fluid (BF). BF can be either water, brine, oil, or synthetic based fluid that suspends solid compositions,

lubricates, and cools the drilling tool. Calcium Carbonate, also known as chalk, is used as weighting agent and bridging material to reduce fluid loss by forming impermeable barrier across formation interfaces. Emulsification of calcium carbonate brine in oil-base or synthetic-base mud provides osmotic wellbore stability while drilling water-sensitive shale zones [32]. While silica, crystalline, quartz, and mica are used to simulate drill cuttings. Physical appearance of OBM is shown in Figure 13.

Table 4: Composition of OBM from field [33]

Composition	Weight %
Barite	30 – 60
Petroleum Distillates, Base Fluid (BF)	10 – 30
Calcium Carbonate	5 – 10
Calcium Chloride	1 – 5
Silica, Crystalline, quartz	1 – 5
Mica	1 – 5

Note: Exact composition varies depending on the well/ application

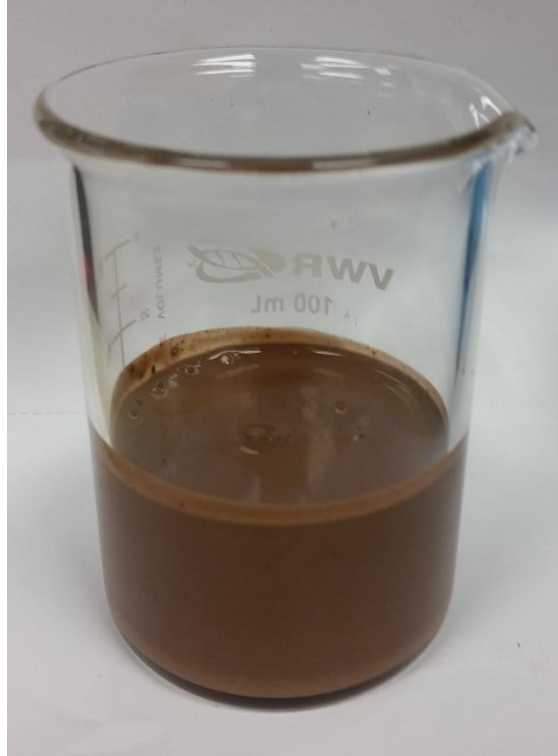


Figure 13: Oil-based mud (OBM) also known as drilling fluid (DF)

2.2.4. Water-based Mud (WBM)/ Water-based Drilling Fluid

KCl Polymer Water-Based Drilling Fluid System is environmentally appropriate alternative to synthetic-based systems to provide high penetration rates, lubricity, wellbore inhibition, and production zone protection. This high-performance water-based drilling fluid system achieves wellbore stabilization and other performance capabilities. Composition as shown in Table 5.

Barium sulfate and limestone/ barite are used to increase viscosity of the drilling mud. Bentonite is used in drilling fluids to lubricate and cool the cutting tools, to remove cuttings, and to help prevent blowouts [34]. Potassium Chloride will dissolve in water phase where its K^+ ions attach to clay surfaces and lend stability to shale formation that is exposed to drilling fluids by the bit.

The ions also help hold the cuttings together, minimizing dispersion into finer particles. [32].

Sodium Hydroxide commonly known as caustic soda is used in most water-base muds to

increase and maintain pH and alkalinity [32]. Kaolin, a material commonly found in clay composition is used to improve flow properties and density of drilling mud [14]. Sodium Carbonate also known as soda ash at the drilling rig is used to treat most types of calcium ion contamination in freshwater and seawater muds such as calcium ions contamination from drilling gypsum or anhydrite, CaSO_4 , causing clay flocculation and polymer precipitation and lower pH [32]. Quartz is found as drill cuttings. Additionally, WBM contains non-solid compositions with unknown concentration such as 2- Ethylhexanol, petroleum distillates (hydrotreated light), ester alcohol, and water.

The main fundamental difference of WBM with OBM are low cost and low environmental damage as discussed in Table 1. Water-based mud is not distinguishable with OBM as shown in Figure 13.

Table 5: Solid composition of WBM [35]

WBM Composition	Weight %
Barium sulfate	15 – 40
Potassium Chloride	15 – 40
Bentonite	1 – 5
Limestone	1 – 5
Kaolin	1 – 5
Sodium Hydroxide	1 – 5
Quartz	1 – 5
Sodium Carbonate	1 – 5

Note: Exact composition varies depending on the well/ application

2.2.5. Friction Modifier Additives

These Organic Friction Modifier (OFM) additives are selected by ExxonMobil Chemicals. Physical appearance of each additives are shown on Figure 14. Although the detail chemical composition of these additives are unknown, most of their functional head groups are known. For instance, EMamide and UltraLube additives are amide based, but amide itself have three varieties, while EvoLube-G has propanoic acid which is a fatty acid. A simple amide weights 44 amu (atomic mass unit), an amide group weights 42 amu, a substituted amide weights 43 amu, and a fatty acid carboxylic head group weights 45 amu. Structure of the head groups are shown in Figure 15. C represents carbon, O represents oxygen, N represents nitrogen, H represents hydrogen, and R represents longer chain C-H organics. These information are especially useful for chemical characterization that will be done in Chapter 4.

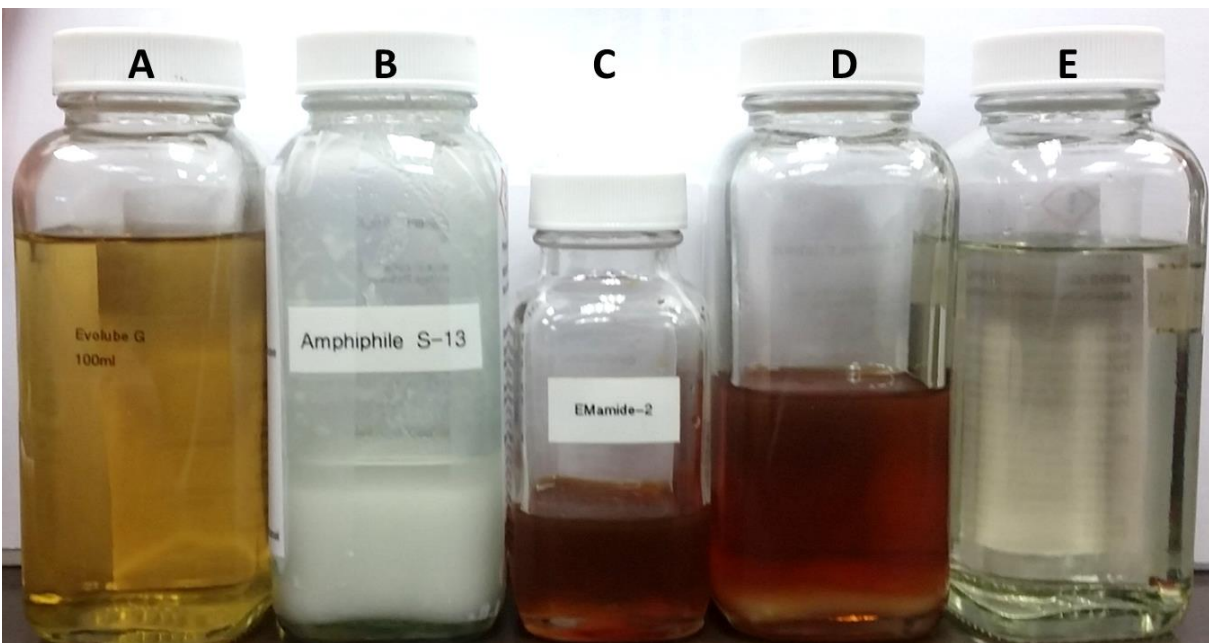


Figure 14: Physical appearance of additives. A) EvoLube-G, B) Amphiphile S-13, C) EMamide-2, D) UltraLube II, E) Amphiphile S

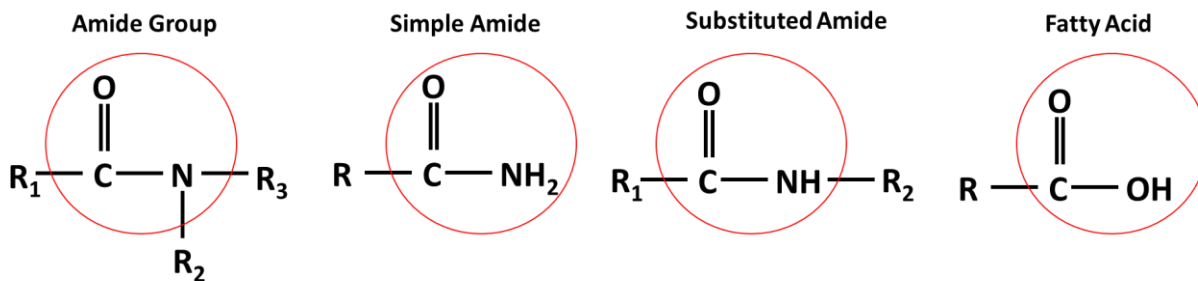


Figure 15: Chemical structure of amide group, simple amide, substituted amide, and carboxylic acid [³⁶]

EMamide-2 and EMamide-7

Experimental Organic friction modifier (OFM) with amide head group that is dark yellow transparent gel (EMamide-2) or liquid (EMamide-7) in room temperature, soluble in synthetic-based fluids. Exact chemical composition dosage is not disclosed. Provided by ExxonMobil Chemicals.

Amphiphile S and Amphiphile S-13

Experimental Amphiphilic Organic friction modifier (OFM) that is yellow transparent liquid in room temperature, soluble in synthetic-based fluids. Exact chemical composition dosage is not disclosed. Provided by ExxonMobil Chemicals.

UltraLube II [³⁷]

Commercial FM consist of mixture of amides and petroleum naphtha Organic friction Modifier (OFM) that is clear brown liquid specifically developed for highly deviated or horizontal drilling applications for both land and offshore use, has a high affinity for metal surfaces, will adhere tenaciously to drill pipe and drill collars, eliminates torque and drag, prevents differential

sticking, and protects the drill pipe from corrosion. UltraLube II is environmentally safe, non-flammable, and does not produce a sheen. Chemical compositions and dosage as recommended by vendor can be found on their website or specification sheet.

EvoLube G [38]

Commercial FM of Organic friction modifier (OFM) with carboxyl head group (fatty acid) that is yellow to dark amber liquid ideal for high-temperature applications due to its greater than 400°F (204°C) thermal stability. It can be used in any type of water-based drilling fluid, effective when used in systems formulated with low clay content or in clay-free formulations. Composed of petroleum distillates and hydrotreated light and 2,2,4-trimethylpentane-1,3 diol monoisobutyrate (propanoic acid). Propanoic acid has a chemical structure as shown on Figure 16, and has a molecular weight of ~74 amu. Recommended dosage is 0.5 – 6 wt % of the total mud system.

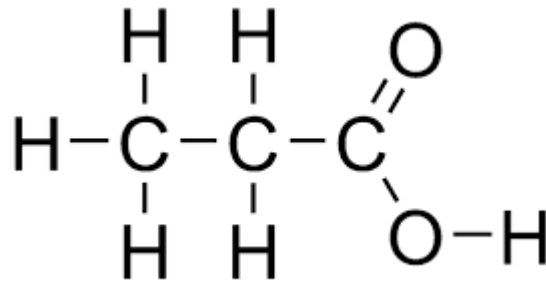


Figure 16: Chemical structure of propanoic acid

2.3. Tribological and Tribochemical Analysis

2.3.1. Coefficient of Friction

The coefficient of friction (COF) is calculated using applied load (F), torsional arm length of Four-ball machine (l), and measured frictional force (f) given by ASTM D5183-05 as shown in

Equation 4) [29]. The constant 0.0023 is used to account for dimensional changes and angular factors. Applied normal load is held constant at 15 kg and the torsional arm length at 7.6 cm.

$$\mu = 0.0023 f l / P \quad \text{Equation 4}$$

Where

f = friction force (g)

l = torsional arm length (cm)

P = applied load (kg)

Data is collected with a National Instrument data acquisition (DAQ) board with a frequency of 100 Hz for the duration of the four-ball test. Then COF is calculated using Equation 4. Then, individual averaged COF and COF standard deviation are calculated using the data from the last portion of the experiment, approximately 30 minutes after the test started. By doing this, no running in COF is accounted for. Total average COF is calculated by averaging the three repetitive tests. Total standard deviation is calculated by taking root mean square of all three repetitive experiments' COF standard deviation.

2.3.2. Hertzian Contact Stress for Sphere-on-Sphere Contact [39]

Calculation of Hertzian contact stress for sphere on sphere point contact is shown in Equation 5 below. Hertzian contact stress is used to determine the maximum stress on the surface.

$$p_0 = \frac{1}{\pi} \left(\frac{6FE^{*2}}{R^2} \right)^{1/3} \quad \text{Equation 5}$$

$$\frac{1}{E^*} = \frac{1 - \nu_1^2}{E_1} + \frac{1 - \nu_2^2}{E_2} \quad \text{Equation 6}$$

$$\frac{1}{R^*} = \frac{1}{R_1} + \frac{1}{R_2} \quad \text{Equation 7}$$

Where,

p_0 = Contact pressure

E^* = effective modulus of elasticity

$\nu_{1,2}$ = Poisson's ratio of sphere 1, 2

F = applied force

R^* = effective radius of sphere

$R_{1,2}$ = radius of sphere 1, 2

2.3.3. Nominal Contact Pressure

The calculation of the nominal contact pressure is shown in Equation 8. Contact pressure is used to determine the maximum pressure that each surface can bear after a tribological experiment.

The experiment is useful to compare the strength of each interface. Contact pressure is calculated by dividing the applied force by surface area of wear on tested sample.

$$p_0 = \frac{F}{A} \quad \text{Equation 8}$$

Where,

p_0 = Contact pressure (Pa)

F = applied force (N)

A = Surface area under contact (m²)

2.3.4. Wear

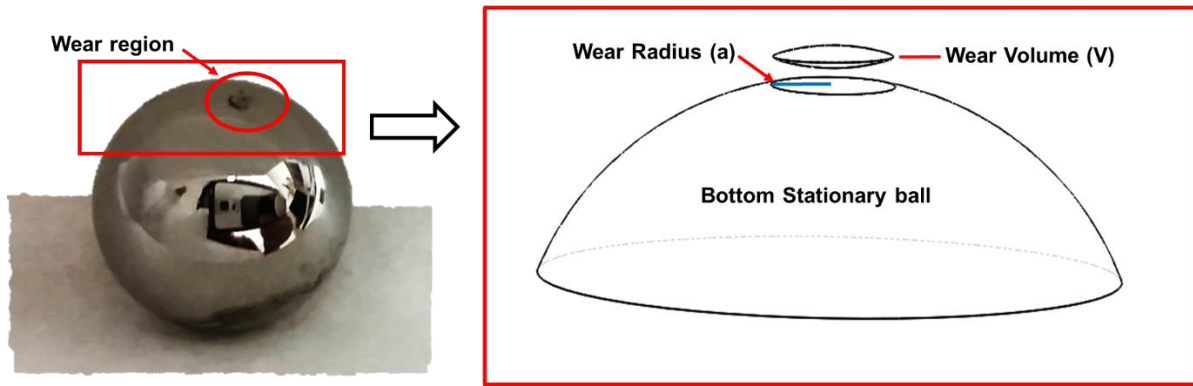


Figure 17: Dome shaped wear on bottom stationary ball

The wear rate was calculated by dividing the averaged wear volume (V) with sliding distance (L) and load (P) as shown in Equation 9. Averaged wear volumes were obtained by averaging double dome shaped wear volume of three stationary balls as shown in Figure 17. Images of balls that represents different additives are also shown in Figure 26, Figure 34, and Figure 46. Equation 10 and Equation 11 are used to calculate the wear volume using the measured wear radius (a) and surface profiling. r is the radius of the steel ball specimen and d is the height of the dome-shaped wear volume.

$$w = \frac{V}{P * L} \quad \text{Equation 9}$$

$$V = \frac{2}{3} \pi d^2 (3r - d) \quad \text{Equation 10}$$

$$d = -\frac{a}{\tan\left(\sin^{-1}\frac{a}{r}\right)} + r \quad \text{Equation 11}$$

Where,

w = Wear rate (m^3/Nm)

V = Wear volume (m^3)

L = Sliding distance (m)

W = Normal force (N)

a = Wear radius (m)

r = Steel ball radius (m)

d = Height of dome shaped wear (m)

2.3.5. Secondary Ion Mass Spectroscopy [⁴⁰]

In this study, the main technique used to analyze the involvement of friction modifier on boundary lubricated surface friction and wear reduction is Secondary Ion Mass Spectrometry (SIMS). SIMS is a characterization technique using the ion beam as the source of energy. In a very simplified manner, primary ion beam is accelerated and bombarded on the target surface. The impact of the primary ion beams with the target sample will ionize the target sample which is then amplified and sorted with a mass analyzer. There are two kinds of SIMS, dynamic and static SIMS. Dynamics SIMS uses higher energy level and is usually used to analyze the bulk element and isotopes of a target sample. Static SIMS uses lower energy and is typically used for analysis of atomic monolayer on material surface to obtain information about molecular species on material surfaces. A detailed SIMS methodology is discussed in Appendix C.

In this study, a Time-of-Flight (ToF) static SIMS is used to analyze the tribochemical process and trace molecules of passive tribochemical layers formed during the tribological processes. In a more detailed manner, a custom-built cluster Time-of-Flight Secondary Ion Mass Spectroscopy (ToF SIMS) equipped with ion source of 50 keV C_{60}^{2+} projectiles is used for (1) determining the chemical composition of lubricant/ additive mixtures as well as for (2) anion analysis of the surfaces of steel balls used in Four-Ball test at 2 areas: a) surface on wear track (Area 1 shown in

Figure 18), and b) area out of contact (Area 2 shown in Figure 18). The specimens are first rinsed with isopropanol and air dried to provide uncontaminated analysis of surface after lubrication.

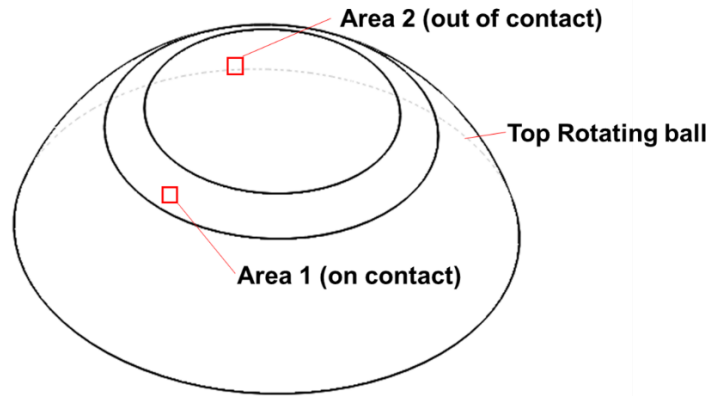


Figure 18: Partial view of top (rotating) ball analyzed with ToF SIMS

This method allows the acquisition of individual mass-spectra corresponding to single projectile impacts (surface emission area $\sim 100 \text{ nm}^2$, depth of emission $< 5 \text{ nm}$), and sorting them by selecting different ion co-emission events. The sum of individual mass spectra over $100 \times 100 \text{ }\mu\text{m}^2$ surface area (total mass spectrum) contains peaks of molecular ions which correspond to the total area analyzed. The information obtained by this technique will provide important information such as oxide/ salt/ tribochemical layer formation generated and tribochemistry of OFM on metal surfaces that is speculated to be the source of COF and wear reduction in this specific boundary lubrication system.

CHAPTER 3

TRIBOLOGICAL TESTING AND ANALYSIS

Tribological experiments are carried to test the effects of various commercial and experimental additives on the friction and wear reducing properties of both oil-based and water-based drilling mud. Experiments are also carried using the base fluid of OBM, Escaid, to fundamentally understand the contrast of friction and wear without solid constituents in the drilling mud. Experiments using base fluid of WBM are not conducted due to the unavailability of the product at the time. Additionally, samples tested with base fluid are useful for tribochemical analysis using ToF SIMS to better understand the lubricating mechanism of additives without the added complexity introduced by solid constituents.

Experiments without additives are conducted on OBM, WBM, and Escaid to establish a reference tribological condition. Experiments are conducted using a Falex Four-Ball Friction and Wear Testing Machine as described in Chapter 2. Lubricant and additives are initially mixed in a separate container using a magnetic stirrer and heated on a heating plate to the target temperature for approximately ~25-30 minutes. In conjunction the sample-holding lubricant cup is also heated on the testing machine by connecting the thermocouple line to the lubricant cup and switching the power on. It is important to note that in this period, the motor and pneumatic loading is not yet operated. When both the lubricant additive mixture and lubricating cup reach the target temperature at the specified time, then the lubricant is poured into the cup. Pneumatic loading is activated and set to the target load. The data acquisition system is activated and the experiment is started. Figure 19 shows the applied load, temperature, and speed of the four-ball experiments with respect to time. Refer to Appendix A for step-by-step Falex-Four Ball Friction

and Wear Testing Machine operation. Refer to Table 6 for tabulated COF vs wear of interfaces data.

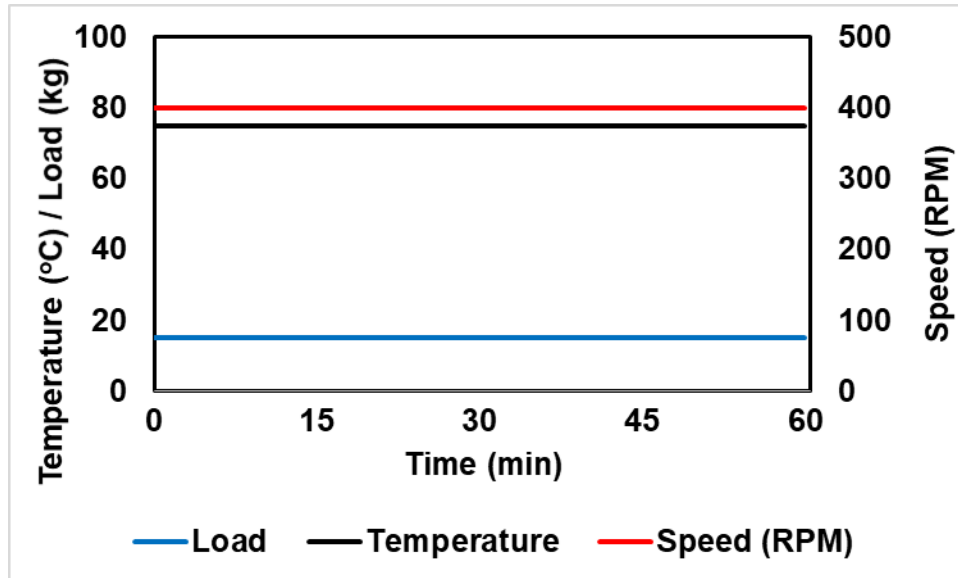


Figure 19: Temperature, speed, and applied load profile with respect to time

3.1. Escaid/ Base Fluid Experiments

3.1.1. No Additives

Four-ball testing with Escaid as lubricating fluid serves as a reference point for friction and wear reduction of additives. It is also an idealized drilling scenario having no solid particles associated in the experiments. The best additives in both Escaid and OBM will be selected for further tribochemical analyses discussed in a later section.

In the first minutes of the experiment, the interface produced a very high pitch noise indicating high metal-to-metal contact, as illustrated by the unstable COF in Figure 20. After ~20 minutes, the COF stabilizes at an average value of 0.333 with an average wear radius on each bottom ball at 473 μm . The final contact pressure of this interface is 77 MPa reduced from the initial Hertzian contact pressure of 2.54 GPa. This data shows that the interface cannot sustain high

GPa pressure and wear progresses until the maximum contact pressure that the interface can maintain is achieved.

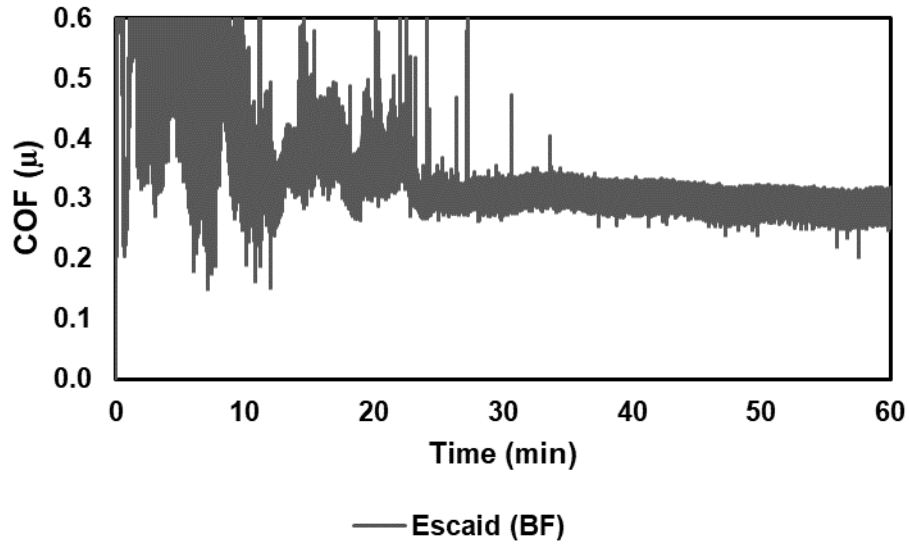


Figure 20: COF versus time of Escaid lubricated interface

3.1.2. EMamide-2 and EMamide-7 Additives

When EMamide-2 is introduced in Escaid, the COF is significantly reduced by 45% and maintained low at an average value of 0.184 illustrated in Figure 21. High pitch noise is no longer observed and the COF remains stable throughout the experiment. The wear radius is found to be 217 μm , a reduction of 54% from Escaid-only experiment.

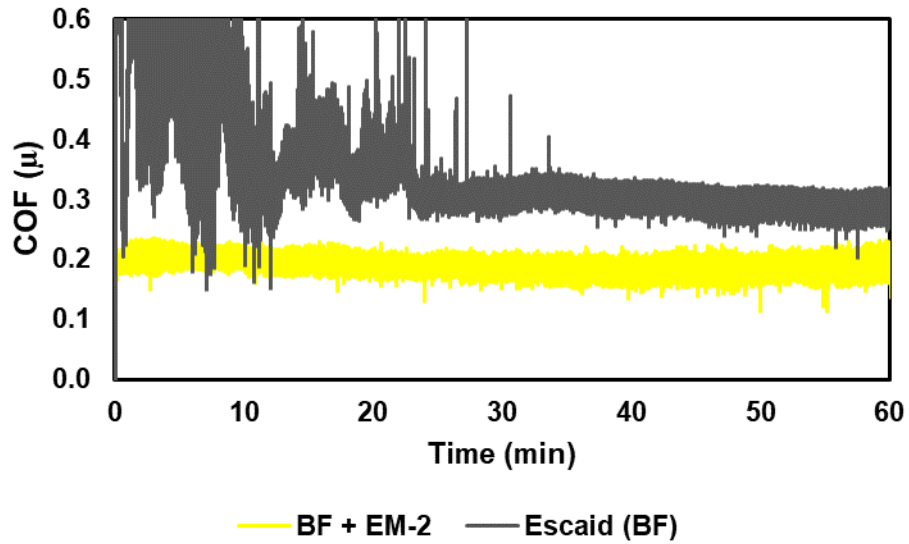


Figure 21: COF versus time of Escaid + EMamide-2 lubricated interface

Another version of EMamide additive, EMamide 7 is tested and found to have a similar COF trend with a slight increase to an averaged value of 0.193, illustrated in Figure 22. Wear is also increased, corresponding to the slight COF increase at an average wear radius of 261 μm , 45% reduction from Escaid lubricated test.

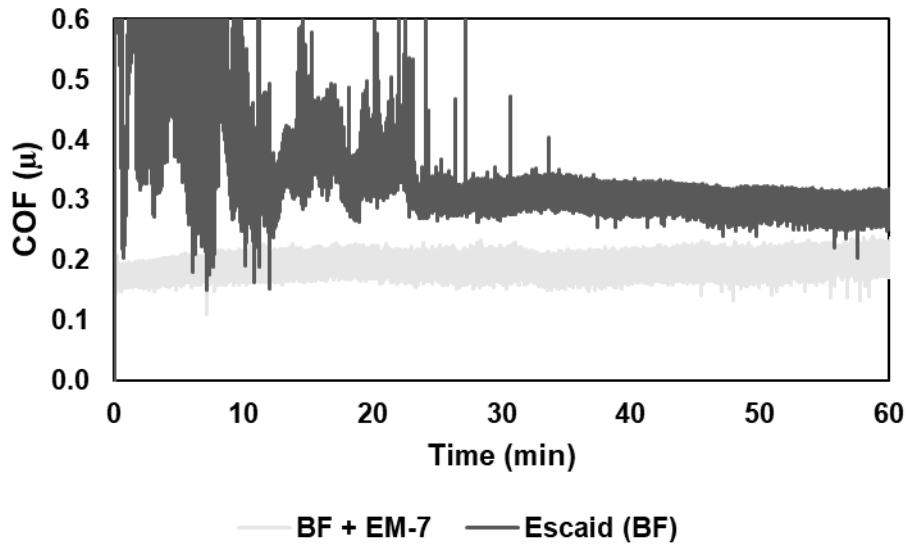


Figure 22: COF versus time of Escaid + EMamide-2 lubricated interface

3.1.3. UltraLube II Additive

The addition of UltraLube II into Escaid lowers the COF and wear by 37% and 30%, respectively compared to Escaid. The COF is stable throughout the experiment as depicted in Figure 23 and no high pitch noise is produced. Although the COF and wear reduction is lower than EMamide-2, UltraLube II still effectively improves the performance of Escaid. The value of COF over the 1 hour duration test is averaged at 0.209 and the wear radius is found to be 332 μm. Like most additives used in this study, the COF performance will eventually start to deplete over the length of operation. This is usually accounted by the addition of additives based on manufacturer recommendation. The recommended amount for UltraLube II is 27.5 gallon per hour for 800-1000 barrel (33,600-42,000 gallons) mud system. [37]

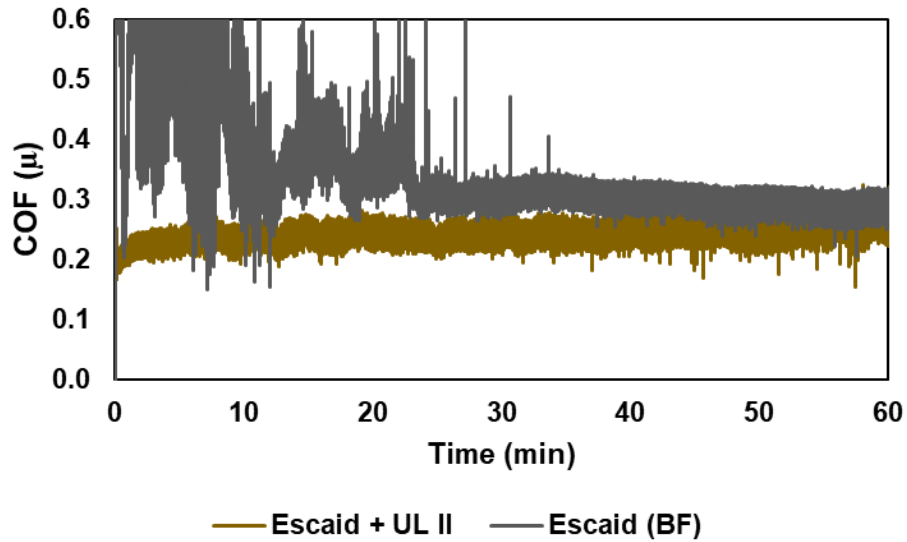


Figure 23: COF versus time of Escaid + UltraLube II Lubricated Interface

3.1.4. Amphiphile S Additives

The progressive increase in COF is even more rapid in the case of Escaid + Amphiphile S, illustrated in Figure 24. The averaged COF is calculated to be 0.207, a 38% reduction from Escaid, although it is lower in the first portion of the experiment. The wear radius is measured to be 373 μ , a 21% reduction from Escaid, lowest wear protection among the other additives used in this study. Amphiphile S-13 is also tested with Escaid, and the result does not show better tribological performance, compared to Amphiphile S with an averaged COF of 0.251 and wear radius of 459 μ m.

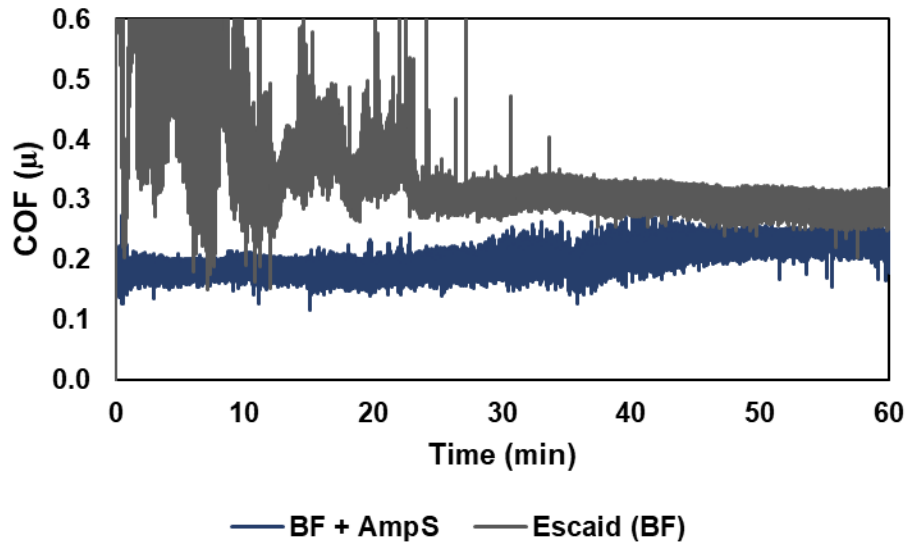


Figure 24: COF versus time of Escaid + Amphiphile S Lubricated Interface

3.1.5. Summary

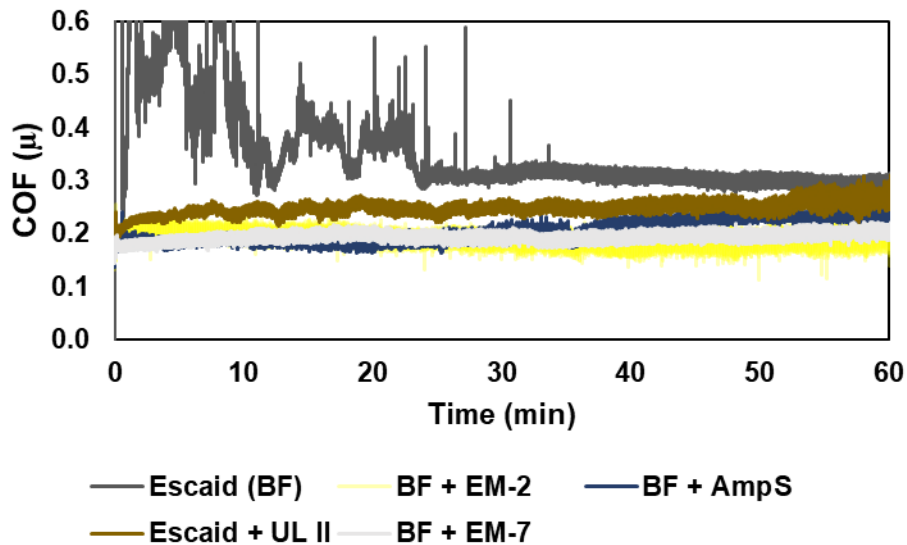


Figure 25: COF versus time of all the additives tested in Escaid

In summary, all OFM additives can significantly improve the tribological performance of Escaid and produce stable interface from the start. EMamide-2 is notably the best performing friction modifier and able to maintain the highest pressure. It reduces COF by 45% and 54% in wear

radius. This translates to a 94% reduction of wear rate in comparison with Escaid lubricated interface. In industry this means large cost and time saving through friction reduction and increase of tool lifetime. Additionally, all additives successfully stabilize the contact and reduce metal-to-metal contact depicted in Figure 25, as a relatively stable COF throughout the experiment. Figure 26 below shows the wear micro-images of all the interfaces tested. Additives arranged based on best wear protection is EMamide-2, EMamide-7, UltraLube II, and Amphiphile S. Wear is mainly abrasive due to the two similar material rubbing against each other. Although this information is useful, experiments in drilling mud are conducted to predict how these additives perform under condition closer to life application.

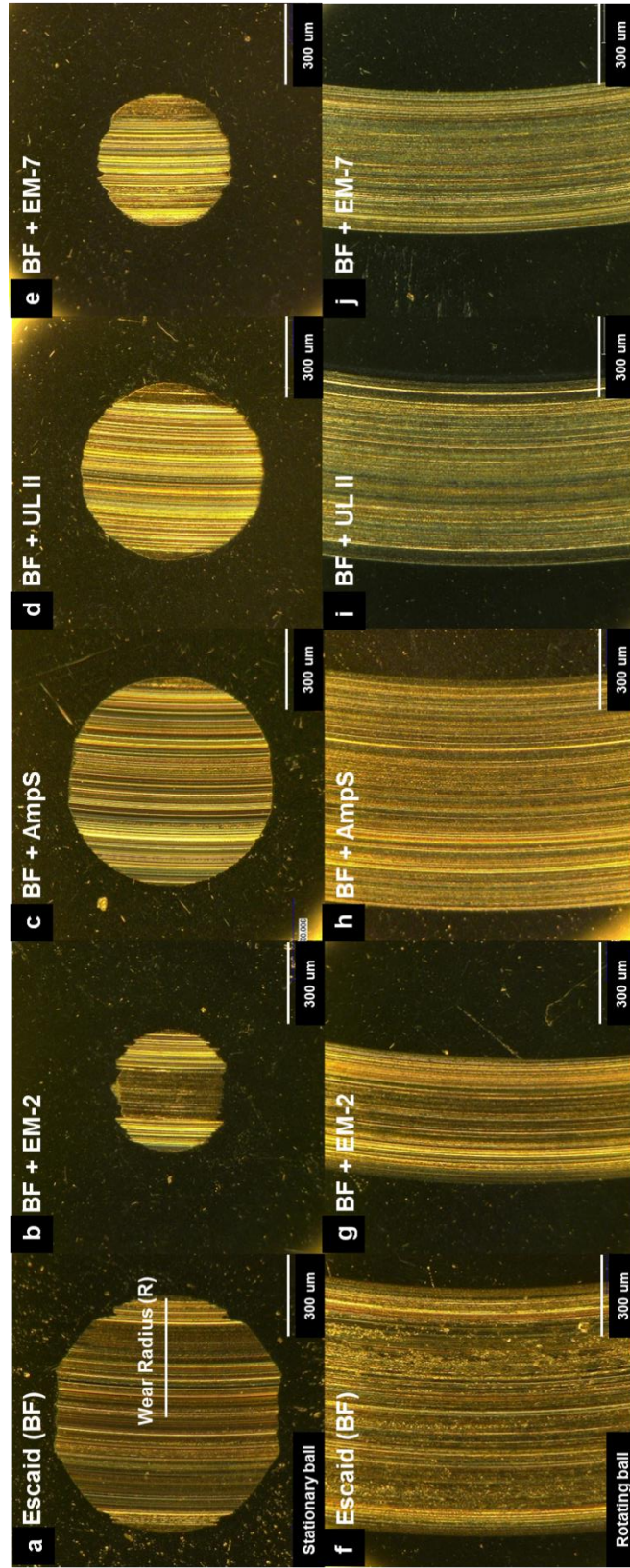


Figure 26: Micro-images of one of the three bottom stationary ball a) Escaid (BF), b) Escaid + EMamide-2, c) Escaid + Amphilphile S, d) Escaid + UltraLube II, e) Escaid + Amps, f) Escaid (BF), g) Escaid + EMamide-2, h) Escaid + Amps, i) Escaid + UltraLube II, j) Escaid + EMamide-7 respectively for the top ball

Experiments with varying test durations were also conducted to understand the wear rate as a function of time as shown in Figure 27. In Escaid lubricated interface, most damage is done in the first 15 minutes. With no additives, lubrication is dependent of hydrodynamic film thickness thus increase in wear reduces the contact pressure which also reduces wear. It is however contrary in the case of OFM additives such as EMamide-2 and Amphiphile S. When OFM is used, lubrication involves tribochemical process such as generation of passive tribochemical layer on metal substrate that is constantly being sheared and regenerated keeping the COF and wear low especially at high contact pressure. As contact area increases, more of this layer is being sheared, thus its rate of regeneration will determine the COF and wear increase. Based on this hypothesis, EMamide-2 has higher tribochemical generation rate than Amphiphile S. ToF SIMS will be conducted on these samples to determine the presence of the passive tribochemical layer.

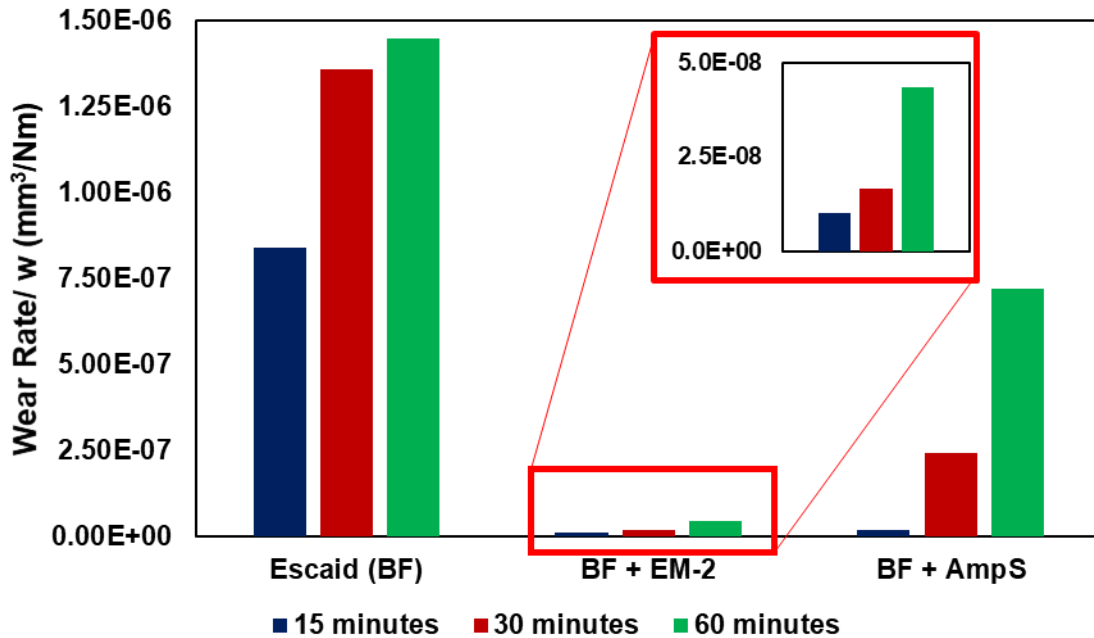


Figure 27: Wear rate of interface versus test duration

3.2. Oil-Based Drilling Mud Experiments

3.2.1. No Additives

Oil-based Mud (OBM) experiment will serve as a reference point in which COF and wear reduction with additives are based on. In comparison to Escaid base fluid (BF), the COF of this interface is lower with no unstable COF seen throughout the experiments as depicted in Figure 28. However, the COF slightly increases after 40 minutes of experimentation. A hypothesis identifies several potential factors such as elevated level of abrasives/ solid particles entrainment to the interface or in a more severe way deterioration of the lubricant. Elevated abrasives entrainment is mainly due to the reduction of the contact pressure caused by increased wear. The averaged COF is found to be 0.233 and averaged wear radius measured to be 425 μm .

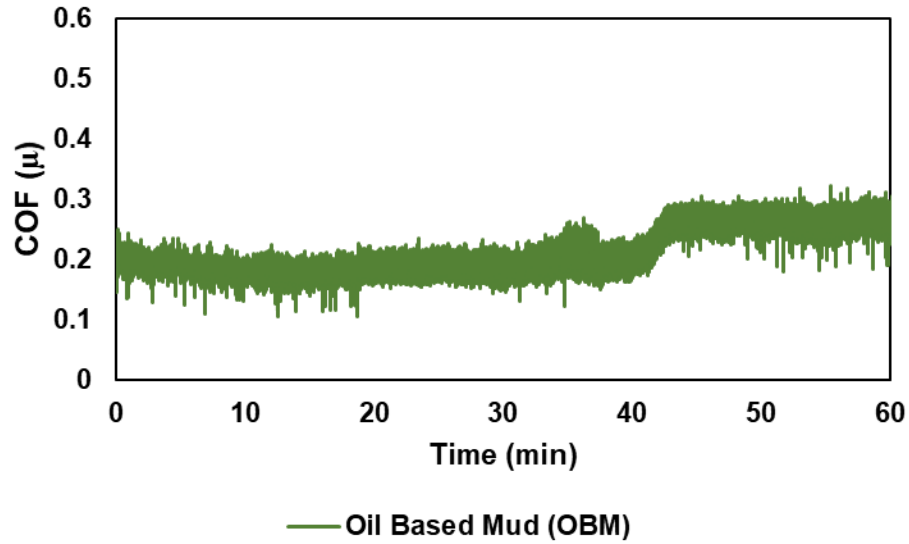


Figure 28: COF versus time of OBM lubricated interface

3.2.2. EMamide-2 and EMamide-7 Additives

Introduction of EMamide-2 into OBM reduces the averaged COF by 25% and the wear radius by 39%. Although the reduction is not as much as what is seen in Escaid, the COF of OBM is already significantly lower than Escaid. In fact, EMamide-2 performs really well reducing the COF to an average of 0.174 and the wear radius to 259 μm . Additionally, the use of EMamide-2 eradicates the progressive increase of COF. Even better the COF reduces over the 1 hour test duration.

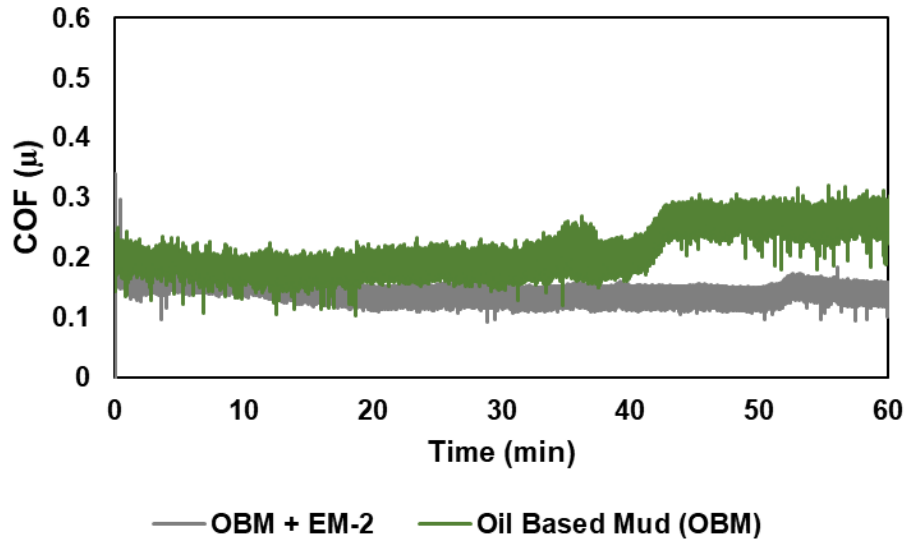


Figure 29: COF versus time of OBM + EMamide-2 lubricated interface

On the other hand, use of EMamide-7 in OBM reduces the COF by only 5% while diminishing the wear protection with 6% increase in wear radius. Then the average COF is measured to be 0.221 and the wear radius is 451 μm. The COF trend of OBM + EMamide-7 lubricated interface in Figure 30 shows high fluctuation, indicating instability of the contact. Additionally, the COF also progressively increases over time.

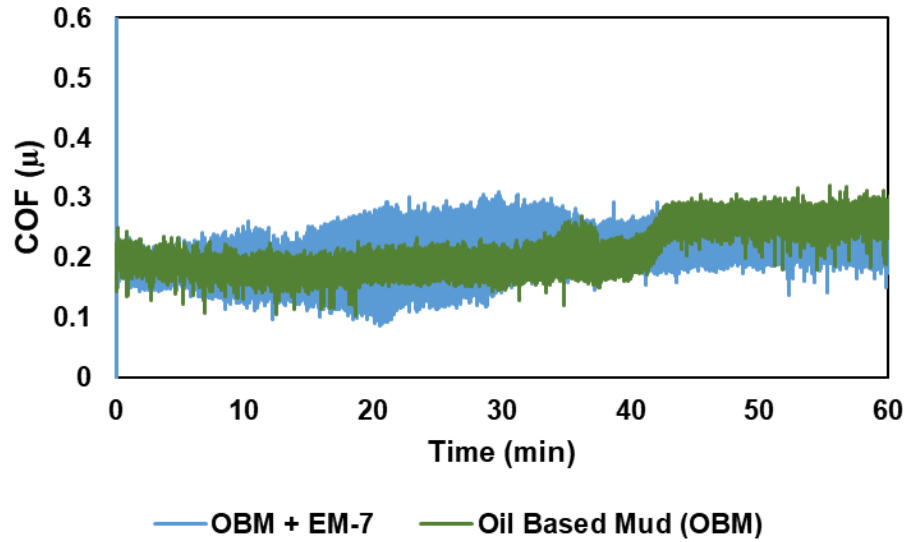


Figure 30: COF versus time of OBM + EMamide-7 lubricated interface

3.2.3. UltraLube 2 Additive

UltraLube reduces the COF of OBM by 12% and wear protection by 9%. Average COF is measured to be 0.204 and wear radius is 387 μm . In addition to lowering the COF, it also removes the step increase of the COF towards the end of the experiment, as illustrated in Figure 31 and progressive increase of COF is not observed in this lubricant mixture.

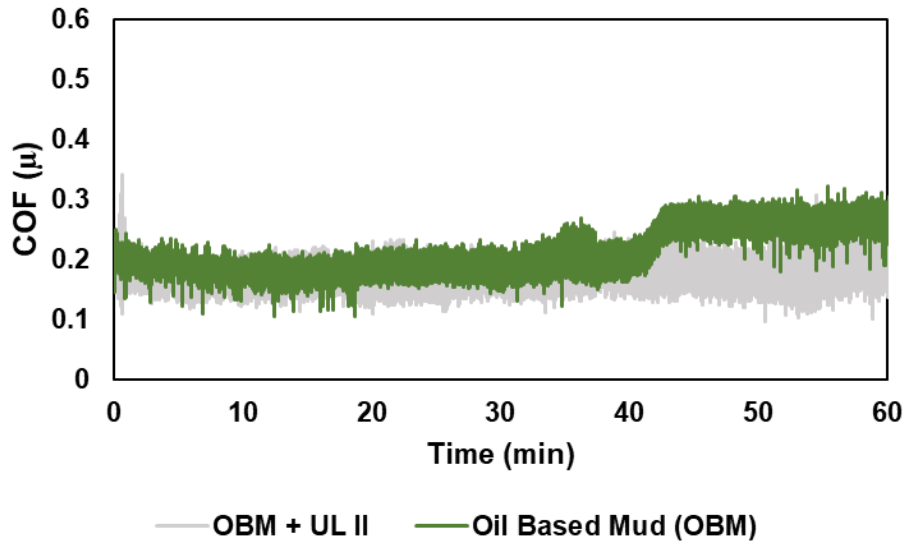


Figure 31: COF versus time of OBM + UltraLube II lubricated interface

3.2.4. Amphiphile S Additives

Addition of Amphiphile S to OBM reduces the COF by 14% while diminishing the wear protection by 1% increase in wear radius. Average COF is measured to be 0.201 and wear radius is 431 μm. The COF initially starts at the same point as OBM without additives, then the COF starts to increase midway through the experiment shown in Figure 32. While improving COF, Amphiphile S does not necessary effected the wear protective property of OBM. Amphiphile S-13 was also tested and the average COF is 0.238. This shows that Amphiphile S-13 causes slightly negative effect to OBM.

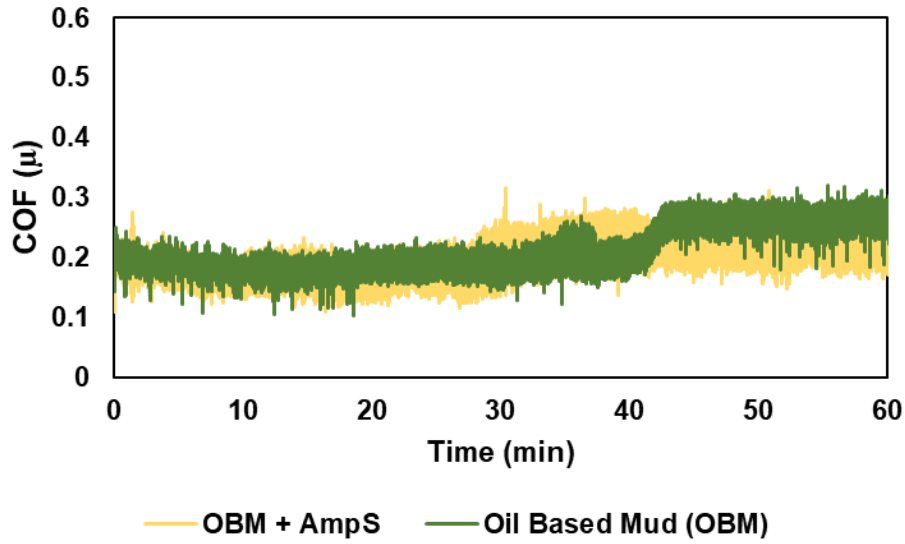


Figure 32: COF versus time of OBM + Amphiphile S lubricated interface

3.2.5. Summary

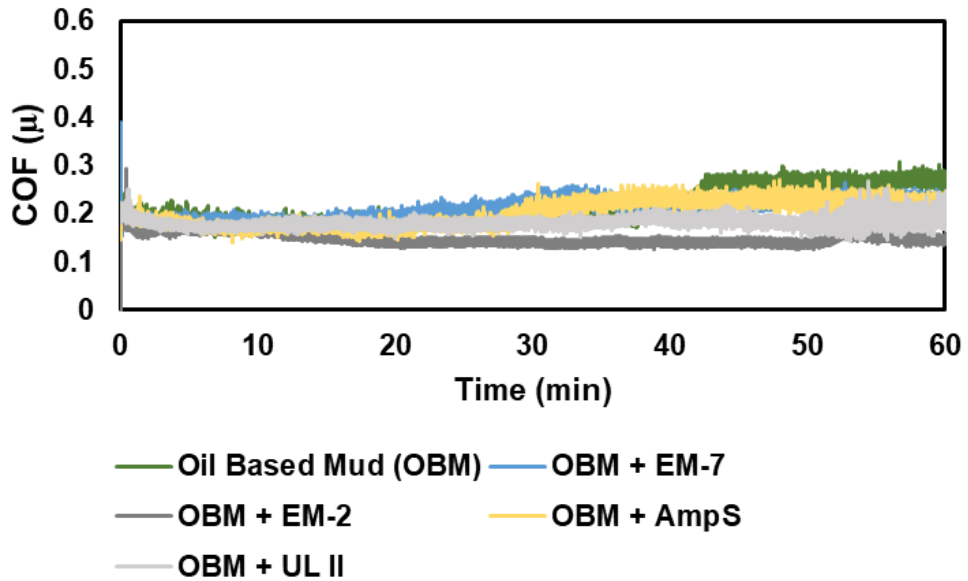


Figure 33: COF versus time of all the additives tested in OBM

Use of all OFM additives chosen for this study reduces friction at the interface. However, they do not necessarily improve the wear protection of OBM particularly due to the presence of 3-

body abrasive that will be discussed next. The tribological results show that EMamide-2 is still the best performing friction modifier reducing COF by 25% and wear radius by 39%. That is a 90% reduction of the wear rate in comparison with OBM lubricated interface. The order of overall performance is EMamide-2, UltraLube II, Amphiphile S, and EMamide-7, partially correlated to the results seen in Escaid except for EMamide-7. Additionally no severe metal-to-metal contact or high pitch noise is seen in OBM experiments as depicted in the summary plot in Figure 33.

Figure 34 below shows the wear micro-images of all the tested interfaces. When EMamide-2 is used in OBM, large erosive wear around the main contact area is observed, shown in Figure 34 (b). This may be caused by EMamide-2's poor dispersing ability that causes flocculation of solid constituents of OBM, and when solid particles settle on the reservoir floor, the spindle motion accelerates these particles, causing erosive wear to the stationary ball, as shown in the figure. On the other hand, Amphiphile S mixtures produce a cleaner cut in both types of fluid, as shown in Figure 34 (c) and Figure 34 (h). This means that Amphiphile S is better in dispersing wear debris to keep the surface clean. In contrast, the addition of Amphiphile S in OBM causes detrimental effect on wear, contrary to its positive effect when used in Escaid. This may be associated to numerous factors such as chemical reaction that weakens the metal. Hypothetically, most OFM will react with steel creating passive tribochemical films that may either protect or weaken the surface depending on the strength of the generated passive films. This film can either be protective like aluminum oxide layer or corrosive like iron oxide that consumes the surface; especially worsen when wear is enhanced by presence of the solid abrasive constituents of mud. Other factors such as passive film thickness and film growth rate also determine the wear rate, especially in the presence of solid abrasives that enhance wear.

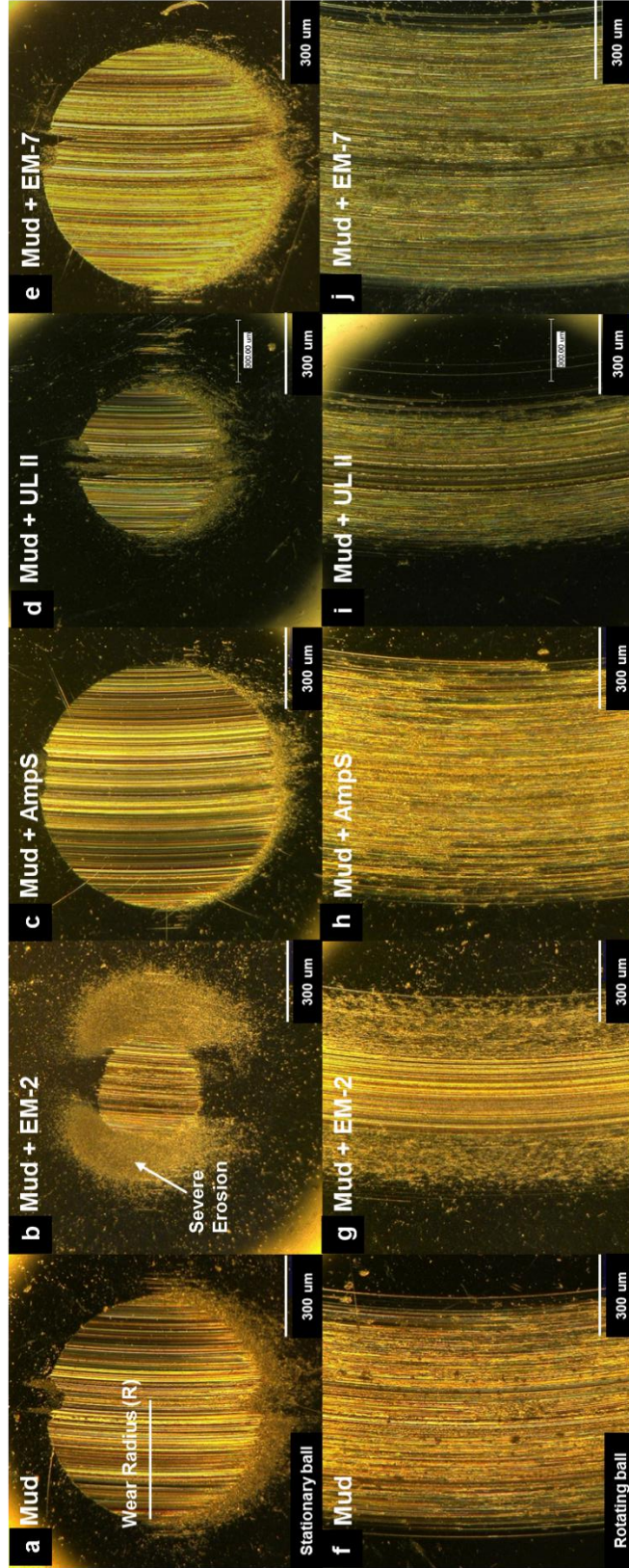


Figure 34: Micro-images of a) oil-based mud (OBM), b) OBM + EMamide-2, c) OBM + Amphiphile S, d) OBM + UltraLube

II, e) OBM + EMamide-7 bottom stationary balls, and f), g), h), i), j) respectively for the top balls

Another study of wear growth rate versus time is conducted to determine how wear grows in OBM, compared to Escaid as shown in Figure 35. As previously hypothesized, the averaged wear rate should increase as averaged wear increases especially when solid abrasives are involved in the lubrication process where they become entrained into the interface and shear the passive tribochemical layer. In the case of EMamide-2, wear does not progress much, possibly due to its strong protective passive layer build on the surface. While in the case of Amphiphile S, the wear rate is similar to OBM itself without additives.

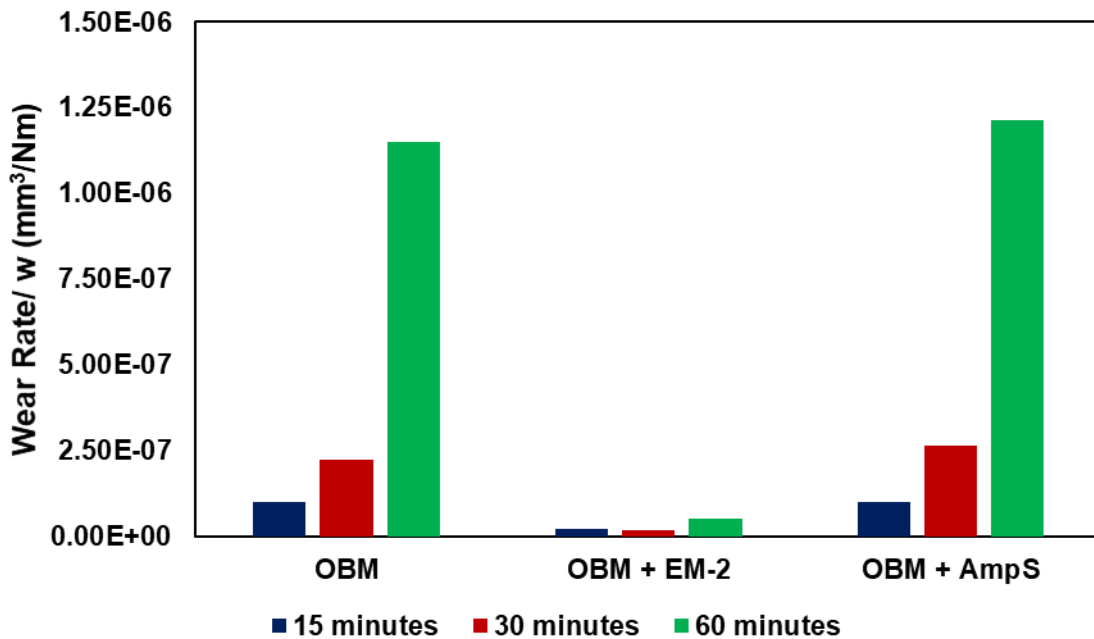


Figure 35: Wear rate of OBM, OBM + EM-2, and OBM + Amphiphile S lubricated interfaces after 15, 30, and 60 minutes test duration

3.3. Water-Based Drilling Mud Experiments

Another variety of drilling fluid is water-based mud (WBM), which is most commonly used for drilling due to its low cost and environmental friendliness. However, WBM typically results in high friction and wear. This is acceptable when drilling most vertical holes as drill string does

not constantly lean on hole-casing, therefore not producing excessive frictional torque or drag. It is highly beneficial and of industry interest to increase the technical performance of WBM such that it can be used in extreme cases such as extended-reach drilling (ERD), where more expensive OBM is currently used.

3.3.1. No Additives

WBM without additives are tested using the same four-ball friction and wear tester. These results will serve as a reference point to determine how OFM effects its friction and wear protection. Tribological result shows an average COF of 0.475 and wear radius of 701 μm , the worst performance among all the drilling fluids tested in this study. Although no high pitch noise is observed during the test, COF is high and remains the same throughout the experiment. Fluctuation in COF indicates unstable frictional behavior and large wear on the interface.

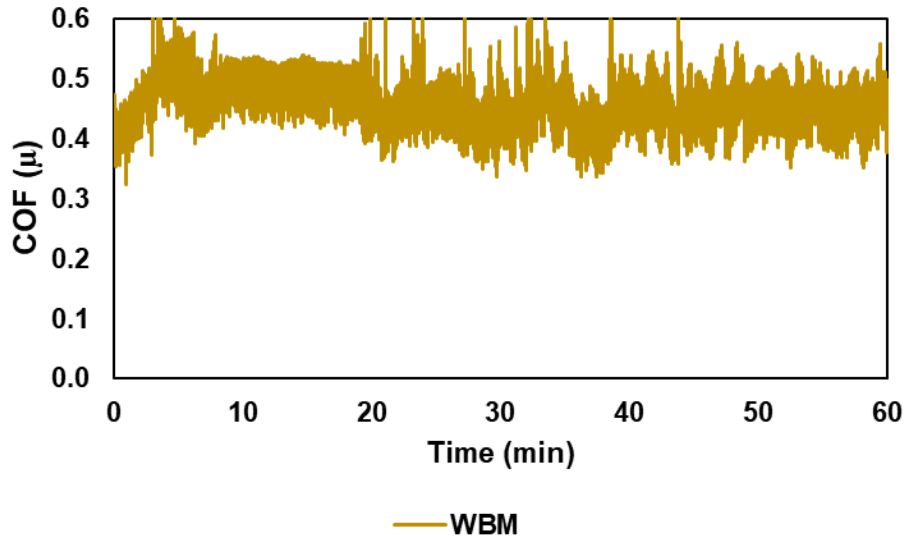


Figure 36: COF versus time of WBM lubricated interface

3.3.2. EMamide-2 and EMamide-7

EMamide-2, the best performing OFM in Escaid and OBM, is tested in WBM and the results show an averaged COF of 0.337, as illustrated in Figure 37 and wear radius of 618 μm , a 29% reduction in COF and 12% reduction in wear radius. Although the COF reduction is higher compared to OBM, it does not protect the surface as much as it does in OBM.

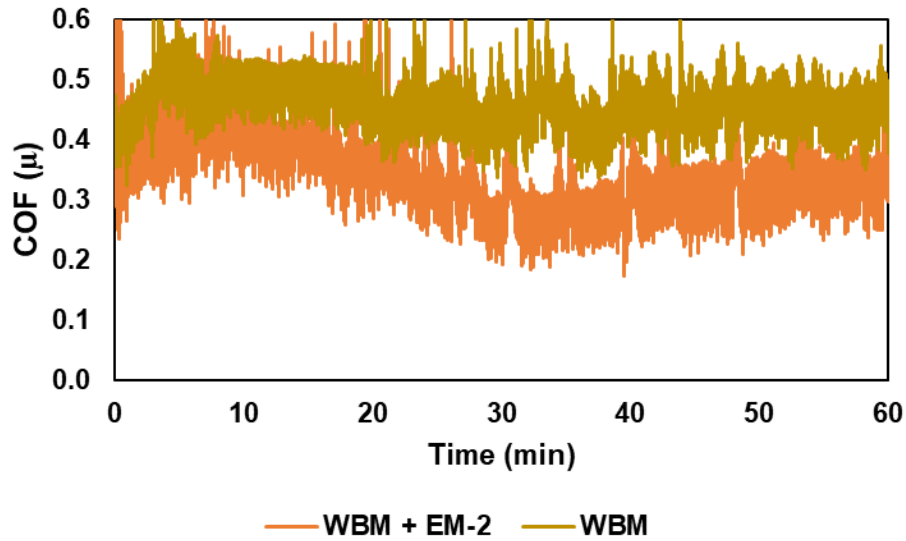


Figure 37: COF versus time of WBM + EMamide-2 lubricated interface

In contrast to OBM results, EMamide-7 performs better in WBM reducing the COF by 38% and wear by 20%. COF is averaged at 0.295 as shown in Figure 38 and wear radius is 565 μm . This result can provide an insight to lubricant additive developers as to why this particular additive is better than the other in the two drilling muds.

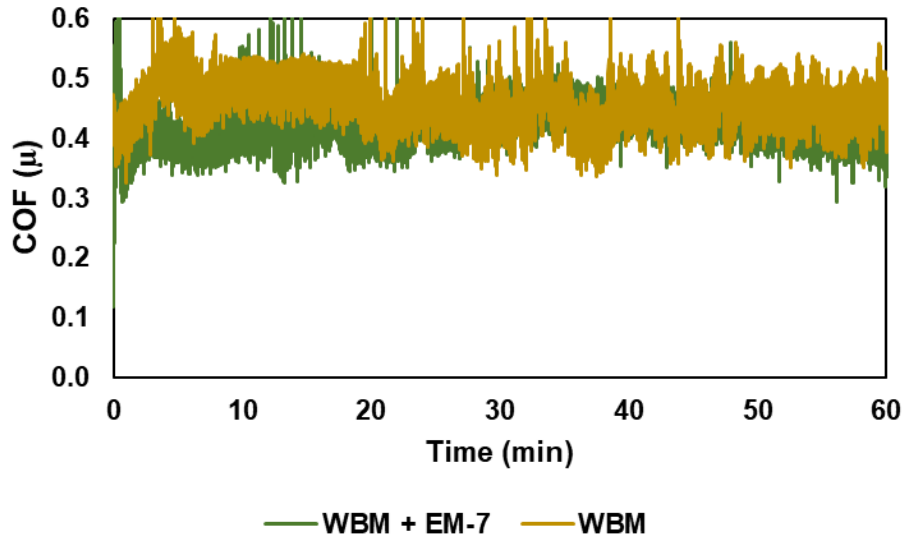


Figure 38: COF versus time of WBM + EMamide-7 lubricated interface

3.3.3. Amphiphile S and Amphiphile S-13

Usage of Amphiphile S in WBM provides one of the best protection in WBM. As seen in Figure 39, Amphiphile S reduces COF by 50% to an average value of 0.236. At the beginning of the experiments, Amphiphile S in WBM has even lower COF than some OBM mixtures. At this level, COF is comparable to that of OBM. Wear radius is reduced by 38% at an average of 437 μm . Amphiphile S's effect in OBM and WBM shows similarity with EMamide-7. Although they do not perform well with oil-based, they are effective in water-based drilling fluids. Similarly, Amphiphile S that impairs OBM performance is able to reduce the COF by 43% and wear radius by 28% in WBM. The COF trend is similar to that of Amphiphile S shown in Figure 40 as COF increases over time. However, it should be noted that the COF of WBM is comparably much higher than OBM without any friction modifier. Thus, these OFM are still effective in OBM as they do in WBM.

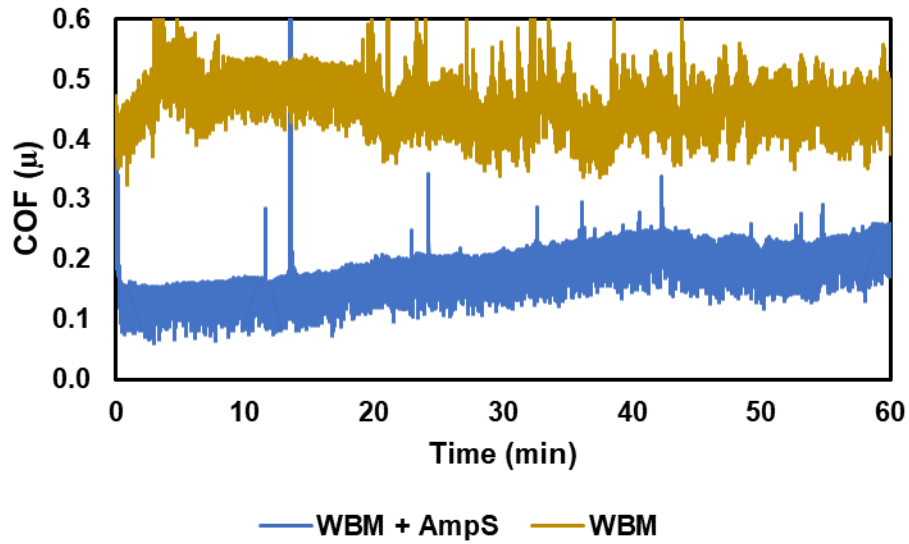


Figure 39: COF versus time of WBM + Amphiphile S lubricated interface

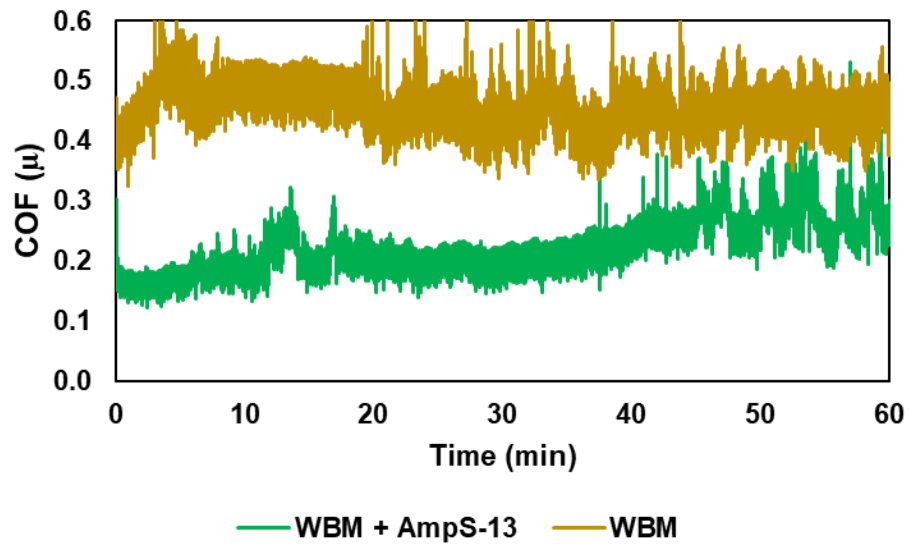


Figure 40: COF versus time of WBM + Amphiphile S-13 lubricated interface

A study of varying Amphiphile S dosage was also performed. A quarter dosage of Amphiphile S is mixed in WBM and tested under the same condition. As shown in Figure 41, reducing Amphiphile S dosage in WBM is terminally effecting the COF. COF is reduced only by 10% at 0.428 and wear radius by 8% at 644 μm.

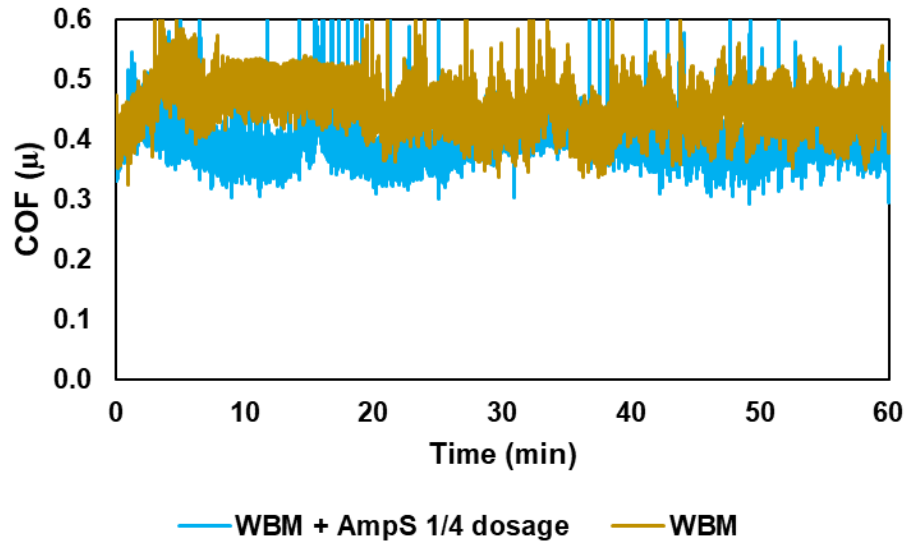


Figure 41: COF versus time of WBM + 1/4 dosage Amphiphile S lubricated interface

3.3.4. UltraLube II

UltraLube II reduces the COF of WBM by 33% and wear radius by 9%. The COF is averaged at 0.319 and wear radius is 641 μm . As shown in Figure 42, the COF initially starts high and decreases over time. This could mean that UltraLube II is more effective in lower contact pressure as wear increases over time.

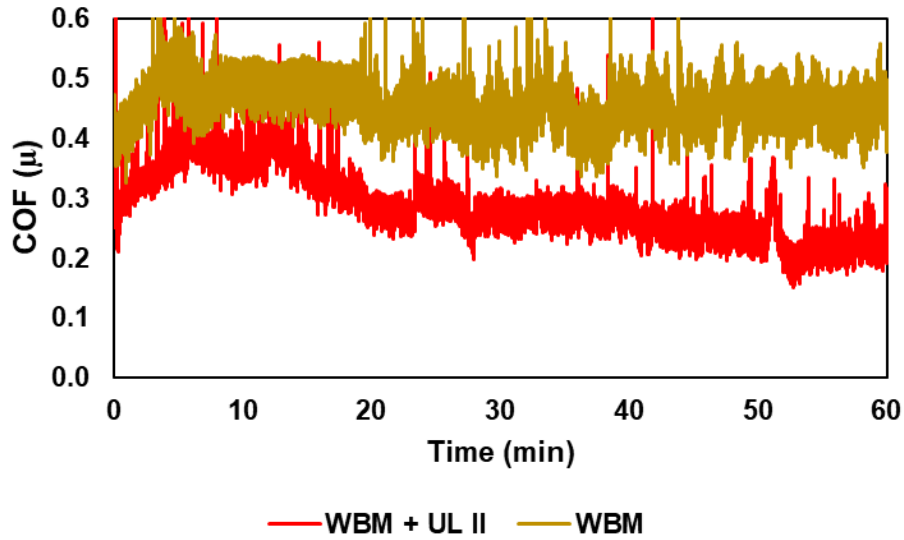


Figure 42: COF versus time of WBM + UltraLube II lubricated interface

3.3.5. EvoLube G

Another addition to OFM additives tested is EvoLube G. It is especially designed to improve performance of WBM. EvoLube G provides the best technical improvement to WBM among the other mixtures. Figure 43 shows that COF initially starts low at ~ 0.2 then progressively increases and reduces again.

Experiments with quarter dosage EvoLube G are also tested and result show even better performance. COF remains low throughout the experiment with quarter dosage of EvoLube G as illustrated in Figure 44. Additional experiments have been conducted to verify the results.

Although it may seem counterintuitive, it is possible that excessive tribochemical layer buildup causes adhesive drag and shear stress that increases COF and wear.

With full dosage, COF is reduced by 43% at 0.272 and wear radius by 23% at 538 μm . At quarter dosage, COF is reduced by 62% at an average value of 0.181 and wear radius by 42% with an average value of 404. In terms of the COF, this interface is even better than most OBM

mixtures except for the one with EMamide-2. However, the amount of wear is inferior in comparison to the best interfaces lubricated by OBM mixtures.

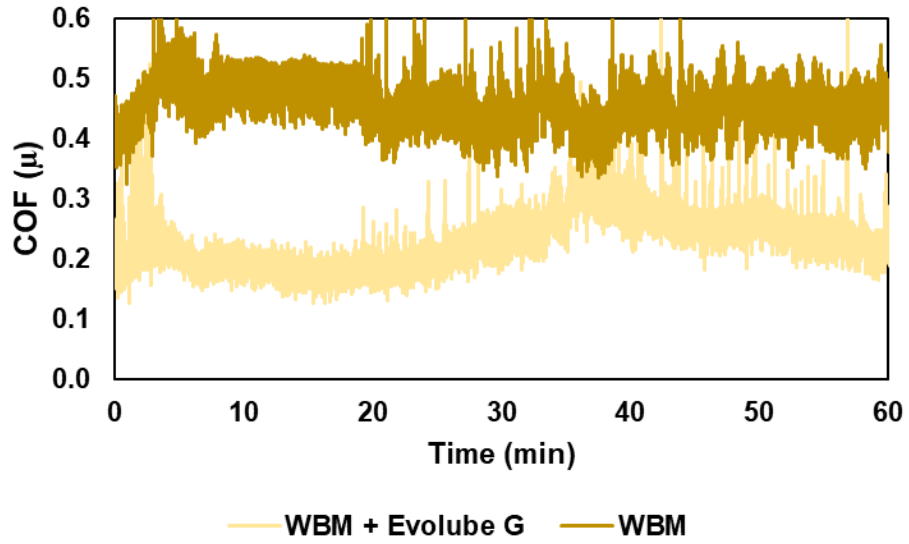


Figure 43: COF versus time of WBM + EvoLube G lubricated interface

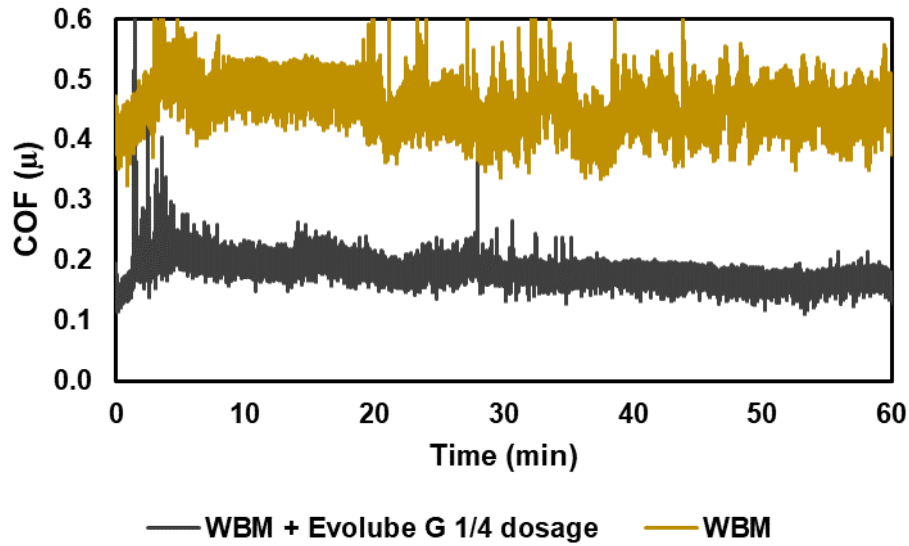


Figure 44: COF versus time of WBM + 1/4 dosage EvoLube G lubricated interface

3.3.6. Summary

Figure 45 shows the effect of each OFM on the COF reduction. As seen in the figure, EvoLube G works effectively in WBM reducing its COF by 62% at an average value of 0.181. At this point, the COF is as low as when OBM is used as drilling mud. This shows that indeed performance of WBM can be increased, to compete with OBM although wear protection is still lower than those lubricated by OBM mixtures. This is favorable for the industry due to WBM's lower toxicity and minimal cost. Another interesting finding from these tests is drawn from experiments with varying EvoLube G dosage that shows increasing dosage does not necessarily increase tribological performance. Additionally, OFMs that work well in OBM do not necessarily work well in WBM and vice versa. Thus it is important to understand the effective amount of OFM needed as well as factors that determine compatibility of OFM in different types of lubricating fluid.

The resulting wear radius of different WBM mixtures are shown in Figure 46 and Figure 47. A similarity in WBM samples is the formation of "reptile skin-like" pattern on the sample surfaces. This is mainly caused by etching of the material due to corrosion. Although WBM + EMamide-2 does not tribologically perform well, it manages to retain mirror-like surface finish on the top rotating ball shown in Figure 47 (b). The degree of reptile skin formation depends on the corrosion rate. However, microimages are not sufficient to determine the rate of corrosion.

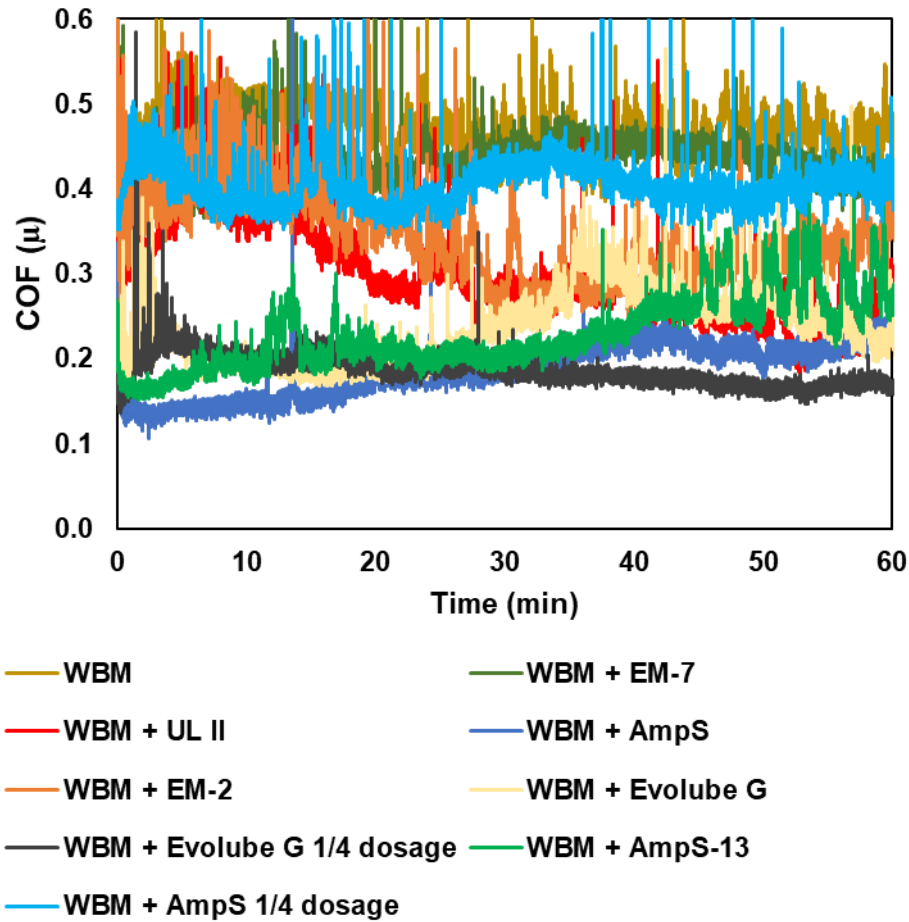


Figure 45: Effect of OFMs on WBM COF versus time

Reptile skin patterns are not observed in WBM only experiments shown in Figure 46 (a) and Figure 47 (b). However the images show rough surfaces outside the wear region after the experiments indicating highest corrosion among the conducted experiments tested. Thus the use of OFM impedes the etching process, but in place generating invisible passive tribochemical layer that is later observed with ToF SIMS.

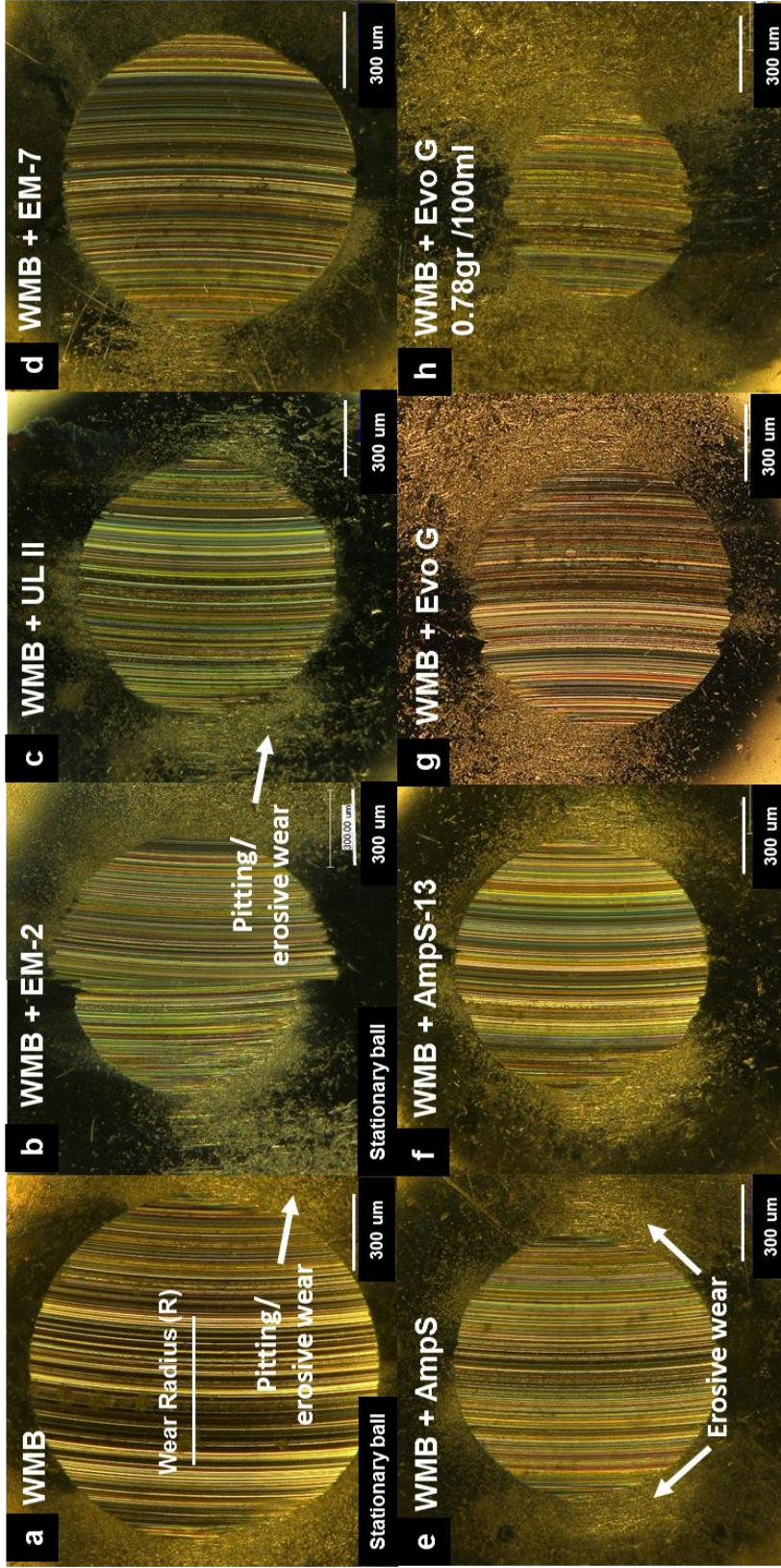


Figure 46: Micro-images of bottom stationary ball of a) water-based mud (WMB), b) WMB + EMamide-2, c) WMB + UltraLube II, d) WMB + EMamide-7, e) WMB + Amphiphile S, f) WMB + Amphiphile S-13, g) WMB + EvoLube G, and h) WMB + ¼ dosage EvoLube G

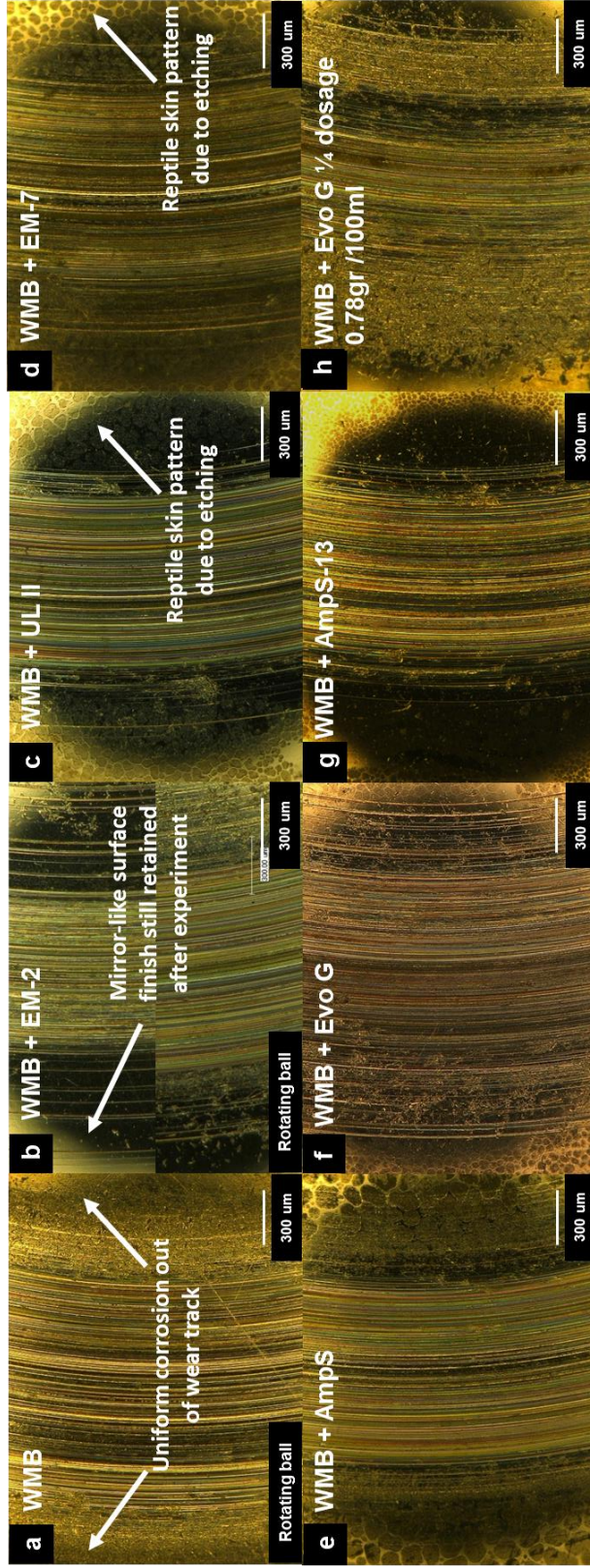


Figure 47: Micro-images of top rotating ball of a) water-based mud (WBM), b) WBM + EMamide-2, c) WBM + UltraLube II, d) WBM + EMamide-7, e) WBM + Amphiphile S, f) WBM + Amphiphile S-13, g) WBM + EvoLube G, and h) WBM + $\frac{1}{4}$ dosage EvoLube G

3.4. COF vs Wear Masterchart

In order to compare the performance of all OFM additives investigated in this study, a master chart is used to plot both the measured wear radius and the wear rates of the bottom balls against COF as depicted in Figure 48 and Figure 49. Additionally, this master chart provides information such as standard deviation of averaged COF and wear radius. Such information plays an importance in determining how repeatable each sets of experiments is. Experiments are color coded with red font for Escaid experiments, black font for OBM experiments, and blue font for WBM experiments. The red arrow shows the direction of improving tribological performance.

With Escaid as lubricating fluid, the best performing OFM is EMamide-2. The order of performance starting from the best FM is EMamide-2, EMamide-7, UltraLube II, and Amphiphile S. With OBM as lubricating fluid, the best performing OFM is also EMamide-2.

The order of performance starting from the best FM is EMamide-2, UltraLube II, Amphiphile S and, EMamide-7. With WBM as lubricating fluid, the best performing OFM is EvoLube G. The order of performance starting from the best FM is EvoLube G, Amphiphile S, Amphiphile S-13, EMamide-7, UltraLube II, and, EMamide-2.

In its totality, OBM performs better than WBM. In terms of tribology, Escaid experiments cannot be directly compared with OBM or WBM because Escaid does not contain solid particles such as barite, silica, quarts. However, petroleum distillate such as Escaid serves as solvent for OBM. Thus, the performance of OFM additives in Escaid can be reflected on OBM making the surface of samples lubricated by Escaid an idealized samples to be used for tribochemical characterization to rule out the complex chemical composition such as solids and other agents in OBM.

Examining the COF and wear trends, they seem to be correlated. In fact, parameters such as subsurface temperature, contact geometry, speed, and even lubricant molecular size have been used to create a complex model of wear prediction. However, even if this information is available, resulting wear of interfaces used in this study cannot be predicted or directly correlated with COF. Another contributing factor of wear in such system is the mechanical properties of tribochemical films generated. The technology to quantify the properties of these product layers is constantly developing. When it becomes available, the mechanical properties of generated tribochemical film can be measured, and a model can be built to predict the performance of different OFMs on different various metal substrate. Nevertheless, the data from Figure 48 and Table 6 shows that the use of OFMs do effect COF and wear in a positive direction.

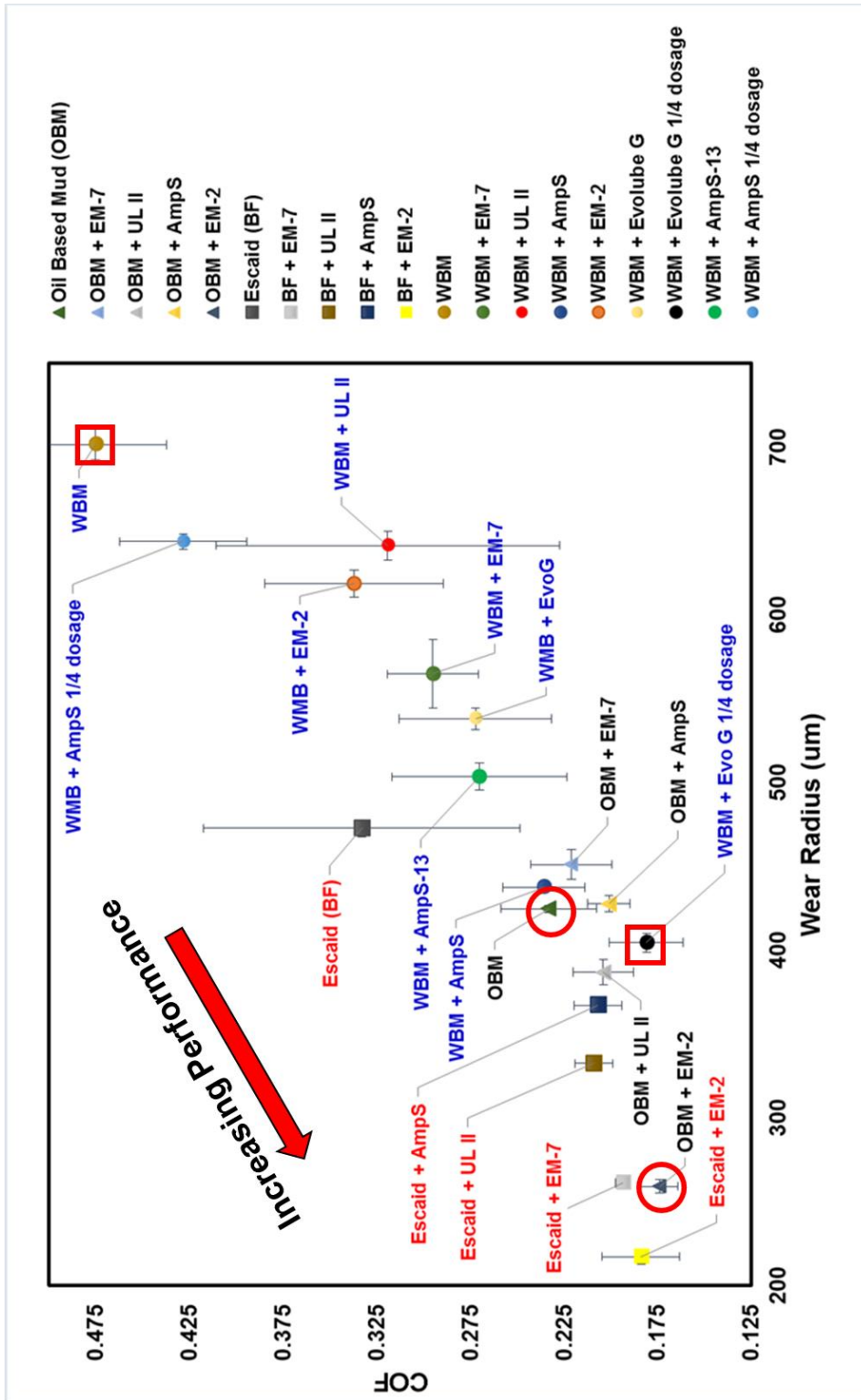


Figure 48: COF vs. wear radius

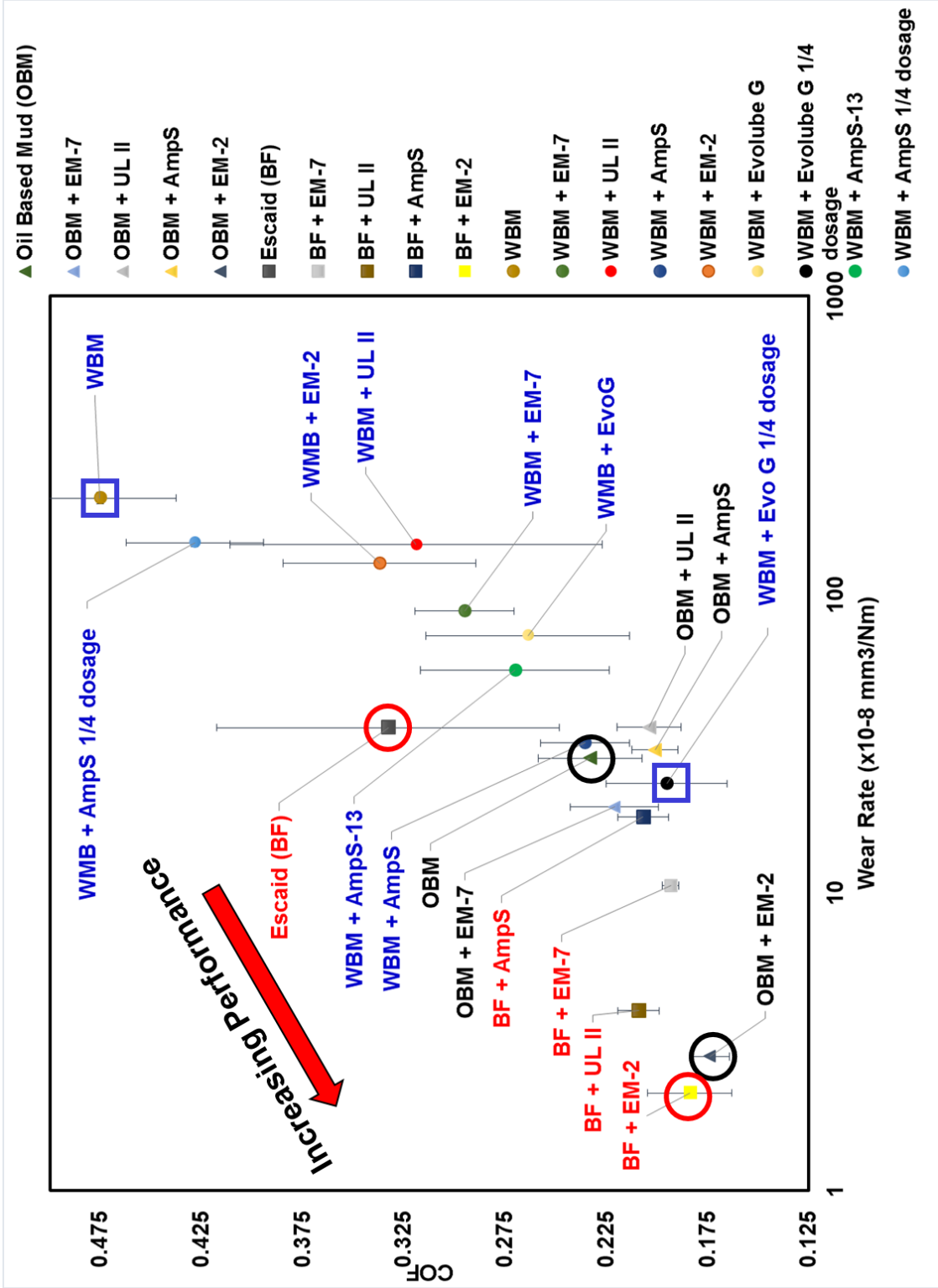


Figure 49: COF versus wear rate

Table 6: Tabulated COF, wear radius, and wear rate of interfaces

Mixture	COF/ μ	$\Delta \mu$	Wear Radius/ R (μm)	ΔR	Wear Rate/ w (mm^3/Nm)	Δw	Contact Pressure/ P (GPa)
Escaid (BF)	0.333		473		3.6E-07		0.077
BF + EM-2	0.184	45%	217	54%	2.1E-08	94%	0.315
BF + AmpS	0.207	38%	373	21%	1.8E-07	50%	0.109
BF + UL II	0.209	37%	332	30%	4.0E-08	89%	0.229
BF + EM-7	0.193	42%	261	45%	1.1E-07	70%	0.141
Mixture	COF / μ	$\Delta \mu$	Wear Radius/ R (μm)	ΔR	Wear Rate (mm^3/Nm)	Δw	Contact Pressure/ P (GPa)
Oil Based Mud (OBM)	0.233		425		2.8E-07		0.087
OBM + EM-2	0.174	25%	259	39%	2.8E-08	90%	0.286
OBM + AmpS	0.201	14%	431	-1%	3.0E-07	-7%	0.084
OBM + UL II	0.204	12%	387	9%	3.6E-07	-27%	0.077
OBM + EM-7	0.221	5%	451	-6%	1.9E-07	31%	0.104
Mixture	COF / μ	$\Delta \mu$	Wear Radius/ R (μm)	ΔR	Wear Rate (mm^3/Nm)	Δw	Contact Pressure/ P (GPa)
Water Based Mud (WBM)	0.475		701		2.1E-06		0.032
WBM + EM-2	0.337	29%	618	12%	1.3E-06	40%	0.041
WBM + AmpS	0.236	50%	437	38%	3.2E-07	85%	0.082
WBM + AmpS-13	0.270	43%	503	28%	5.6E-07	74%	0.062
WBM + UL II	0.319	33%	641	9%	1.5E-06	30%	0.038
WBM + EM-7	0.295	38%	565	20%	8.8E-07	58%	0.049
WBM + EvolubeG	0.272	43%	538	23%	7.3E-07	65%	0.054
WBM + EvolubeG ¼ dose	0.181	62%	404	42%	2.3E-07	89%	0.095
WBM + AmpS ¼ dose	0.428	10%	644	8%	1.5E-06	29%	0.038

3.5. Nominal Contact Pressure

Although the contact geometry complicates the linearity of the wear growth, the four-ball test is an excellent tool to compare the maximum contact pressure that the interface can bear at the end of the test, as shown in Figure 50. In the beginning of the test when contact between top and bottom is still point-to-point, an elastic Hertzian contact pressure is calculated to be 2.24 GPa with Hertzian contact radius of 102.5 μm . When the surface is lubricated with Escaid, final contact pressure is calculated at only 0.077 GPa. This indicates that the interface cannot sustain that high pressure therefore surface is worn to sustain the loading. Meanwhile when EMamide-2 is added into Escaid, final contact pressure is measured at 0.315 GPa, nearly four times increase from Escaid lubricated interface. The same mechanism applies for OBM lubricated interfaces, and addition of EMamide-2 increase that number to 0.286 GPa.

In WBM lubricated interface, final contact pressure is calculated to be only 0.032 GPa. The best performing OFM in WBM, EvoLube G, increases that number nearly three times higher at 0.095 GPa, but still a very low number compared to when EMamide is added to Escaid or OBM. Meanwhile, EMamide in WBM is performing poorly increasing the final contact pressure to only 0.041 GPa.

This information shows the importance of molecular size of the lubricating fluid. Water in WBM has a comparably much smaller molecular size compared to distilled hydrocarbon used in OBM. Although the COF of WBM lubricated interface can be significantly reduced with the use of FM like EvoLube G to the order of magnitude of OBM lubricated interface, the size of the lubricating fluid may not be sufficient to separate the contact preventing asperities contact. Thus wear is still high although wear is lowered.

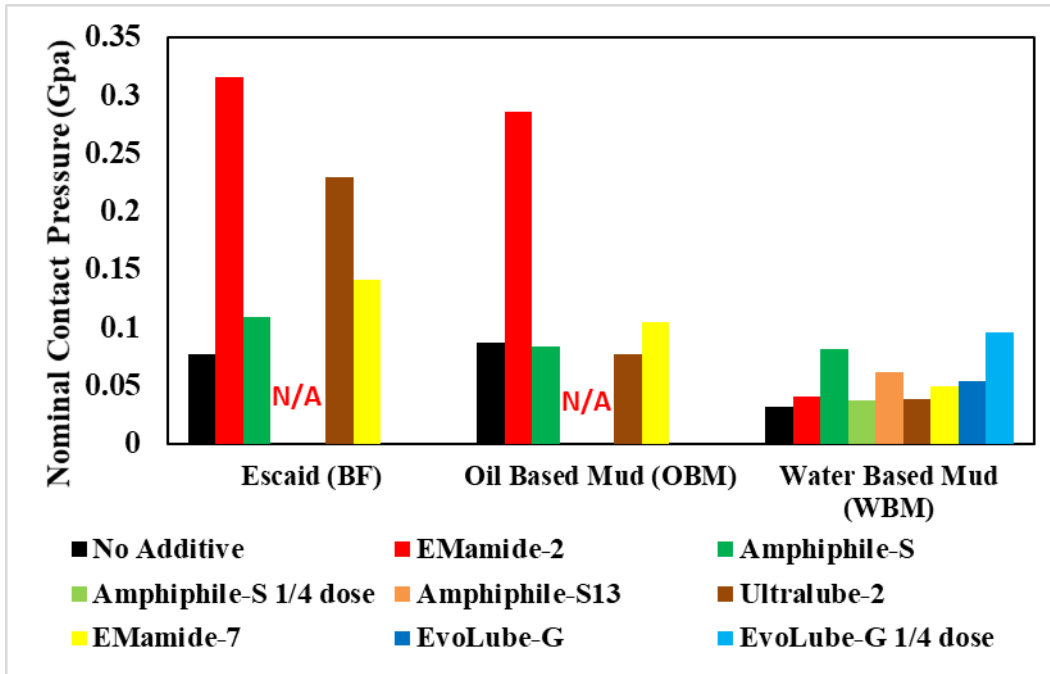


Figure 50: Nominal contact pressure of interfaces at the end of testing

3.6. Electrochemistry and Tribo-corrosion

The submersion of dissimilar alloy steel composition in drilling fluid creates an electrochemical system where drilling fluid acts as electrolyte. Electrochemical process are redox (oxidation-reduction) reactions in which the energy release by a spontaneous reaction is converted to electricity or in which electrical energy is used to cause a spontaneous reaction to occur. For an electrochemical process to happen, electrodes such as anode and cathode, as well as electrolyte needs to be present in the system. In drilling process in particular, the electrochemical reaction that happens spontaneously such as corrosion is called galvanic cell ^[41].

To understand the electrochemical reactions in the drilling process, the half-reaction and standard electrode potentials relevant to the materials used are shown in Table 7. This information is used to predict which materials will get oxidized and reduced in the tribological experiment based on highest electrode potential difference. Based on the order of pairs, species

toward the top of the table will be oxidized while its pairing species toward the bottom of the table will be reduced.

Table 7: Standard reduction potentials of species found in drilling system at 25°C^[41]

Half-Reaction	Standard electrode potentials E° (Volts)
Oxidized Form → Reduced Form	
$K^+_{(aq)} + e^- \rightarrow K_{(s)}$	-2.93
$Ba^{2+}_{(aq)} + 2e^- \rightarrow Ba_{(s)}$	-2.90
$Al^{3+}_{(aq)} + 3e^- \rightarrow Al_{(s)}$	-1.66
$2H_2O_{(l)} + 2e^- \rightarrow H_2 + 2OH^-_{(aq)}$	-0.83
$Cr^{3+}_{(aq)} + 3e^- \rightarrow Cr_{(s)}$	-0.74
$Fe^{2+}_{(aq)} + 2e^- \rightarrow Fe_{(s)}$	-0.44
$Ni^{2+}_{(aq)} + 2e^- \rightarrow Ni_{(s)}$	-0.25
$2H^+_{(aq)} + 2e^- \rightarrow H_{2(g)}$	0.00
$SO_4^{2-}_{(aq)} + 4H^+_{(aq)} + 2e^- \rightarrow SO_{2(g)} + 2H_2O_{(l)}$	+0.20
$Cu^{2+}_{(aq)} + 2e^- \rightarrow Cu_{(s)}$	+0.34
$O_{2(g)} + 2H_2O_{(aq)} + 4e^- \rightarrow 4OH^-_{(aq)}$	+0.40
$O_{2(g)} + 4H^+_{(aq)} + 4e^- \rightarrow 2H_2O_{(l)}$	+1.23
$Cl_{2(g)} + 2e^- \rightarrow 2Cl^-_{(aq)}$	+1.36

*For all half-reactions the concentration is 1 Molar for dissolved species and the pressure is 1 atm for gases. These are the standard-state values.

In the case of OBM lubricated surface as seen in Figure 34, surface pitting and etching are very minor. The reason is because hydrocarbon-based Escaid which is acting as the electrolyte is very poor in transferring electrons. Thus, corrosion is controlled. In the case of incorporating

EMamide-2 into the system, performance is superior in terms of tribology; however, localized attack is observed as major erosion on regions just outside the abrasive contact. This indicates that EMamide-2 presents a chemical change into the system that causes this localized attack.

In the case of using WBM as drilling fluid, issues with corrosion are more severe as seen in Figure 46 and Figure 47. With WBM alone, surface outside abrasive contact is uniformly corroded. This is indicated by the absence of mirror-like surface finish characteristic to untested samples. The use of OFM such as Amphiphile-S, EMamide-7, UltraLube II, and EvoLube G reduce corrosion with different potency, observed as the different level of reptile-skin pattern cause by etching process. In the case of incorporating EMamide-2 into the system, mirror-like surface finish of the surface outside abrasive contact is still retained. Some OFMs also cause localized corrosion observed as major pitting and erosion on surface surrounding the main abrasive contact.

WBM itself has a very high content of strong electrolyte such as KCl and BaSO₄ that will dissociate in aqueous solution like water producing Cl⁻ and SO₄²⁻ ions. In a simplified reactions, metals like iron will also be oxidized from its bulk form into Fe²⁺ and electrons. Electrons will be donated to deionize water into hydrogen and hydroxide ions where they will then again bond with K⁺ and Ba²⁺ that previously deionized from KCl and BaSO₄ forming KOH and Ba(OH)₂. The remaining ions such as Fe²⁺, Cl⁻, and SO₄²⁻ will bond creating FeCl₂ and FeSO₄ observed as material loss such as pitting and oxidation. In the real case, especially when OFM is present and tribology is involved, the electrochemical process is far more complex because of the presence of oxygen, metals, humidity, temperature, organics, and biological organism that will contribute to different level uniform and localized corrosion. Therefore, it is very important to

have a balanced tribological and corrosion performance studied as a field commonly known as tribo-corrosion.

3.7. Surface Profile

A selection of samples are chosen for surface profiling to understand the contour of the worn surface. The best performing additives for each types of fluids such as EMamide-2 in Escaid and OBM and EvoLube-G 25 % dosage are selected for surface profiling. The surface profile of BF + EMamide-2 as shown in Figure 51 for example is very useful to understand Figure 26 (b) better. Additionally, the significant reduction of wear can be easily visualized when additives are incorporated into lubricating fluid using surface profilometry. From microimages, questions are raised regarding the presence of trough or ridge on the center of wear and what may cause them to occur. Figure 51, Figure 52, and Figure 53 show that when wear is small by the use of FM additives, a ridge is maintained on the center of wear. This is mainly due to several factors such as the geometry of the steel ball, elasticity of the surface under contact, and protection by additives that contributes to the reduction of shearing of material on the center of contact, allowing the ridge to be formed during experiment. As wear increases, the ridge profile will eventually be removed.

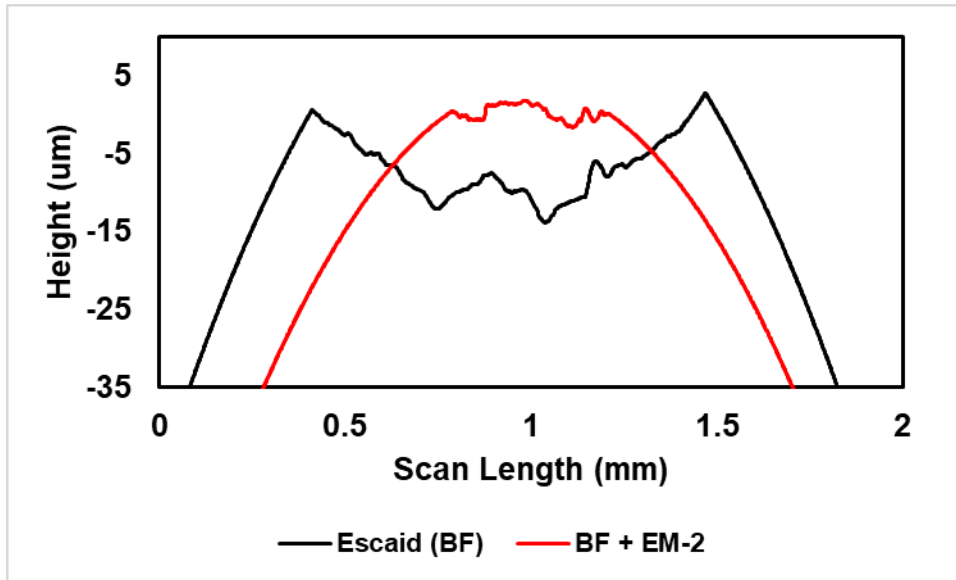


Figure 51: Surface profile of BF and BF + EMamide-2

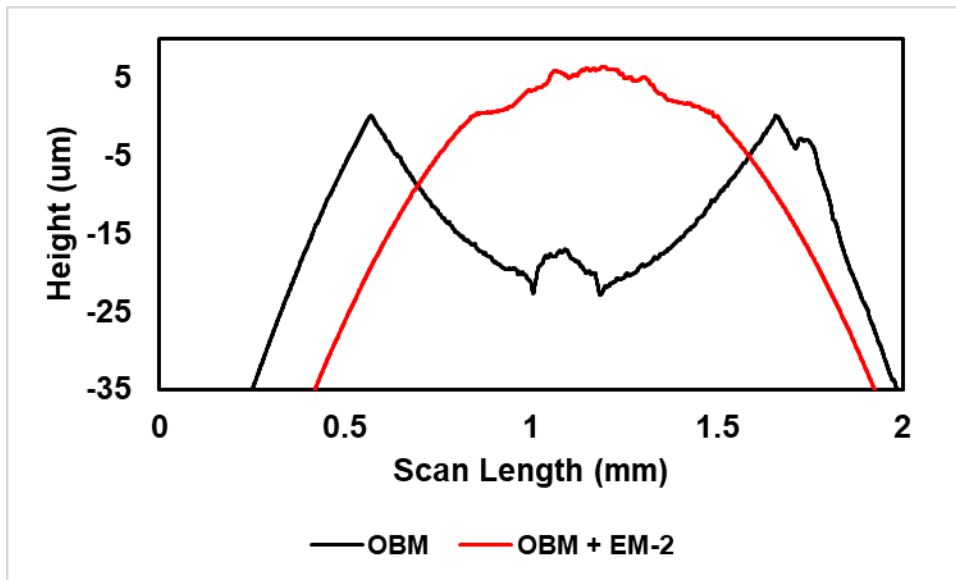


Figure 52: Surface profile of OBM and OBM + EMamide-2

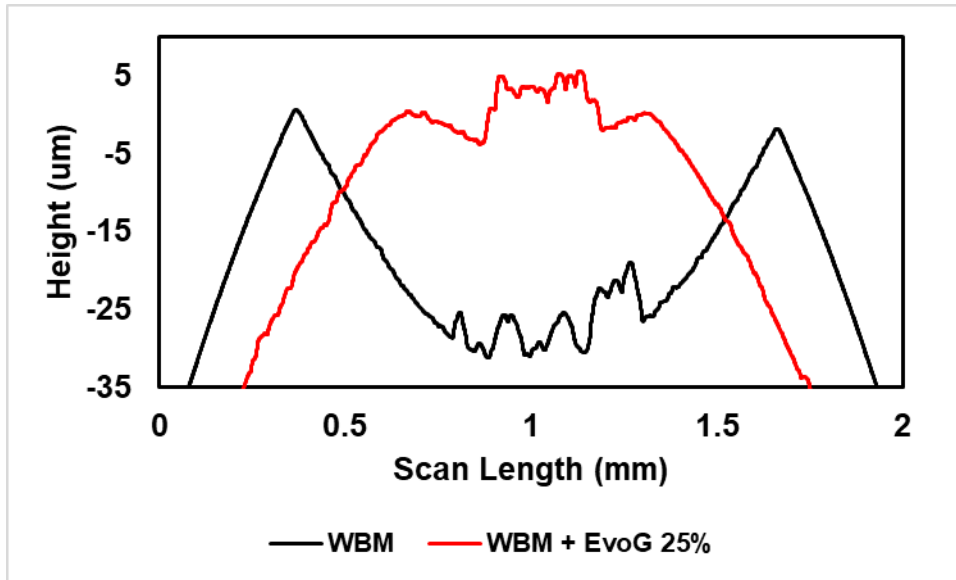


Figure 53: Surface profile of WBM and WBM + EvoLube-G 25% dosage

CHAPTER 4

TRIBOCHEMISTRY OF FRICTION AND WEAR REDUCTION

Tribochemistry can be defined as the chemical reactions that occur between the lubricant/environment, and the surfaces under boundary lubrication conditions. However the precise nature of the chemical reactions and the causes of the reactions are only subjects of speculation due to the lack of techniques to characterize them [10]. When a lubricant OFM mixtures such as Escaid + EMamide-2 is used in boundary lubrication, it is found that OFM participate in tribochemical interactions generating passive lubricating layer substrate also known as metallic soap or salt or tribochemical layer. This was proven in Bowden and Tabor's sliding friction experiments when they found that adding lauric acid into paraffin oil used as lubricant significantly lowers the COF [42]. Although the tribochemistry of lubricant additive mixtures on metal surfaces is not well understood, it is speculated that the generation of organic salt layer is one of the key mechanisms in COF and wear reduction [11].

Recent observations of surface emissions of electrons, charged particles, from rubbing surfaces invites speculation that this emission provides the source of energy causing tribochemical reactions to take place [10]. Analysis tools such as ToF SIMS fills in the gap by providing elemental composition of tribological interfaces to analyze the reactions between OFM, lubricating fluid, and metal substrate that causes the reduction of COF and wear. Three Escaid and two WBM lubricated interfaces are tribochemically characterized using ToF SIMS to understand its lubricating mechanism in OBM. They are Escaid, Escaid + EMamide-2, Escaid + Amphiphile S, WBM, and WBM + ¼ dose EvoLube G.

4.1. Chemical Analysis of Lubricating Fluid/ Additive Mixture

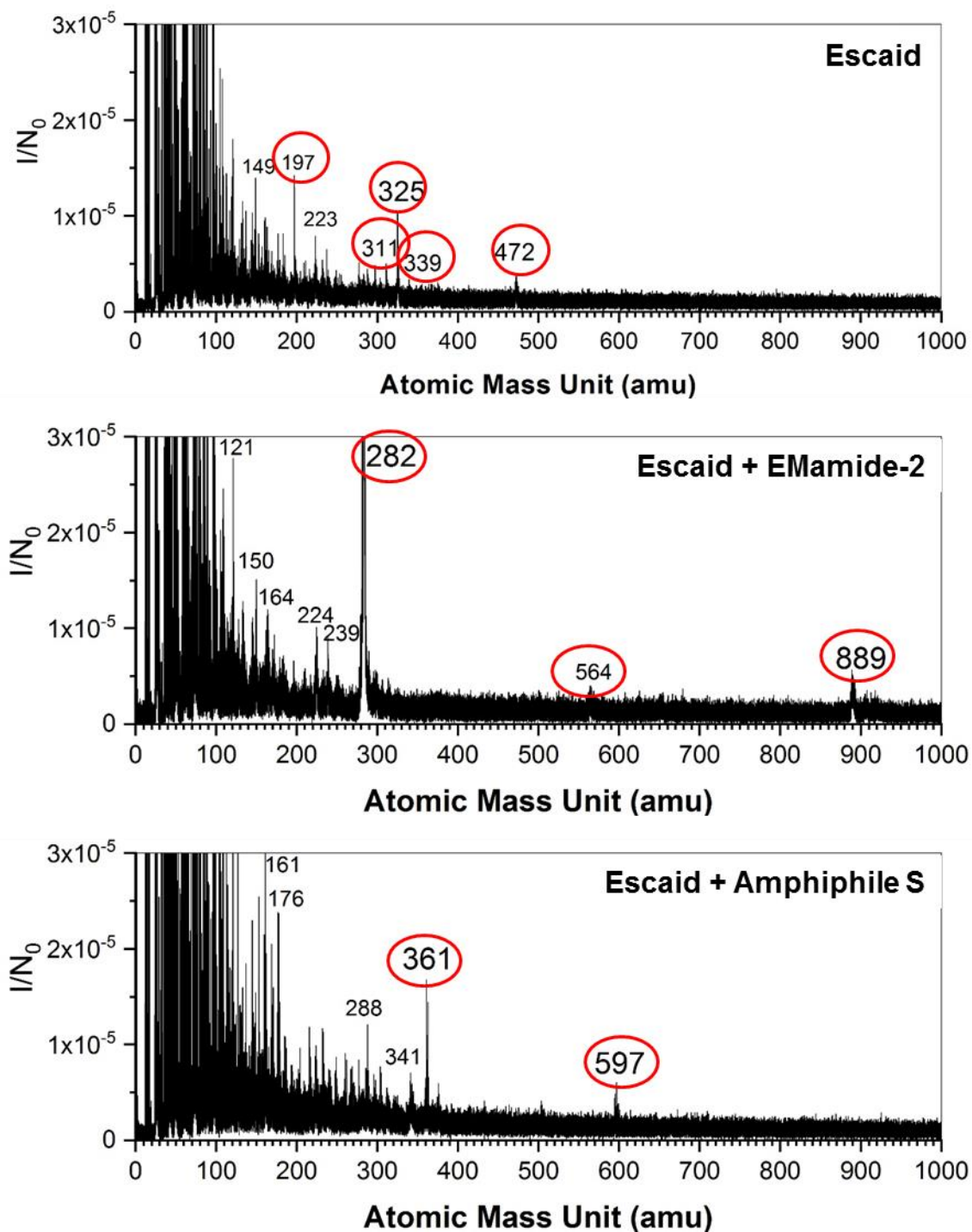


Figure 54: Mass spectrum of a) Escaid (BF), b) Escaid + EMamide-2, c) Escaid + Amphiphile S in carbon nanotube (CNT) structure

Before analyzing the surface of tribologically tested samples, the molecular composition of the OFM-lubricant mixtures are analyzed. This information is crucial for observing the presence of both the lubricating fluid and OFMs and their changes on the contact interface following tribological experiments. The following analyses are for Escaid, Escaid + EMamide-2, and Escaid + Amphiphile S. Escaid is chosen because the presence of solid compositions in both OBM make them impossible to characterize due to the need for ultra-high vacuum. In the case of WBM, chemical analyses are not conducted due to the unavailability of the WBM base fluid; however, it is known that KCl brine is the base stock with the addition of some polymer and that the chemical composition of EvoLube G is mostly known.

For Escaid mixtures, porous carbon nanotube (CNT) is used as a sponge that holds the lubricant when the sample chamber of SIMS is being vacuumed. Illustrated in Figure 54, the mass spectrum for the mass range of 0-150 shows collection of small molecular fragments of BF, additive molecules, and other ionic compositions, while molecular mass larger than 150 comes from larger fragments of Escaid and/ or OFM molecules. Larger ionic fragmentation of Escaid yields a lower intensity because Escaid is made of covalent bonds; thus, harder to deionize.

Figure 54 (a) shows the mass spectrum of Escaid having high molecular peaks of 311, 325, 339, and 472 atomic mass units (amu). In comparison, spectrum of Escaid + EMamide-2 in Figure 54 (b) shows that the peaks associated to Escaid are weakened but a very high molecular weight (MW) 282, 564, and 889 peaks that belong to EMamide-2 are introduced. In comparison when analyzing Escaid + Amphiphile S, peaks of MW 361 – 363 and 597 amu dominate the spectrum in the analysis as shown in Figure 54 (c). In conjunction, the MW of Escaid weakens as well.

As an explanation to the disappearance of Escaid molecules, when an ion beam characterization technique such as ToF SIMS that works best for ion detection is used to characterized covalent species, even small presence of ionic species such as EMamide-2 or Amphiphile S will dominate the intensity. This is the reason why detection of BF molecules are obscured in the presence of EMamide-2 and Amphiphile S although the dosage of both OFMs in Escaid are relatively low. Additionally, MW 564 that is found in EMamide-2 is exactly double the MW 282 amu, implying that the additive form a dimer of two molecules.

Knowing the MW of EMamide-2 and the fact that it is an amide, NIST handbook is used to find the potential exact chemistry of EMamide-2. Some chemicals such as Acetamide, N-[2-(2-cyanoethyl)-1-cyclohexen-1-yl]-N-(phenylmethyl)- with chemical formula $C_{18}H_{22}N_2O$ are one of the possible answers [43]. When the chemical compositions of the additives are known, their chemical reactions with metals can be predicted using thermodynamic and electrochemistry relationship.

4.2. Tribochemical Analysis of Tribological Surface

In this section, tribochemical analyses are conducted on surfaces of samples that are on wear track, labeled as “In wear track”, as well as surfaces of samples that are out of tribological contact but submerged in the lubricant mixture, labeled as ”Out of wear track”, to study the formation of protective tribochemical layer.

4.2.1. Escaid

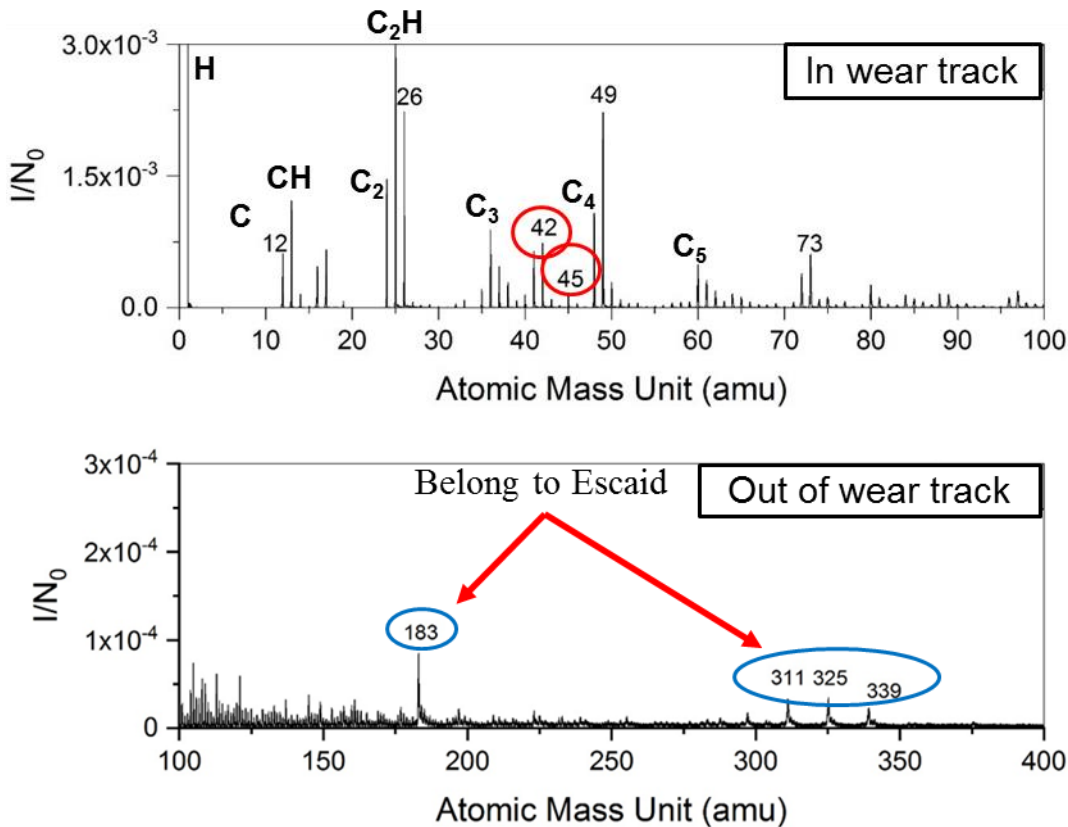


Figure 55: Mass spectrum of wear track surface on sample lubricated with Escaid
Analysis conducted on the ball lubricated with Escaid discovers deposit of three previously characterized Escaid-associated molecular species on damaged wear track surface as depicted in Figure 55. These molecules may be adsorbed and act as bearing element during the tribological process without chemically reacting with the metal substrate. In the lubrication process, superior lubricants will separate the two contacting surface to reduce metal-to-metal contact which is what lubricating fluid like Escaid is designed to do. Analysis on undamaged surface is not conducted provided that no significant chemical reactions are found even in undamaged surface lubricated with either Escaid + EMamide-2 or Escaid + Amphiphile S, aside from the reduced intensities, as shown in Figure 56 and Figure 57.

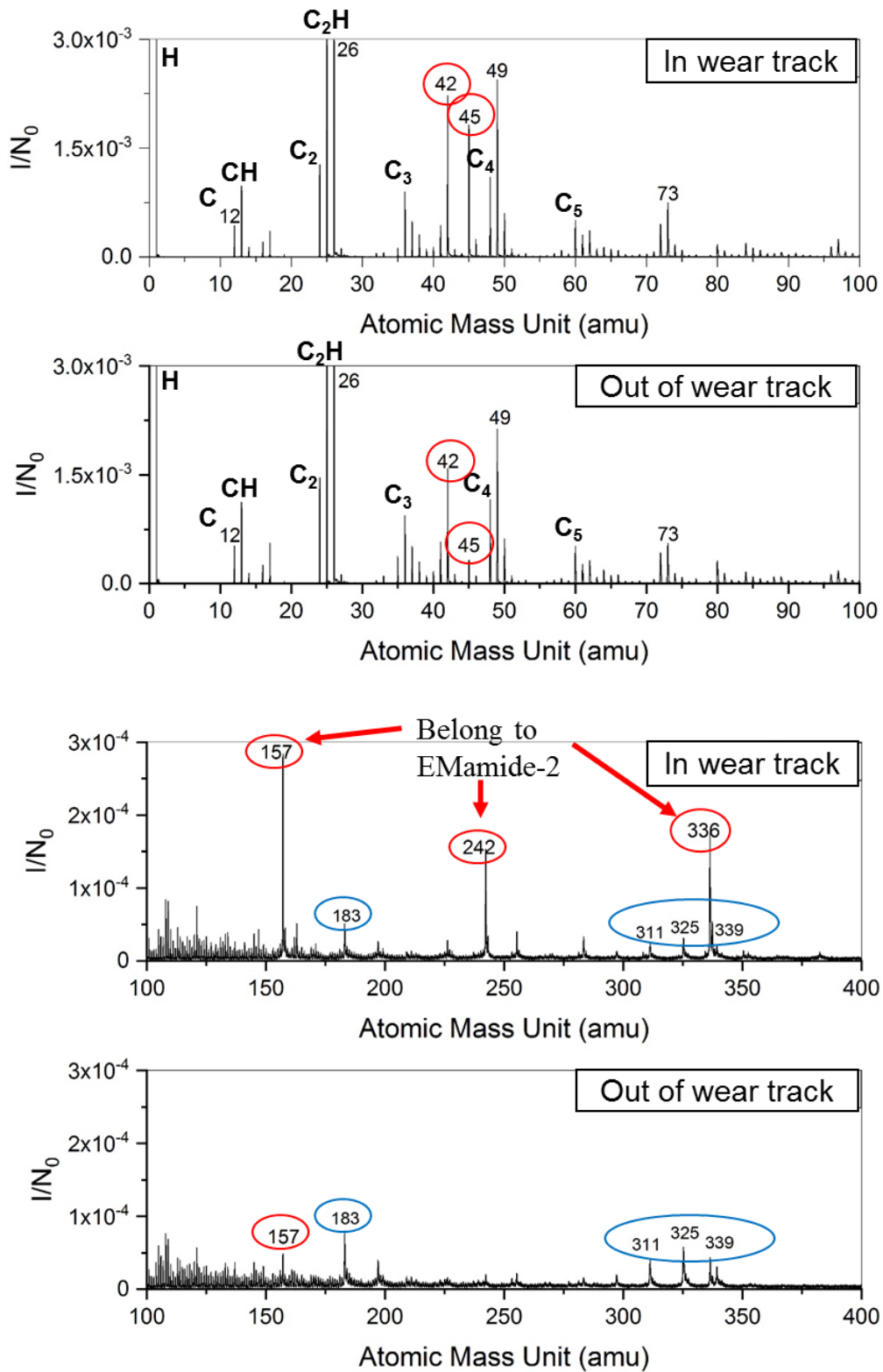


Figure 56: Mass spectrum of surfaces on sample lubricated by Escaid + EMamide-2

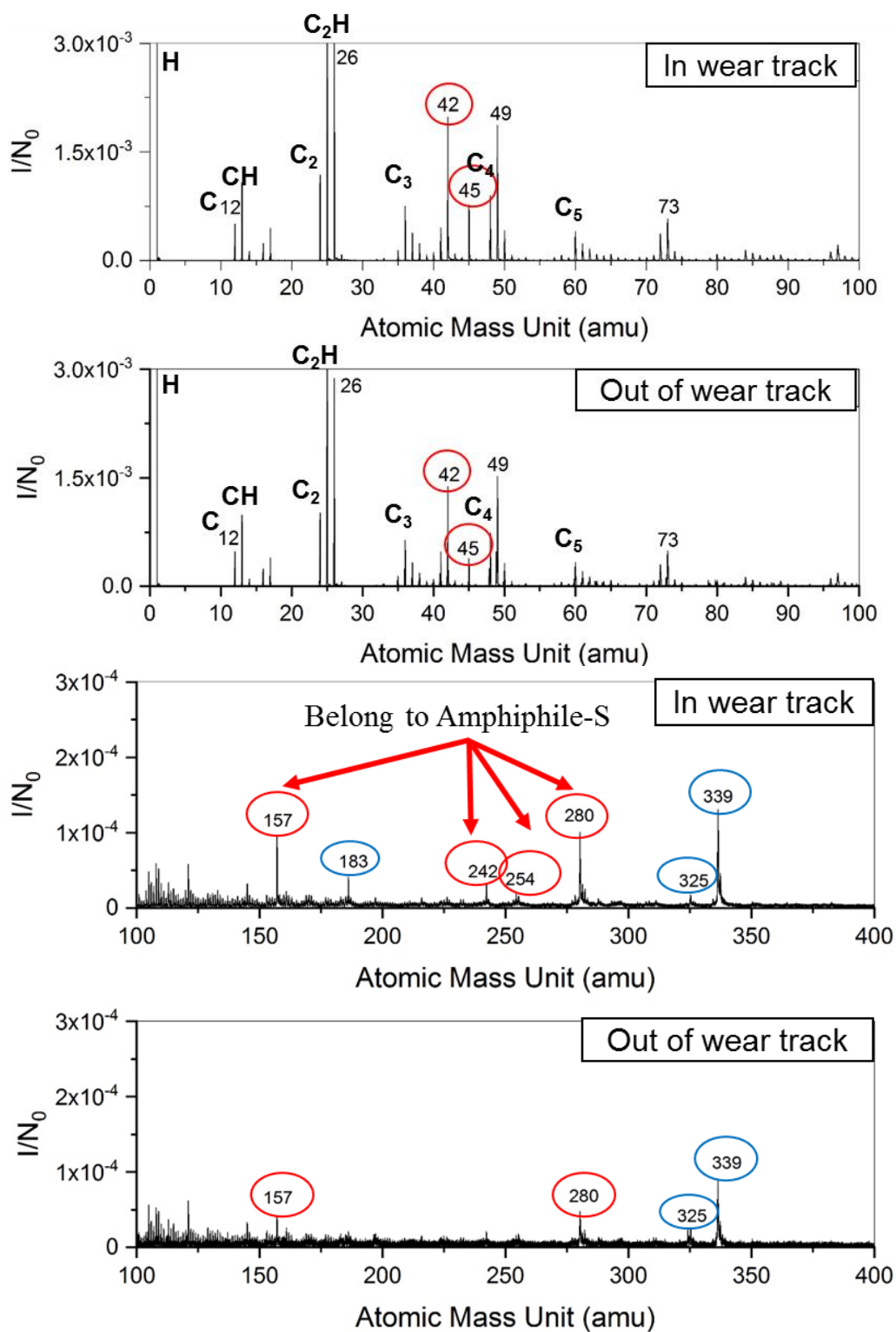


Figure 57: Mass spectrum of surfaces on sample lubricated by Escaid + Amphiphile S

In the case of incorporating OFM into lubricating fluid such as Escaid + EMamide-2, based on literature discussed in Chapter 2, OFM molecules are designed to reduce COF and wear by forming a protective layer. Analysis of surface on wear track that is lubricated by Escaid + EMamide-2 traces significant compounds on sample surface that belongs to EMamide-2 such as molecular mass 157, 242, and 336 and several other lower intensity molecules including 311, 325, 336 that belongs to Escaid as shown in Figure 56. Except that of Escaid, the species are suspected to be fragments of EMamide-2's original molecule that bonds with metal surface in tribological process. Using information from oil and additives chemical analysis, we know that EMamide-2 has characteristic molecular weight 282 amu. ToF SIMS analysis on the surface also found an increase of 42 and 45 amu that from literature discussed in Chapter 2 are speculated to be amide and fatty acid head group. Subtracting amide (42 amu) from EMamide-2 (282 amu), we get 240 amu, which is close to 242 amu detected. Prior hypothesis stated that OFM will bond with metal iron (55 amu) generating protective iron organic salt layer. Additionally, its lipophilic tails attracts Escaid molecules, and suspend them as a protective oil layer that reduces metal-to-metal contact. On undamaged surface, low intensity of molecular mass 157, 242, 336 are detected, showing that high temperature and pressure in tribological process supply additional energy for these reactions to occur. Additionally, EMamide-2 reduces O⁻ level on metal surface by 74% and FeO₃⁻ level by 53% compared to Escaid lubricated surface.

Analysis of surface on wear trace that is lubricated by Escaid + Amphiphile S traces evidence of Amphiphile S such as molecular mass 157, 280, and 339 and lower intensity species as shown in Figure 57. Some of these peaks show similarity with Escaid + EMamide-2 sample although their intensities are much lower relatively. Theoretically, Amphiphile S would experience the same tribochemical layer generation process during tribological experiments. Only two of the three

species that belong to Escaid, 311 and 325, are discovered on the surface which can also possibly be fragments of Amphiphile S instead. Possible explanation to this is because the organic salts formed by Amphiphile S only attract Escaid molecules mildly or generate a fairly weak tribochemical layer leading to higher COF in comparison with EMamide-2. On undamaged surface of this sample, the variety of molecular species is reduced. This result supports the previously made statement about how tribological experiment provides energy for some tribochemical process to occur.

4.2.2. Water-Based Mud

Due to unavailability of water-based base fluid (BF), ToF SIMS is conducted on WBM lubricated samples. This adds complexity to the analysis as solid compositions such as barium sulfate, silica, and other salts may be embedded on the surface and read by ToF SIMS. Two samples from tribological experiment are chosen, WBM and WBM + ¼ dose EvoLube G lubricated samples. Before characterized with ToF SIMS, samples are cleaned with isopropanol to ensure the surface is free of contaminants. Two areas with different degree of damage on wear track are analyzed. Analysis conducted on severely damaged surface of ball lubricated with WBM discovers deposit of various molecular species embedded on sample surface as depicted in Figure 58. High level of chlorine MW 35 amu from potassium chloride is observed, as well as MW 16, 17, 76, 77, 119, 137, 148, and 179 amu species that are found with lower intensity on moderately damaged surface. High intensity of species associated to petroleum distillates, 311, 325, 339 amu are also observed on surface mildly damaged surface indicating the presence of oil molecules. Presence of silicon oxide clusters are found on wear track depicted as mass 60, 77,

119, and some other high molecular mass most likely originated from solid composition of mud and oxidized metals.

Figure 59 shows the mass spectrum of surface lubricated with WBM + ¼ dosage EvoLube G. The mass spectrum shows more similarity with Escaid lubricated surface than with WBM lubricated surface with the addition of MW 277, 288, 297 amu. Even on severely damaged surface, there is no trace of silicon oxide clusters. This shows that EvoLube G protects the surface from damage and inhibits formation or embedment of some compounds found on severely damaged surface lubricated with WBM.

In Escaid lubricated tests, we know that the occurrence of peaks are associated to generation of tribochemical film or chemical reactions, and that peaks contribute to the decrease of COF and wear. However, in WBM, solid composition of mud may become embedded on damaged surface, adding complexity to the analysis. These embedments may be abrasive and causing increase to COF and wear. Therefore, for the case of WBM, SIMS result itself cannot be used to conclude whether certain molecular peaks correspond to tribochemical layer and whether if they are improving tribological performance or not.

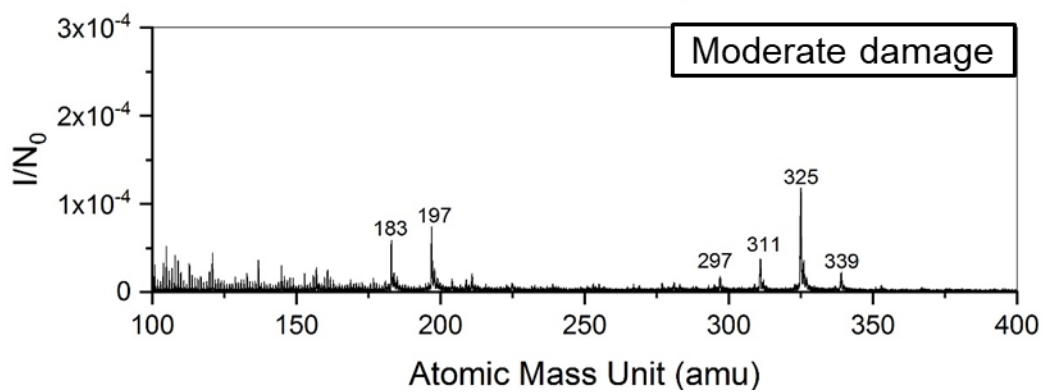
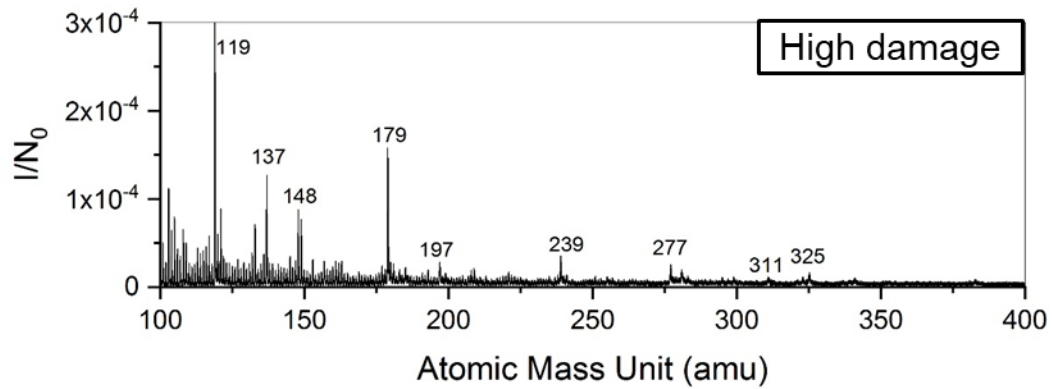
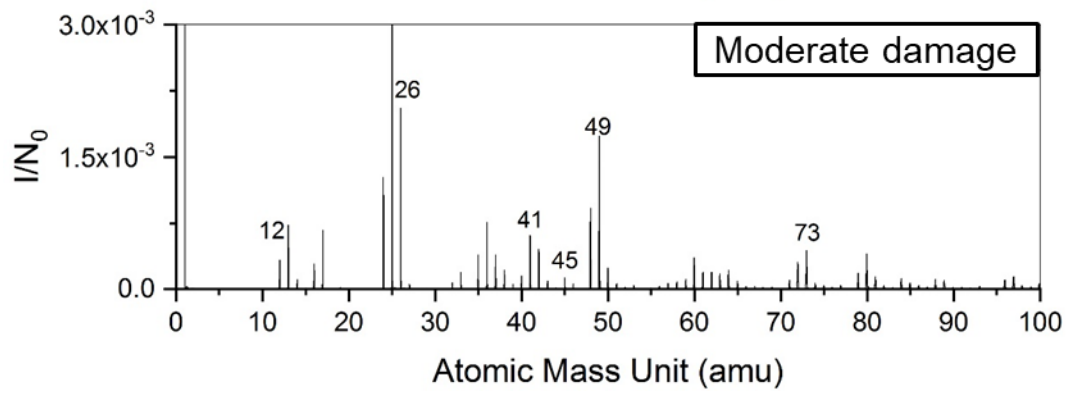
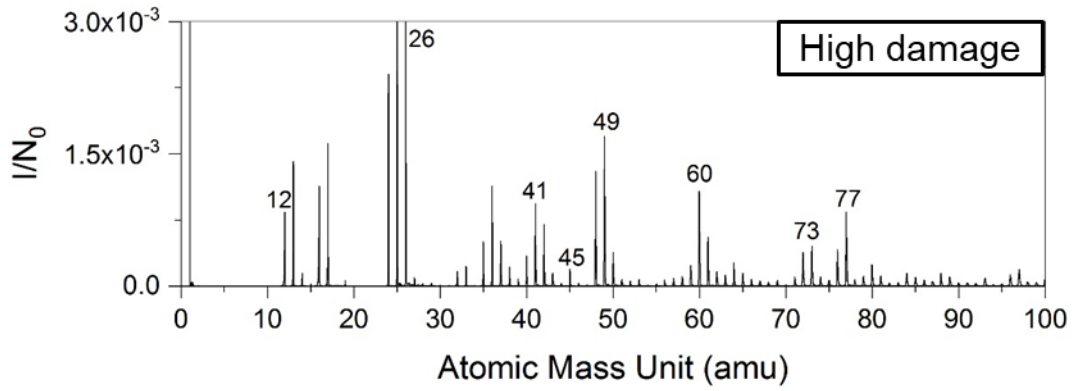


Figure 58: Mass spectrum of surfaces on sample lubricated by WBM

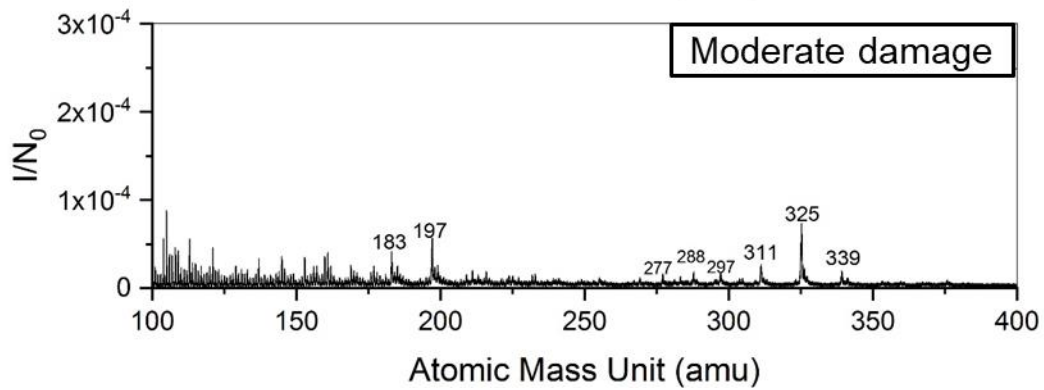
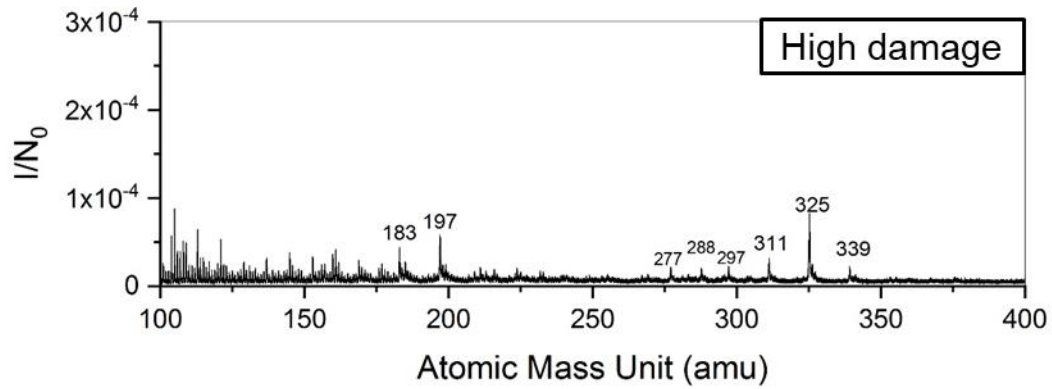
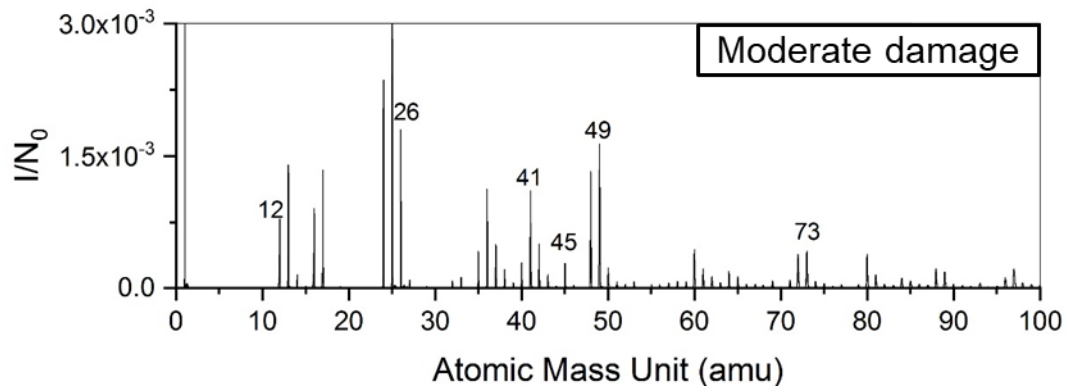
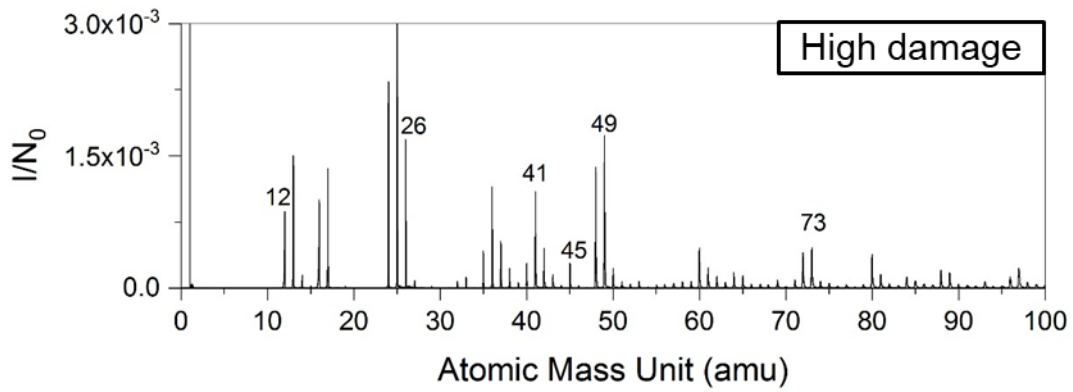


Figure 59: Mass spectrum of surfaces on sample lubricated by WBM + EvoLube G

4.3. Coverage Level Analysis and Summary

Another information obtained from ToF SIMS analysis is the coverage of additive molecules on the metal surface. Such information is important in determining tribological synergy as well as for engineers and scientists to optimize the amount additive dosage needed for particular interfaces. Degree of coverage calculation of ToF SIMS is discussed by Stanislav [44]. Coverage analysis of sample lubricated Escaid + EMamide-2 discovers that molecular compounds associated to EMamide-2 cover 50 to 63% of total wear track surface, while molecular compounds associated to Amphiphile S cover 38 to 48% of total surface of wear track. The optimum dosage of additive can then be determined by studying the effect of dosage variation on COF and wear reduction and using ToF SIMS to trace the level of additive coverage on surface.

Thus, for OFM to effectively increase lubricant's technical performance, they have to sufficiently cover contact surface area, which is a challenge especially in large sums lubrication systems such as oil and gas drilling where heterogeneity is present. Additionally, excess tribochemical film may even increase adhesive wear or shear stress leading to increase COF and wear as seen on tribological test result in Chapter 3. Therefore, the right balance of additive is critical in improving technical performance and reducing cost. Statistical approach may be used to determine the appropriate amount of additives needed in such dynamic lubrication process.

Although OFM is proven to be effective to reduce friction and wear, another important factor needs to be considered is the mechanical properties of this tribochemical layer such as melting temperature and shear-strength of the tribochemical film generated [42]. Based on J.A. Williams, the effect of temperature on surface films comes to play when temperature of the interface reaches melting point of the tribochemical film [42]. For instance, tribochemical layer generated

by Amphiphile S may deteriorate faster due to subsurface temperature increase caused by elevated solid particles entrainment in OBM experiments. To encounter the need to perform in extreme elevated temperature and pressure such as the oil and gas drilling, OFM alone may not be sufficient to reduce COF and wear. Other form of low-shear-strength film is required and can be obtained with the use of extreme-pressure or e.p. additives that provides excellent lubrication for high-temperature applications up to 300-400°C, a typical condition in a deep drilling. E.p. additives generally consist of small quantities of organic compound containing chlorine, sulfur, and phosphorus that will react with hot metallic surface forming protective films of solid metal chloride, sulphide, and phosphide. Since these compounds are inert in low temperature, OFM and e.p. additives are used in conjunction to widen range of lubricant operating temperature as observed by Fuller [45].

In summary, some of the major ToF SIMS findings from this study are as follows:

1. OFM chemically bond with metal substrate creating one or more organic salt compounds that protect the surface. Lipophilic fragments of OFM that bonds with metal may attract oil molecules and suspend them as hydrodynamic film.
2. EMamide-2 associated species cover 50 to 63% of total surface area on wear track.
3. Amphiphile S associated species cover 38 to 48% of total surface area on wear track.
4. The formation of tribochemical layer is enhanced with tribological process. This can be observed as undamaged surface in both EMamide-2 and Amphiphile S yield lower level of organic salt compared to surface on wear track.
5. Excessive tribochemical film may increase adhesive wear or shear stress leading to an increased COF.

CHAPTER 5

CONCLUSION AND FUTURE WORK

Use of lubricant additives such as Organic friction modifier (OFM) can significantly improve technical performance of lubricating fluids in terms of friction and wear reduction. It lowers industry operating expenses by reducing energy, materials, and time consumption. Use of EMamide-2 reduces COF of OBM by as high as 36% and wear by 90%, while use of EvoLube G reduces COF of WBM by 62% and wear by 42%. However, improving friction and wear may be challenging when the solution has undesirable tradeoffs. In this case, EMamide-2 causes agglomeration of solid mud compositions which may lead to other technical complications in the drilling process such as difficulty in hole-cleaning. Thus, it is very important to fundamentally understand how these additives impacted mud lubricity. Surface characterization of worn samples using ToF SIMS discovers that tribological process provides additional activation energy for EMamide-2's molecules to chemically bond with metal substrate creating one or more organic salt compounds. Due to EMamide-2's amphiphilic properties, its lipophilic tails attract oil molecules and suspends them as a protective film. This process known as tribochemistry generates layer of lubricating compounds called tribochemical layer that covers 50 to 63% of wear surface lubricated with Escaid + EMamide-2. The tribochemical layer generation process is also valid for Amphiphile S and EvoLube G. However, tribological shows that Amphiphile S does not produce strong enough protective layer especially considering its low effect on COF and negative wear reduction of OBM where solid particles are present. As the effect of different OFM head groups on lubricity had been studied, this study is expected to be the first step in quantifying lubricity and mechanical properties of various tribochemical layers generated by those OFMs.

The conclusion of this study are as follows:

1. Use of OFM in drilling fluid can reduce COF by up to ~60% and wear volume by up to ~95%.
2. WBM has comparably higher COF and wear in comparison to OBM, but the effect of OFM is more potent in WBM. Its performance can be improved to compare with OBM and is desirable due to its lower cost and environmental impact
3. Literature shows that OFM will readily bond with metal substrate forming an organic salt film also known as tribochemical layer or metal soap. The three factors that determine the effectiveness of OFM in producing the protective layers are:
 - a. Chemical bonding strength between OFM and metal substrate.
 - b. Mechanical properties of the generated tribochemical layer such as its melting temperature and shear strength.
 - c. Degree of coverage of generated tribochemical layer on a tribological interface.
4. Using ToF SIMS, the molecular weight (MW) of Escaid, EMamide-2, and Amphiphile S are found. Tribochemical analysis on the wear surface of Escaid (BF) + EMamide-2 lubricated sample also found molecular species that are speculated to be tribochemical layer contributing to the reduction of COF and wear. In comparison, the surface lubricated by Escaid does not produce them. Surface lubricated by Escaid (BF) + Amphiphile S produce molecular species of different kind.
5. The degree of coverage study shows that molecular species associated to EMamide-2 cover 50 – 63% of the wear track surface of the sample lubricated by Escaid + EMamide-2. While on the wear surface of sample lubricated by Escaid + Amphiphile S, the

molecular species associated to Amphiphile S cover only 38 – 48% of the lubricated surface.

6. Although the composition of some of the OFMs are unknown, using ToF SIMS result, NIST handbook, and the knowledge of head group presenting the OFM, the chemistry of OFM can be found to better understand their reactions with metals that generate protective tribochemical layer and the mechanical properties of corresponding layers that contributes to the reduction of COF and wear.

Based on this study, recommendations for future work are as follows:

1. Incorporate extreme pressure additive such as organics with active chloride, sulfur, and phosphorus group into OFM additives to meet desired drilling mud performance.
2. Select OFM and e.p. additives that chemically react and bond strongly with drill string and casing materials without impairing COF performance.
3. Tribological performance of lubricant mixtures with field materials such as drill string and casing aluminum and steel alloys and hardfacing materials
4. Tribological performance of OFM in WBM base stock/ base fluid and their tribochemical analysis.
5. Quantify mechanical shear strength of tribochemical layer generated to understand what type of active OFM and e.p. head groups are most effective in reducing friction and wear, perhaps using nanoscratch method, when technology available.

REFERENCES

1. Payne, M. L., Cocking, D. A. & Hatch, A. J. Critical Technologies for Success in Extended Reach Drilling. in *SPE Annual Technical Conference and Exhibition* (1994). doi:10.2118/28293-MS
2. Allen, F., Tooms, P., Conran, G., Lesso, B. & Slijke, P. Van De. Extended-Reach Drilling : Breaking the 10-km Barrier. *Oilf. Rev.* **Winter**, 32–47 (1997).
3. Blix, P. E. M. United States Patent (19). (1975). doi:10.1016/j.(73)
4. Bray, B. U. B., Moore, C. C. & Merrill, D. R. Improvements in Diesel-Engine Lubricating Oils. 35–42 (2017). doi:10.4271/390125
5. Prutton, C. F., Frey, D. R., Turnbull, D. & Dlouhy, G. Corrosion of Metals by Organic Acids in Hydrocarbon Solvents. *Ind. Eng. Chem.* **37**, 90–100 (1945).
6. Herschel G. Smith, Wallingford, and Troy L. Cantrell, Drexel Hill, Pa., and J. G. P. Mineral Oil Compositions Containing Amidic Acids or Salts Thereof. (1955).
7. Eckert, G. W. Adducts of Aliphatic Monocarboxylic Acids and Aliphatic Amines in Gasoline. 2–3 (1962).
8. Schick, J. W. & Kaminski, J. M. Lubricant Composition for Reduction of Fuel Consumption in Internal Combustion Engines. (1981).
9. Sirianni, A. F. & Puddington, I. E. Friction Reducing Additives for Lubricants. (1954).
10. Hsu, S. M., Zhang, J. & Yin, Z. The nature and origin of tribochemistry. in *Tribology Letters* (2002). doi:10.1023/A:1020112901674
11. Spikes, H. Friction Modifier Additives. *Tribol. Lett.* **60**, 1–26 (2015).

12. Okabe, H., Masuko, M. & Sakurai, K. Dynamic behavior of surface-adsorbed molecules under boundary lubrication. *ASLE Trans.* (1981). doi:10.1080/05698198108983044
13. Jahanmir, S. & Beltzer, M. Effect of Additive Molecular Structure on Friction Coefficient and Adsorption. *J. Tribol.* (1986). doi:10.1115/1.3261129
14. Larsen, D. H. Use of Clay in Drilling Fluids. *Clays Clay Miner.* **1**, 269–281 (1952).
15. Williams, J. The friction of solids. in *Engineering Tribology* 132 (205AD).
16. Holmberg, K. & Erdemir, A. Influence of tribology on global energy consumption, costs and emissions. *Friction* (2017). doi:10.1007/s40544-017-0183-5
17. Bol, G. M. Effect of Mud Composition on Wear and Friction of Casing and Tool Joints. *SPE Drill. Eng.* **1**, 369–376 (1986).
18. Woydt, M. & Wäsche, R. The history of the Stribeck curve and ball bearing steels: The role of Adolf Martens. *Wear* **268**, 1542–1546 (2010).
19. Williams, J. Wear and Surface Damage. in *Engineering Tribology* 166–192 (2005). doi:10.1017/CBO9780511805905
20. Chilingarian, G.V. ; Vorabutr, P. *Drilling and Drilling Fluids*. (Elsevier Scientific, 1981).
21. Caenn, R., Darley, H. C. H. & Gray, G. R. *Composition and Properties of Drilling and Completion Fluids. Composition and Properties of Drilling and Completion Fluids* (2011). doi:10.1016/C2009-0-64504-9
22. Caenn, R. & Chillingar, G. V. Drilling fluids: State of the art. *J. Pet. Sci. Eng.* **14**, 221–230 (1996).

23. SPE. Drilling fluid types. (2001). Available at:
http://petrowiki.org/Drilling_fluid_types#Synthetic-based_drilling_fluids.
24. Al., P. et. Oil Based Synthetic Hydrocarbon Drilling Fluid. (1993).
25. Noria Corporation. Lubricant Additives - A Practical Guide. Available at:
<https://www.machinerylubrication.com/Read/31107/oil-lubricant-additives>.
26. Institute for Reduction of Cognitive Entropy in Organic Chemistry. Illustrated Glossary of Organic Chemistry - Amphiphilic. Available at:
<http://www.chem.ucla.edu/~harding/IGOC/A/amphiphilic.html>.
27. Kier, L. B. Quantitation of solvent polarity based on molecular structure. *J. Pharm. Sci.* **70**, 930–3 (1981).
28. ASTM. Standard Test Method for Measurement of Extreme-Pressure Properties of Lubricating Fluids (Four-Ball Method) 1. **03**, 1–9 (2013).
29. ASTM. Standard Test Method for Determination of the Coefficient of Friction of Lubricants Using the Four-Ball Wear Test Machine 1. *Annu. B. ASTM Stand.* **95**, 1–5 (2007).
30. ASTM. Standard Specification for High-Carbon Anti-Friction Bearing Steel. *Astm* 1–4 (2015). doi:10.1520/A0295
31. Lake, L. W. & Mitchell, R. F. *Petroleum Engineering Handbook, Volume 2: Drilling Engineering. Drilling Fluids Processing Handbook* (2005).
doi:<http://dx.doi.org/10.1016/B978-075067775-2/50003-2>
32. Schlumberger. Schlumberger Oilfield Glossary: Where the Oilfield Meets the Glossary.

Available at: <http://www.glossary.oilfield.slb.com/>.

33. Lan, P. & Polycarpou, A. A. High temperature and high pressure tribological experiments of advanced polymeric coatings in the presence of drilling mud for oil & gas applications. *Tribol. Int.* **120**, 218–225 (2018).
34. Hosterman, J. & Patterson, S. Bentonite and fuller's earth resources of the United States. *U. S. Geol. Surv. Prof. Pap. 1522* **1522**, 45 (1992).
35. Newpark Resources Inc. *KCL Polymer Water-Based Drilling Fluid System*.
36. LibreText, C. Structure of Amides. Available at:
[https://chem.libretexts.org/Textbook_Maps/Organic_Chemistry/Supplemental_Modules_\(Organic_Chemistry\)/Amides/Properties_of_Amides/Structure_of_Amides](https://chem.libretexts.org/Textbook_Maps/Organic_Chemistry/Supplemental_Modules_(Organic_Chemistry)/Amides/Properties_of_Amides/Structure_of_Amides).
37. Integrity Industries. UltraLube II. Available at: <http://www.integrityindustries.com/ultra-lube-ii.html>.
38. Newpark Resources Inc. EvoLube G. Available at: <https://www.newpark.com/evolube-g/>.
39. Williams, J. Contact between surfaces. in *Engineering Tribology* 92–96 (2005).
40. Geochemical Instrumentation and Analysis. Secondary Ion Mass Spectrometer (SIMS). Available at:
https://serc.carleton.edu/research_education/geochemsheets/techniques/SIMS.html.
41. Chang, R. Chemistry. in *McGraw-Hill* 814–850 (2011). doi:10.1007/s00044-012-9998-9
42. Williams, J. Boundary Lubrication and friction. in *Engineering Tribology* (2005). doi:10.1017/CBO9780511805905

43. WebBook, N. C. Acetamide. Available at:
<https://webbook.nist.gov/cgi/cbook.cgi?ID=C82365251&Units=SI>.
44. Verkhoturov, S. V. *et al.* ‘Trampoline’ ejection of organic molecules from graphene and graphite via keV cluster ions impacts. *J. Chem. Phys.* (2018). doi:10.1063/1.5021352
45. Fuller, D. D. *Theory and Practice of Lubrication for Engineers.* (Wiley, 1984).

APPENDIX A

FOUR-BALL TEST PROCEDURE

1. Sample Cleaning

- a) Rinse 4 52100 alloy steel bearing balls lightly with acetone and rub with wipes
- b) Ultrasonically clean for 15 minutes (start Step 2 while sonic cleaning)
- c) Rinse setup lightly with acetone and rub with wipes
- d) Rinse balls lightly with acetone and dry with wipe

2. Drilling Fluid/ Lubricant Preparation

- a) Prepare 25 ml of lubricant per trial
- b) If not using an additive
 - Don't need to be exact with 25 ml/trial, just be close
- c) If using an additive
 - Need to be exact with 25 ml/trial
 - Add the additive using the scale and chart with how much additive to use
- d) Clean a stirring magnetic bar with acetone and air dryer
- e) Place mixture on the room temperature hot plate with the stir bar and a plastic science paper covering
- f) Set hot plate to 75C and 400 RPM, heat for 30 minutes

3. Falex Four-ball Friction and Wear Test Machine Setup

- a) Load balls into holder, tighten main bolt down tightly
- b) Set machine Hc = 1, HL = 18 (starting at 22C, this takes approximately 20 min)
- c) Note: make sure other values are set correctly:

1. $P_b = 1$
 2. $t_i = \text{off}$
 3. $t_d = 5$
 4. $AP = 1.00$
- d) Once the machine reaches 72C, set machine $H_c = 5$, $HL = 12$
4. Begin experiment
 - a) Pour lubricant in holder, set holder in machine
 - b) Make sure load is zeroed, then load to 15 kg
 - c) Put friction force chain in place, “zero” to 655
 - d) Adjust the time to desired time, plus one minute (for example, if running a 60 minute experiment, set to 61 minutes)
 - e) Check to make sure labview saves the data
 - f) Start Labview data collection
 - g) Start machine “Drive Start”
 - h) Make sure “Specimen RPM” = 400 to 403, “Load Kilograms” = 15.0, Temperature = 73C to 77C
 - i) Remember to turn off heating for the rest of the oil for next experiment.
 5. Prepare for next experiment (while the previous experiment is running)
 - a) Prepare mixture
 - b) If running a trial with the same lubricant, begin heating at the 40 minute mark of the running trial. If running a trial with a different lubricant, begin the steps at the beginning under Step 1 “Prepare Mixture”

6. Finish experiment

- a) Click “STOP” in Labview, (NOT THE RED STOP SIGN), change file name
- b) “Unload” setup
- c) Slightly loosen the main bolt
- d) Pour excess lubricant into the waste collection
- e) Clean setup

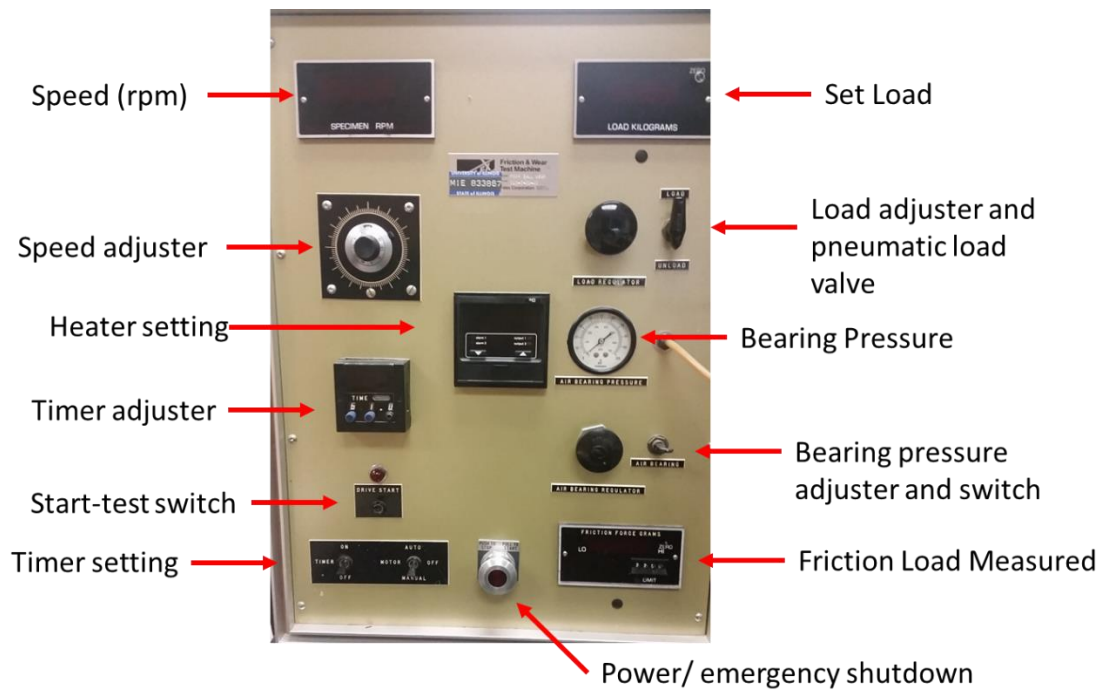


Figure 60: Falex Four-Ball user interface

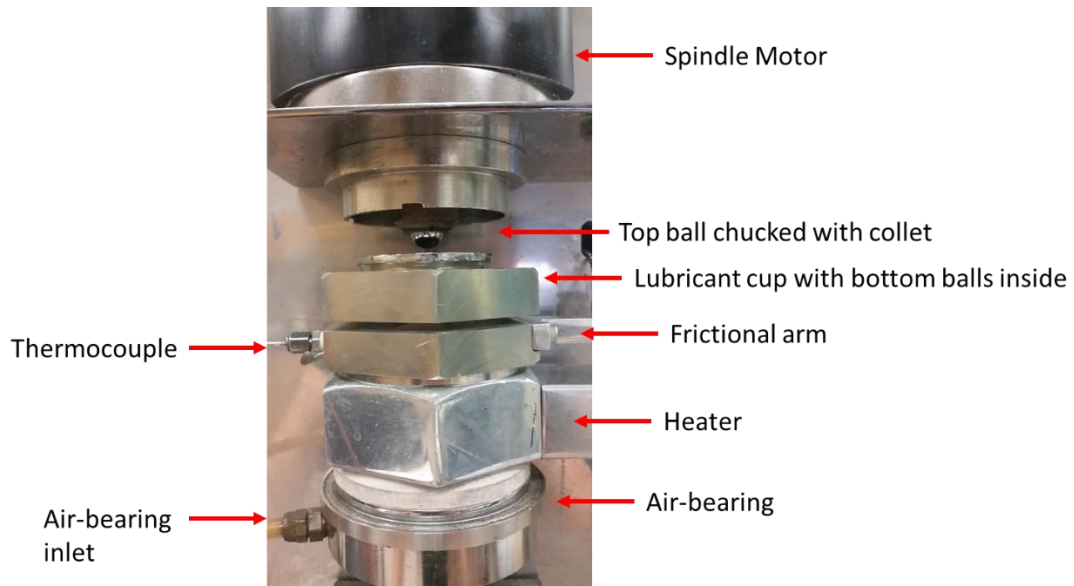


Figure 61: Falex Four-Ball setup before experiment

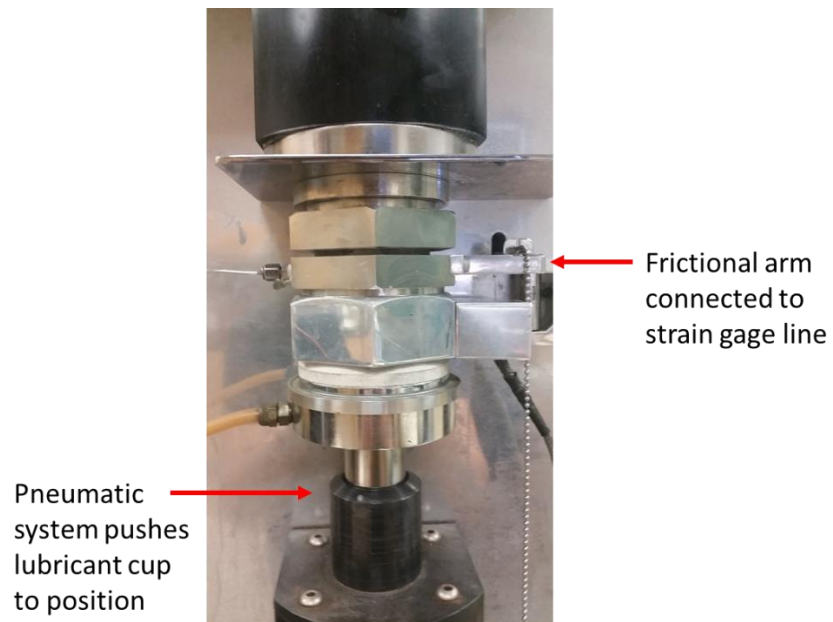


Figure 62: Falex Four-Ball setup during experiment

APPENDIX B

FALEX FOUR-BALL TESTER DAQ WIRING

Data acquisition of Falex Four-ball tester are wired as shown on Figure 63 and Figure 64.

Analog output is then collected by Labview as written in chapter 2.

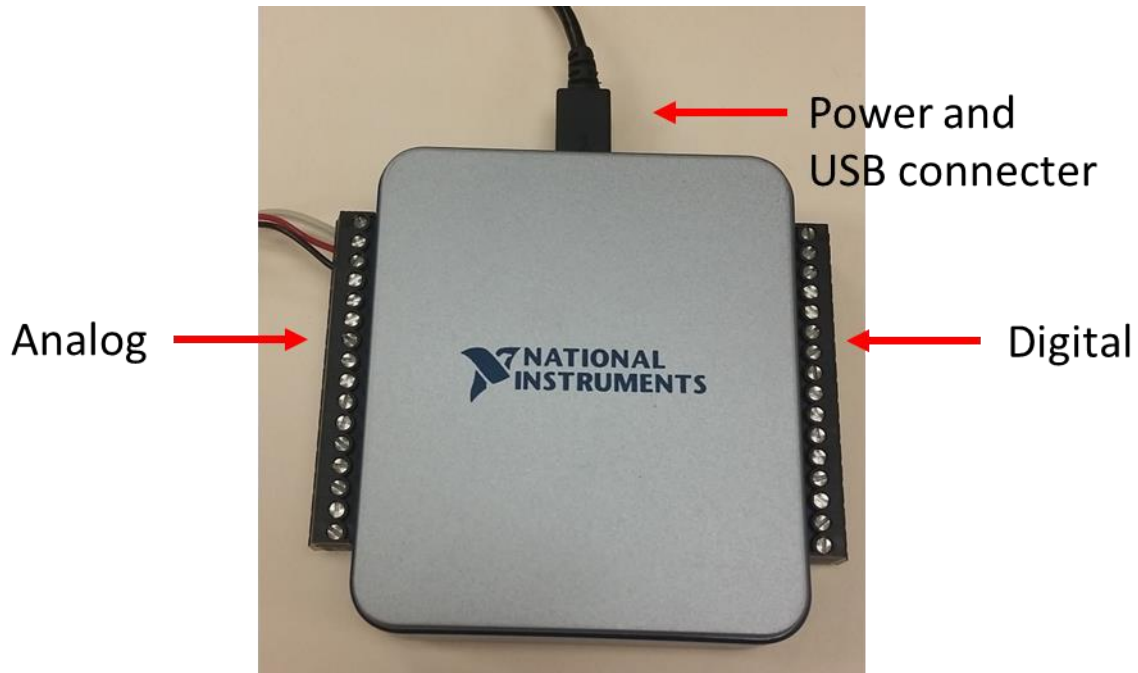


Figure 63: NI USB-6001 takes analog input from Falex Four-Ball tester

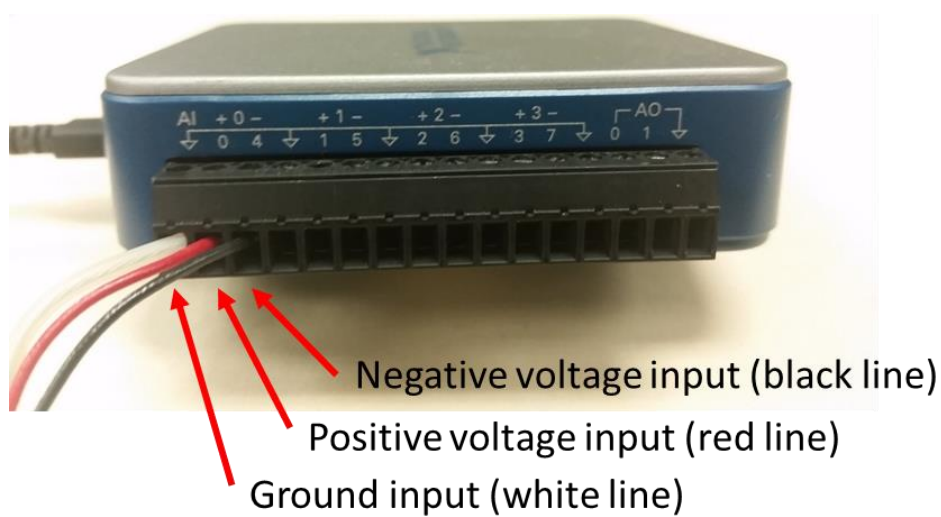


Figure 64: Analog inputs are in the form of negative and positive voltage

APPENDIX C

SECONDARY ION MASS SPECTROSCOPY

SIMS is a surface characterization technique utilizing ion beam as its source of energy. It is an important family of modern analytical techniques involving the use of MeV ion beams to probe the composition and obtain elemental depth profiles in the near-surface layer of solids. The two kinds of ion beams used in SIMS are cation (positive ion) and anion (negative ion). SIMS is highly sensitive and allow the detection of elements in the sub-monolayer range with an accuracy of a few percent. The depth resolution of SIMS on a sample surface is typically in the range of a few nanometers to a few ten nanometers.

The basic working principle of SIMS is to bombard surface with primary ion beams and use mass spectrometer to collect secondary ions that are ejected by the bombardment. A time to digital converter is used to the measure the time of flight of secondary ions from the sample surface to the mass analyzer. Alternatively, mass quadrupole is used to filter different mass passing through it and chart the mass spectrum. Mass spectrum is then used to supply insight of the elemental, isotopic and molecular composition of its uppermost atomic layers from Hydrogen to Uranium and above. SIMS is applicable to any solid that can be kept under vacuum. Figure 65 below shows how primary ion beam bombard the target surface and as a result cause secondary ions, electrons, and other entities to be ejected from the surface.

and basic elemental profiling can be conducted. Figure 67 below shows how ion beam interact to the surface in Dynamic SIMS technique.

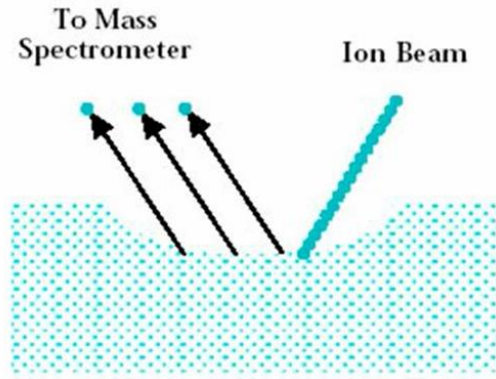


Figure 67. Dynamic SIMS ion beam interaction

The other SIMS technique is Static SIMS with several variants such as ToF SIMS as an example. Static SIMS is less destructive in terms of primary ion bombardment and thus this technique is able to collect information such as elemental and molecular analysis without destroying the molecular compounds before acquiring results. It operates by bombarding single or a short cluster of primary ion into the surface. It also penetrate only on small atomic level of layers on the surface and that is why it is called Ultra-surface analysis. Figure below shows how primary ion interact with surface in Static SIMS.

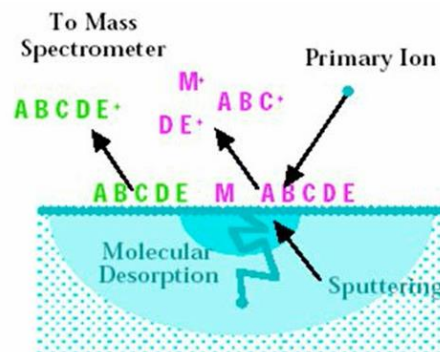


Figure 68. Static SIMS ion beam interaction

APPENDIX D

ADDITIONAL TRIBOLOGICAL DATA

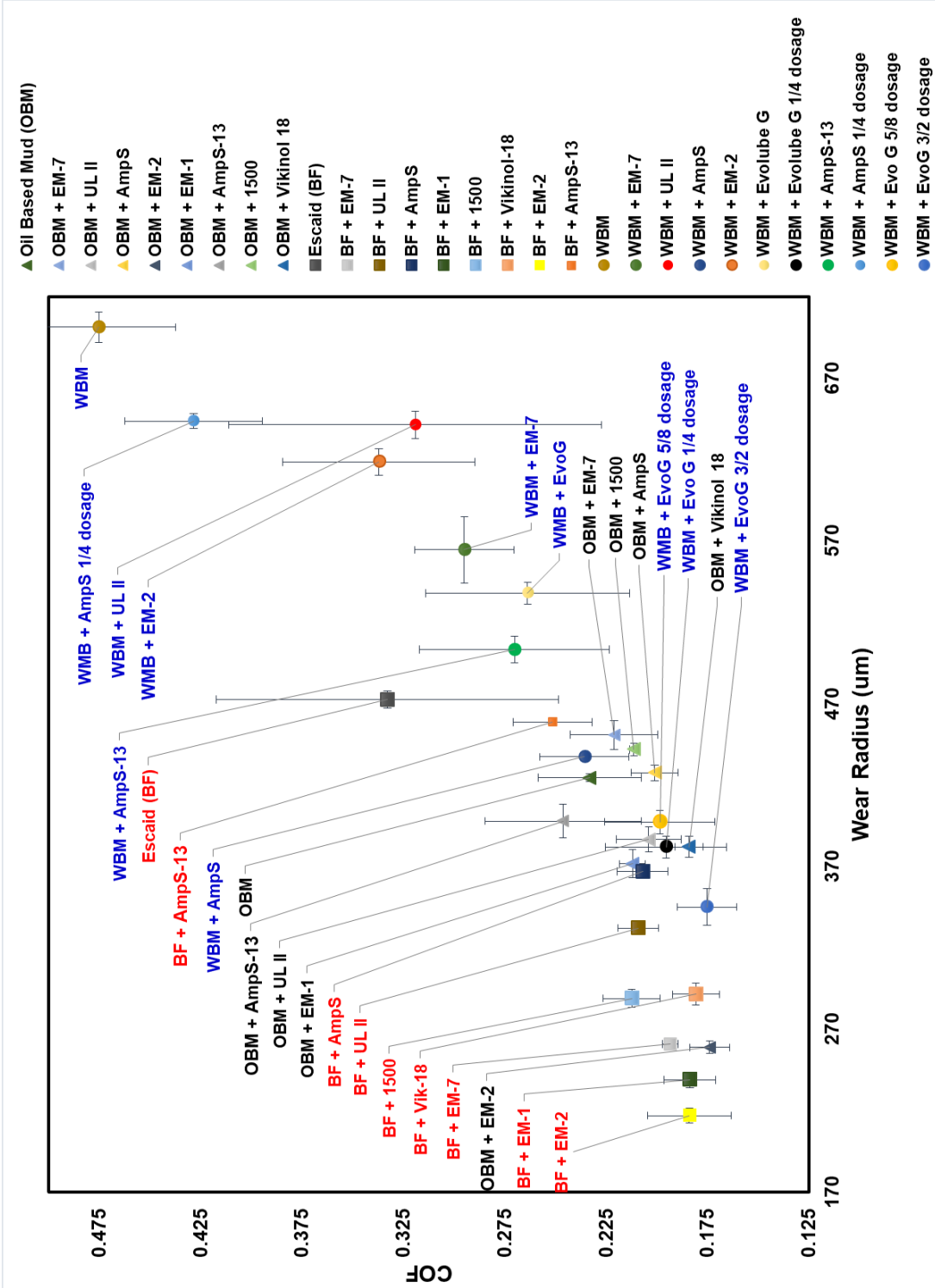


Figure 69: Master Chart of additional Four-Ball results

APPENDIX E
EFFECTS OF SURFACE HARDENING AND LUBRICANT VISCOSITY ON SURFACE
SEIZURE

This work is adopted from a project with Ingersoll Rand, contact person Wasim Akram, Ph.D., phase 5. Dr. Akram is interested in publishing the result of this project as it may be beneficial for industry interest.

This testing is conducted with Hi-Pressure Tribometer (HPT) as shown on Figure 70.

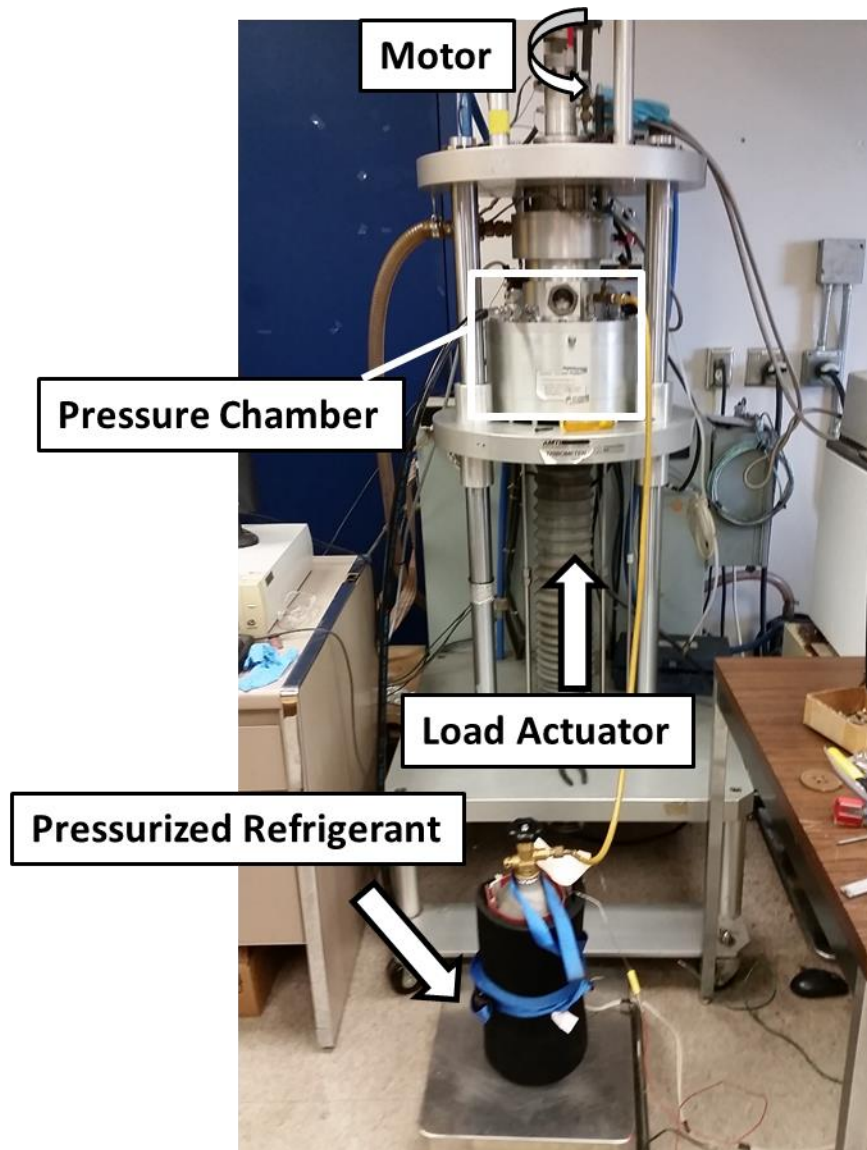


Figure 70: High-pressure tribometer (HPT) used for testing

The testing matrix used is shown in Table 8

Table 8: Testing matrix

Exp #	Pin	Disk	Lubricant	Speed	Load	Lubrication	Environment	Temp.	Failure Time (min)	Failure Load (lb)
1	4340N	4340H	Lub1	2.4 m/s	89N/min	Wick Method	Air	Room	8.3	145
2	4340N	4340H	Lub1	2.4 m/s	89N/min	Wick Method	Air	Room	4.02	85
3	4340N	4340N	Lub1	2.4 m/s	89N/min	Wick Method	Air	Room	58.3	792
4	4340N	4340N	Lub1	2.4 m/s	89N/min	Wick Method	Air	Room	20.1	325
5	4340N	4340N	Lub1	2.4 m/s	89N/min	Wick Method	Air	Room	40	625
6	4340N	4340H	Lub2	2.4 m/s	89N/min	Wick Method	Air	Room	5.1	100
7	4340N	4340H	Lub2	2.4 m/s	89N/min	Wick Method	Air	Room	2.5	55
8	4340N	4340N	Lub2	2.4 m/s	89N/min	Wick Method	Air	Room	43.5	670
9a	4340N	4340N	Lub2	2.4 m/s	89N/min	Wick Method	Air	Room	4.4	85
9b	4340N	4340N	Lub2	2.4 m/s	89N/min	Wick Method	Air	Room	30.5	475
10a	4340N	4340H	Lub3	2.4 m/s	89N/min	Wick Method	Air	Room	3.75	70
10b	4340N	4340H	Lub3	2.4 m/s	89N/min	Wick Method	Air	Room	3.05	70
11	4340N	4340H	Lub3	2.4 m/s	89N/min	Wick Method	Air	Room	NA (60)	819
12	4340N	4340N	Lub3	2.4 m/s	89N/min	Wick Method	Air	Room	NA (60)	819
13	4340N	4340N	Lub3	2.4 m/s	89N/min	Wick Method	Air	Room	49.9	673
14	4340N	4340H	Lub4	2.4 m/s	89N/min	Wick Method	Air	Room	TBA	TBA
15	4340N	4340H	Lub4	2.4 m/s	89N/min	Wick Method	Air	Room	TBA	TBA
16	4340N	4340N	Lub4	2.4 m/s	89N/min	Wick Method	Air	Room	TBA	TBA
17	4340N	4340N	Lub4	2.4 m/s	89N/min	Wick Method	Air	Room	TBA	TBA

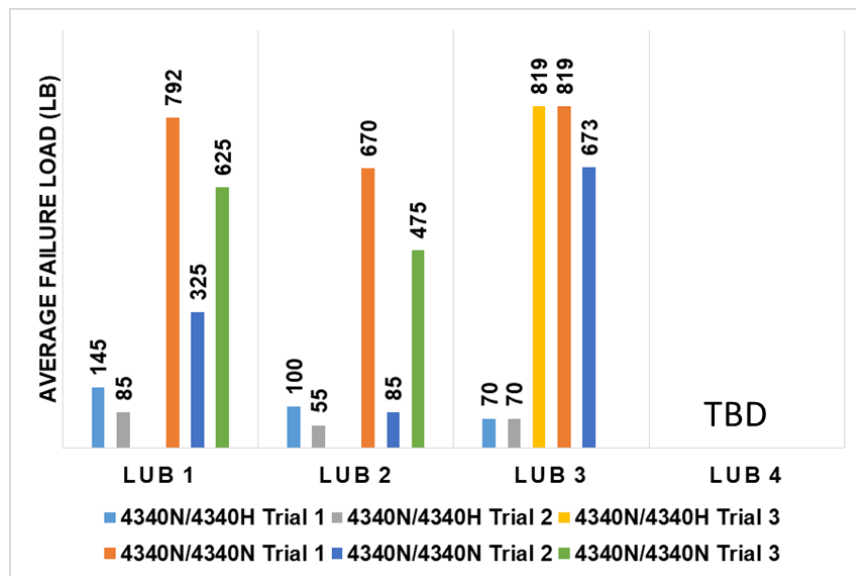


Figure 71: Summary of load at seizure for different interfaces

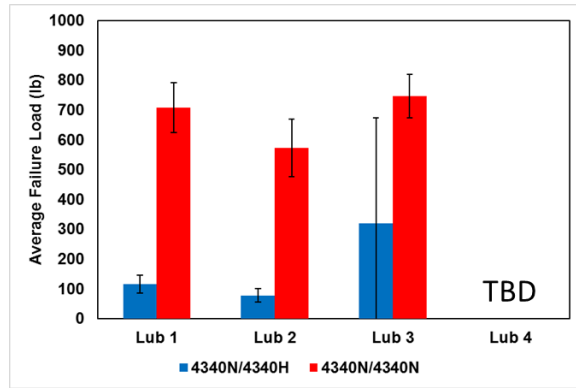


Figure 72: Average failure load of interfaces

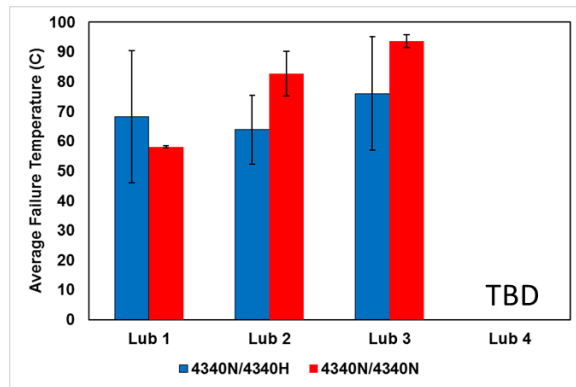


Figure 73: Average failure temperature of interfaces

Table 9: Summary of results

Rank	Material	Lubricant	Note
1	4340N / 4340N	Lube 3	Very good interface, high failure load
2	4340N / 4340N	Lube 1	Very good interface, high failure load
3	4340N / 4340N	Lube 2	Good interface, high failure load
4	4340N / 4340H	Lube 3	Moderate interface, moderate failure load, inconsistent
5	4340N / 4340H	Lube 1	Poor interface, low failure load
6	4340N / 4340H	Lube 2	Poor interface, low failure load